Grundmann, J. T. et al. (2019) Capabilities of Gossamer-1 derived small spacecraft solar sails carrying MASCOT-derived nanolanders for in-situ surveying of NEAs. *Acta Astronautica*, 156, pp. 330-362. (doi:10.1016/j.actaastro.2018.03.019)

This is the author's final accepted version.

There may be differences between this version and the published version. You are advised to consult the publisher's version if you wish to cite from it.

http://eprints.gla.ac.uk/159269/

Deposited on: 19 March 2018

Capabilities of GOSSAMER-1 derived Small Spacecraft Solar Sails carrying MASCOT-derived Nanolanders for In-Situ Surveying of NEAs

Jan Thimo Grundmann[(1)]*, Waldemar Bauer[(1)], Jens Biele[(2)], Ralf Boden[(3)], Matteo Ceriotti[(4)], Federico Cordero[(5)], Bernd Dachwald[(6)], Etienne Dumont[(1)], Christian D. Grimm[(1)], David Herčík[(7)], Tra-Mi Ho[(1)], Rico Jahnke[(1)], Aaron D. Koch[(1)], Alexander Koncz[(8)], Christian Krause[(2)], Caroline Lange[(1)], Roy Lichtenheldt[(9)], Volker Maiwald[(1)],Tobias Mikschl[(10)], Eugen Mikulz[(1)], Sergio Montenegro[(10)], Ivanka Pelivan[(8)], Alessandro Peloni[(4)], Dominik Quantius[(1)], Siebo Reershemius[(1)], Thomas Renger[(1)], Johannes Riemann[(1)], Michael Ruffer[(10)], Kaname Sasaki[(1)], Nicole Schmitz[(8)], Wolfgang Seboldt[(11)], Patric Seefeldt[(1)], Peter Spietz[(1)], Tom Spröwitz[(1)], Maciej Sznajder[(1)(12)], Simon Tardivel[(13)], Norbert Tóth[(1)], Elisabet Wejmo[(1)], Friederike Wolff[(9)], Christian Ziach[(14)]

[(1)]*DLR German Aerospace Center, Institute of Space Systems, Robert-Hooke-Strasse 7, 28359 Bremen, Germany*
+49-(0)421-24420-1107, jan.grundmann@dlr.de
[(2)]*DLR German Aerospace Center, Space Operations and Astronaut Training – MUSC, 51147 Köln, Germany*
[(3)]*Institute of Space and Astronautical Science (ISAS), Japan Aerospace Exploration Agency (JAXA), Solar Power Sail ISAS Pre-Project, 3-1-1 Yoshinodai, Chuo, Sagamihara, Kanagawa, 252-5210, Japan*
[(4)]*University of Glasgow, Glasgow, Scotland G12 8QQ, United Kingdom*
[(5)]*Telespazio-VEGA, Darmstadt, Germany*
[(6)]*Faculty of Aerospace Engineering, FH Aachen University of Applied Sciences, Hohenstaufenallee 6, 52064 Aachen, Germany*
[(7)]*Institute for Geophysics and Extraterrestrial Physics, Technical University Braunschweig, Germany*
[(8)]*DLR German Aerospace Center, Institute of Planetary Research, Rutherfordstr. 2, 12489 Berlin, Germany*
[(9)]*DLR German Aerospace Center, Robotics and Mechatronics Center, 82234 Wessling, Germany*
[(10)]*Informatik 8, Universität Würzburg, Am Hubland, 97074 Würzburg, Germany*
[(11)]*Consultant to DLR Institute of Space Systems*
[(12)]*Institute of Physics, University of Zielona Góra, Szafrana 4a, 65-069 Zielona Góra, Poland*
[(13)]*CNES, Future Missions Flight Dynamics, 18 avenue E. Belin, 31401 Toulouse cedex 9, France*
[(14)] *High-Tech Gründerfonds Management GmbH, Schlegelstraße 2, 53113 Bonn, Germany*

ABSTRACT

Any effort which intends to physically interact with specific asteroids requires understanding at least of the composition and multi-scale structure of the surface layers, sometimes also of the interior. Therefore, it is necessary first to characterize each target object sufficiently by a precursor mission to design the mission which then interacts with the object. In small solar system body (SSSB) science missions,

this trend towards landing and sample-return missions is most apparent. It also has led to much interest in MASCOT-like landing modules and instrument carriers. They integrate at the instrument level to their mothership and by their size are compatible even with small interplanetary missions.

The DLR-ESTEC GOSSAMER Roadmap NEA Science Working Groups' studies identified Multiple NEA Rendezvous (MNR) as one of the space science missions only feasible with solar sail propulsion. Parallel studies of Solar Polar Orbiter (SPO) and Displaced L_1 (DL1) space weather early warning missions studies outlined very lightweight sailcraft and the use of separable payload modules for operations close to Earth as well as the ability to access any inclination and a wide range of heliocentric distances.

These and many other studies outline the unique capability of solar sails to provide access to all SSSB, at least within the orbit of Jupiter. Since the original MNR study, significant progress has been made to explore the performance envelope of near-term solar sails for multiple NEA rendezvous.

However, although it is comparatively easy for solar sails to reach and rendezvous with objects in any inclination and in the complete range of semi-major axis and eccentricity relevant to NEOs and PHOs, it remains notoriously difficult for sailcraft to interact physically with a SSSB target object as e.g. the HAYABUSA missions do.

The German Aerospace Center, DLR, recently brought the GOSSAMER solar sail deployment technology to qualification status in the GOSSAMER-1 project. Development of closely related technologies is continued for very large deployable membrane-based photovoltaic arrays in the GoSolAr project.

We expand the philosophy of the GOSSAMER solar sail concept of efficient multiple sub-spacecraft integration to also include landers for one-way in-situ investigations and sample-return missions. These are equally useful for planetary defence scenarios, SSSB science and NEO utilization. We outline the technological concept used to complete such missions and the synergetic integration and operation of sail and lander.

We similarly extend the philosophy of MASCOT and use its characteristic features as well as the concept of Constraints-Driven Engineering for a wider range of operations.

1. INTRODUCTION

1.1 A brief history of…

The idea of an outward propulsive force of sunlight, and thus the concept of sunlight as a practical source of energy, goes back to Kepler's observations and remarks published in 1619 on the directionality of comets' tails [1]. It was predicted to equal magnitude in 1873 by Maxwell on the basis of his electromagnetic theory [2] and in 1876 by Bartoli based on the Second Law of Thermodynamics [3]. The same year, the foundations for modern semiconductor-based electronics and photovoltaics were laid by Adams' and Day's discovery of an electrical current driven by selenium exposed to light. [4]

Kepler's propulsive force was finally experimentally demonstrated as pressure due to radiation by Lebedev in 1901 [5] and by Nichols and Hull in 1903 [6]. Solar sailing as a method of space propulsion was proposed repeatedly throughout the 20th century [7], beginning with Oberth and Tsiolkovsky in 1923 and 1924, respectively [7][8]. The term 'solar sailing' as such was only introduced by Garwin in 1958. [9]

Based on the same principle as Adams' and Day's selenium cell of 1876 but refined by the knowledge of quantum mechanics, the silicon junction solar cell was first serendipitously created in 1953 by Pearson, Chapin and Fuller at Bell Labs. It turned photovoltaic devices from sensor-level signal generators into a technically viable power source by 1956. It was the first source of electrical power that does not require a constant supply of chemicals, fuel, water, or hard labour, and it was lightweight and portable. However, it was at first commercially restricted to the novelty toy and beach radio market. [10]

Realizing the limits and limitations of chemical batteries in powering remote and expensive electronic experiments (cf. [11] [12] [13] [14] [15] [16] [17] [18]), Ziegler [4] and Liderenko [19] introduced photovoltaic cells on Vanguard-1 and Sputnik-3, respectively, which successfully operated low-power optimized solid-state electronics for the entire functional respectively orbital lifetime of these spacecraft. However, at this time, photovoltaic generators were viewed as only an interim power generation method on the way from simple battery-powered missions using 'experimental' low-power devices such as transistors to complex long-duration missions using nuclear power and 'proper' vacuum tube based high-performance electronics for high reliability (*sic!*). [4] [17] [18]

Up to the early 1960s, it was consensus that the lowest energy trajectory to any planetary target, the Hohmann transfer, also corresponded to the lowest *launch* energy solution to that target. The Hohmann transfer is also the trajectory with the longest flight time, with two impulses, to any given target. It was commonly assumed that entirely new methods of propulsion would be required to even reach all but the nearest planets on one-way trips or to complete a round trip to any of the planets including the nearest. These new methods of propulsion included high-thrust nuclear-electric and nuclear-thermal rockets which became major development programmes.

The resulting massive reactor-powered escape stages easily carried the then-envisaged near-term exploration spacecraft based on contemporary avionics to Mars and Venus but were almost as challenged by the velocity requirements of a trip beyond the asteroid belt as was the technology of the day by the lifetime requirements of a Hohmann transfer to the outer planets. Such journeys and return trips to Mars or Venus required the development of hyper-giant launch vehicles which, like nuclear propulsion, were begun in earnest. Nova, much larger versions of what would become the Saturn V, went to the limit of land-based launch pads. Sea Dragon made the nuclear aircraft carrier which was required to power its fuelling plant after it was towed empty to the open ocean look small next to it ([20] *and references therein)*.

Perturbations by the planets were recognized but regarded as a disturbance to be actively cancelled out to preserve trajectories considered favourable such as Hohmann's Mars-Venus return roundtrip based on a sequence of his minimum

energy transfers from planet to planet [21]. At best, planetary perturbations were arranged to mutually compensate and thus reduce the propulsive effort in their elimination [22].

However, a paradigm change occurred in the first half of the 1960s. Minovitch realized the propulsive potential of strong planetary perturbations in controlled very close fly-bys, turning planetary gravitational perturbations from an annoyance into the main if not exclusive post-launch propulsion mechanism for interplanetary exploration. He developed an interplanetary free-fall trajectory design method and the tools to study the trajectories for identified line-ups of the planets [23] [24] [25]. Using these tools, following the leads already placed in [23] [26], and equipped with a new high-quality planetary ephemeris extended beyond 1980 [27], Flandro singled out the 'Grand Tour' trajectories around the 1977 launch window, in particular the one to be flown by Voyager 2 to all the gas giants taking advantage of a planetary line-up occurring only every ≈175 years in this quality [28].
Provided one puts enough effort in finding such planetary line-ups and is patient enough to await their occurrence, tours to any combination of all the planets are possible starting from the ones easiest to reach, Venus [23] or Earth itself [29] [30] [31].

With the acceptance of this newly discovered method of planetary gravity-assists and the contemporary difficulties encountered in realizing high-energy nuclear propulsion and giant launch vehicles, all exploration missions beyond the Moon became immediately feasible and based on off-the-shelf conversion launch vehicles of the mid-1960's. Within half a decade, any mission beyond Venus or Mars employed gravity-assists. [20]
Thus, the exploration of the outer planets and Mercury based on gravity-assists and the respectively smallest feasible launch vehicles became the third pillar after the U.S. ICBM programmes and the Apollo Guidance Computer development [32] supporting the development of lightweight, highly integrated and reliable electronics able to survive for decades in space. Planetary probes and their avionics suddenly had to fit inside a phone booth sized fairing now instead of the previously envisaged twin garage of the future, and still include a digital sequencer if not a full-blown computer. The only vacuum tubes remaining in space applications were those in high-power microwave transmitter output stages, for a while. [33]
With the concurrent reduction of power requirements by the transition from vacuum tube to solid-state electronics and available space in launch vehicles beneath that required for deployable radiators of nuclear reactors, photovoltaic generators became the prime power source in space [10] [16], relegating all the others to niche applications mainly in exploration science missions. [11] [12] [13] [14] [15] [16] [34] [35] [36] At first confined to the region of the terrestrial planets, the feasibility photovoltaic power has meanwhile been proven out to Jupiter [37] and beyond [38] [39], and photovoltaic spacecraft are considered in studies reaching as far out as Uranus [40].

The avalanche of change set off by gravity propulsion enabled the exploration of the whole solar system out to Pluto and beyond but at the same time focused work on missions that were feasible without entirely new technologies in mission-critical functions such as propulsion.

Nuclear-thermal propulsion went the way of the vacuum tube before the end of the decade. Electric propulsion development adjusted itself to the power capabilities of photovoltaics and thus proceeded on a long-term effort of efficiency optimization, creating the concept of interplanetary cruise low thrust reaction propulsion. First demonstration missions employing solar-electric propulsion in cruise to planetary targets came along in the 1990s [41] [42] and have led to its use in flagship missions [30] [43] [44].

Although non-nuclear, propellant-free, and by the concept of deployable lightweight membrane structures inherently suited to small spacecraft, solar sailing largely receded into the realm of trajectory studies and optimization. For several decades, the last application of the propulsive force of sunlight were the adjustable attitude trim panels at the outer ends of MARINER 4's solar panels. Nevertheless, the development of complete concepts and designs of sailcraft was occasionally carried through to the stage of hardware production and full-scale ground testing, sometimes even suborbital deployment trials. However, despite the – in terms of mechanisms technology development research programmes – substantial effort invested in these projects, only simplified and/or sub-scale demonstrators were flown at least in orbit [45] before the sole exception, the Interplanetary Kite-craft Accelerated by Radiation Of the Sun (IKAROS) [46], which accompanied JAXA's atmosphere observation orbiter, AKATSUKI, to Venus. The IKAROS first demonstrated solar sail effect in space, successfully and as predicted. It also performed the first gravity-assist of a solar sail on December 8th, 2010, passing Venus at 80800 km distance and achieving about 20° deflection of the trajectory.

1.2 Solar sailing at DLR

The development of solar sail technology has been ongoing at DLR for many years at varying levels of intensity since the 1990s. A first phase culminated in a successful ground deployment test of a (20 m)² boom-supported sail on December 17th, 1999 – Figure 1.

Figure 1 – Ground deployment test of a (20 m)² sail, DLR Cologne, in the EAC hall (note space station practice modules in the background) December 17th,1999

This work was subsequently evolved over almost a decade at relatively low intensity in the hope of achieving flight status through a mission with propulsion requirements suitable for the solar sail technology of the day but too challenging to be met by conventional means of propulsion. [47] [48] [49] [50] [51]

However, space exploration projects requiring a very high ΔV are almost always funded primarily to fulfil a planetary science objective, not to initiate technology development to optimize their propulsion. Also, interplanetary missions already are a rare occurrence when compared to the launch cadence of global spaceflight activities; not even a handful of the spacecraft launched each year leave Earth gravity behind. Missions to a specific interplanetary target are yet rarer. With the exception of the nearest planets a generation or more may pass before it comes to a revisit.

1.2.1 The Gossamer Roadmap

In the wake of the GEOSAIL technical reference study [52] [53] [54] the previous work at DLR was finally extended into the framework of the DLR-ESTEC GOSSAMER Solar Sail Technology Roadmap in November 2009 by an agreement between DLR and ESA [55] [56]. The key programmatic difference to previous national and European solar sail related studies and projects was its character as a pure technology development undertaking with the explicitly stated complete abandonment of any

scientific payload – and thus of any mainstream big mission scale funding. The technology demonstration mission based approach was chosen in the hope that it could more readily provide an environment that would lead to the successful development of ultra-lightweight deployable structures as it became apparent that these would only require a very modest fraction of the funding required by a typical mission on the science-driven path where propulsion is just one among many service-providing subsystems.

The GOSSAMER Roadmap consisted of three steps:
- GOSSAMER-1: low cost technology demonstrator for membrane deployment technology with a (5 m)² sail in very low Earth orbit (LEO).
- GOSSAMER-2: validation of solar sail attitude control technologies on a (20 m)² sail in Earth orbit at altitudes where photonic pressure becomes dominant.
- GOSSAMER-3: fully functional (50 m)² solar sail to validate the design approach and prove sufficient guidance, navigation and attitude control to conduct planetary science and space weather missions.

1.2.2 The GOSSAMER-1 Qualification Model

GOSSAMER-1 was intended as a low cost technology demonstrator for the mechanics and coordination of the membrane deployment process, only. It deploys a (5 m)² sail using technology that is already suitable for the next step in terms of sail size to be deployed, GOSSAMER-2's (20 m)². The GOSSAMER-1 design was compatible with all low Earth orbits (LEO) that ensure orbital decay of all spacecraft units within 25 years [57] including very low altitudes below the ISS. The last baseline design was an independent free-flyer spacecraft optimized for the widest possible spectrum of secondary payload ("piggy-back") launch opportunities. An alternative upper stage attached mission option was also studied in detail.
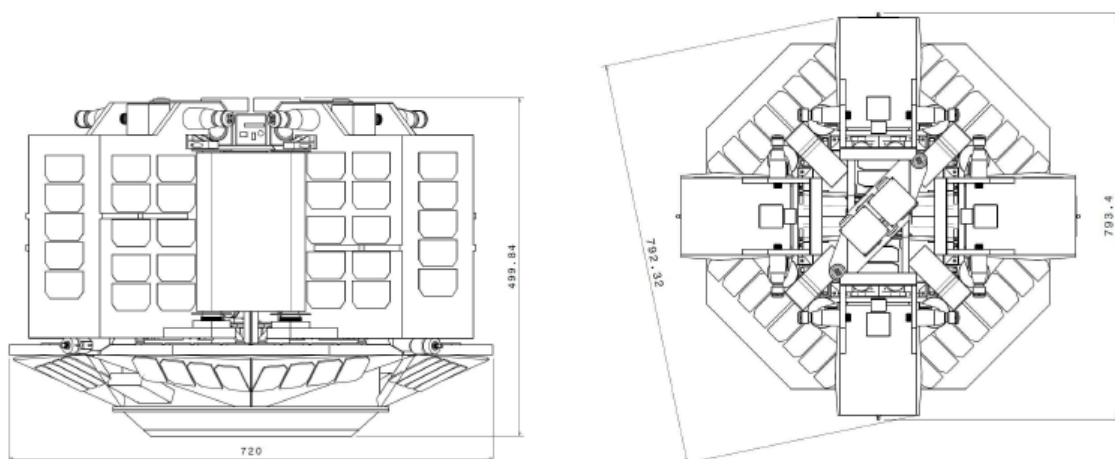

Figure 2 – GOSSAMER-1 free-flyer design with operational photovoltaics based on conventional triple-junction cells (placeholders shown, only) for independent operation

The GOSSAMER-1 design was carried forward to full qualification testing. The integration of the qualification model (QM) and test campaign planning re-used the concurrent AIV approach pioneered by MASCOT [58] [59] (also cf. [60]). The

GOSSAMER-1 QM consisted of one fully functional train of the deployment relevant units and two adjacent membrane quadrants. It completed qualification testing in 2016, including venting, vibration testing, thermal-vacuum testing with initial deployment phase testing only restricted by the size of available facilities, and laboratory full deployment. The development of the solar sail specific technology was stopped after the qualification process on a TRL five full ground deployment tests. Several components were also subjected to environmental qualification testing. The QM was applicable for all possible GOSSAMER-1 launched system configurations, from upper stage attached payload to independent free-flyer. [61]
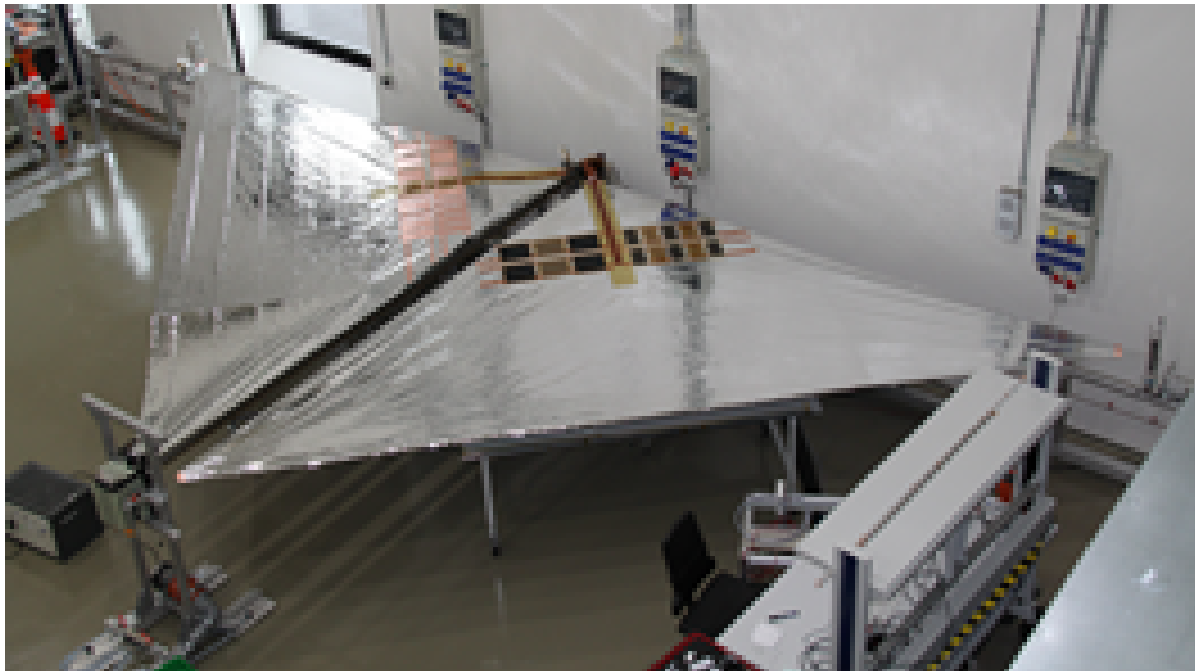

Figure 3 – GOSSAMER-1 QM fully deployed

The development of the solar sail specific technology was stopped after the qualification process on a technology readiness level (TRL) of 5 (cf. [62] [63] [64] [65] [66], also for comparison regarding TRL definitions). The further development of deployment technologies will focus on membrane-based solar arrays using thin-film photovoltaics. [67] [68] [69] [70]

2. PATHS OF CONVERGENCE FROM A DIVERGENT PAST

The recent achievements in solar sail trajectory design [71] [72] and sailcraft hardware development [46] [73] [74] [75] [76] [77] [78] [79] [80] [81] [82] [83] [84] [85] [86] [87] [88] [89] [90] made clear that a point has been reached where a review of the results and ongoing efforts should be made for a determination which road they should take. The development towards this point happened in trajectory analysis and technology development during more than a decade, on the background of a sustained resurgence of interest in small solar system bodies (SSSB). It saw the successful conclusion of the HAYABUSA and ROSETTA/PHILAE missions, the launch of HAYABUSA2 [29] with the small lander MASCOT aboard [34], the launch of OSIRIS-REx [31], the flight of the IKAROS [46] [60] [75] [76] [77] [78], and the first steps

towards a long-term Solar Power Sail (SPS) propelled sample-return mission to the Trojan asteroids of Jupiter [79] [80] [81].

Among small solar system bodies, the near-Earth asteroids (NEA) in many ways may hold keys to our future on Earth and in space: for planetary science, they appear to represent a fairly good mix of the building blocks of the terrestrial planets while orbiting at an accessible distance; for planetary defence, they are the reservoir of almost all potential threats which we need to understand to protect Earth from dangerous impacts; and for the new emerging field of asteroid mining, their surfaces and interiors are the promising terra incognita to be mapped and prospected.

2.1 Small Spacecraft

Within about the project lifetime of the ROSETTA/PHILAE mission, from its inception in 1985 to the landings of PHILAE in 2014 and beaching of ROSETTA in 2016, the broad if not exclusive trend towards ever larger, heavier, more capable, more difficult and more expensive space missions was disrupted by the emergence of small spacecraft. [91]

We define small spacecraft in analogy to commonly used small Earth satellite class definitions. There is no consensus on mass boundaries between classes in the many academic as well as practical definitions around. [92] [93] [94] [95] Also, interplanetary spacecraft inherently have additional requirements for propulsion and communication which can significantly affect the mass or size of a specific design without changing the underlying characteristic design concept features it shares with the class of small Earth satellites that it appears to resemble. Thus, we rely on a practical combination of criteria based on launch accommodation implying mass of the spacecraft separated from its carrier [96] [97], as well as design concepts considering key features commonly associated with the respective Earth-orbiting small spacecraft class, project schedule, team size, development and AIT/AIV requirements, and cost. [98] With this in mind, we use the SI unit prefixes for spacecraft smaller than 'minisatellites' which are commonly applied in the classification of small spacecraft.

Consequently, we classify MASCOT (9.8 kg) and its derivatives as 'nanolanders' also for the features they share with Earth-orbiting nanosatellites such as a common integrated electronics compartment (E-Box) even though their mass is close to or sometimes exceeds the most commonly applied 10 kg boundary. We classify PHILAE (96 kg) or the JAXA Solar Power Sail Jupiter Trojan Asteroid Lander as a 'microlanders' not just for their mass being slightly below 100 kg but also for their similarity in design with highly compact microsatellites such as BIRD (92 kg) [99], TET-1 (110 kg) [100], or AsteroidFinder (~127 kg) [101].

In the secondary ('piggy-back') payload launch situation common for small spacecraft, the launch opportunity or the set of launch opportunities combined place requirements and constraints on the payload. A secondary payload is in no position to put requirements on the launch. At best, it can request the use of surplus performance e.g. of available fuel margins of a restartable upper stage. Thus, in the preferable situation of having a set of prospective launch opportunities, the envelope of the most adverse constraints become design requirements on the payload to be launched. For tertiary payloads, i.e. subsatellites carried by another usually larger payload of the same launch and not on the launcher directly, the same

considerations apply, although a set of constraints to be enveloped will only appear if the carrying spacecraft is itself a secondary payload working with a set of launch opportunities. Regarding sailcraft, the requirements of launch opportunities to conveniently-high Earth orbits or Earth escape ($c_3 \geq 0$) are key constraints driving the design of small sailcraft directly in terms of mass and stowed envelope size, and indirectly by the set of accessible orbits at the technically feasible times of separation from the launcher, by the resulting schedule options and the respective cost. If several launch opportunities present themselves, they may need to be traded based on technical as well as programmatic aspects. These design-driving constraints apply mainly to the launch configuration of the sailcraft, and the implementation of design features characteristic of the respective Earth-orbiting small satellite classes is very likely to follow by constraints-driven design.

Thus, we define 'micro' sailcraft as those which fit secondary launch opportunities using the U.S. ESPA small spacecraft rideshare platform and/or the various Arianespace ASAP and VESPA platforms' 'micro' positions, i.e. are clearly too large to ride in place of the largest cubesat dispensers but do not exceed 180…200 kg mass and somewhat less than $(1 \text{ m})^3$ envelope. (The precise geometry of the volume envelope varies between launch vehicles and is also often negotiable depending on the primary payload.) We define 'mini' sailcraft as those which exceed these 'micro' payload envelopes but fit the Arianespace ASAP or VESPA platforms' 'mini' positions and/or similar accommodations on launch vehicles using ESPA or proprietary structures. [96] [97] As a corollary, 'nano' sailcraft would be those small enough to ride in place of cubesats or their dispensers and thus not requiring a 'micro' slot on any of these platforms, such as NEAscout [82] [83] or proposed Advanced Composites-Based Solar Sail System (ACS3) based [90] future small spacecraft exploration precursor missions [88]. Together, we refer to all of these as 'small' sailcraft.

2.2 Multiple NEA Rendezvous

A near-term mission scenario for solar sails is the multiple NEA rendezvous (MNR). [71] [72] [102] It is a means to increase the knowledge on NEAs by vastly accelerating the rate of their exploration and to open up a more representative sample of the NEA population. All asteroid user communities – planetary science, planetary defence, and in-space resource utilisation – have an expressed need or desire to expand their respective body of knowledge on a reasonable time scale.

The DLR-ESTEC GOSSAMER Roadmap NEA Science Working Groups studies identified Multiple NEA Rendezvous (MNR) as one of the space science missions presently only feasible with solar sail propulsion. [102] The parallel Solar Polar Orbiter (SPO) study showed the ability to access any inclination and a wide range of heliocentric distances. It used a separable payload module conducting the SPO mission after delivery by sail to the proper orbit. [103] The Displaced L_1 (DL1), spaceweather early warning mission study, outlined a very lightweight sailcraft operating close to Earth, where all objects of interest to planetary defence must pass. [104]

Current MNR trajectory studies demonstrate the feasibility of exploring 5 different NEAs in a rendezvous scenario for >100 days, each, with one near-term first-generation sailcraft within 10 years from Earth departure ($c_3 \geq 0$). [71] [72] This rendezvous duration is comparable to the mission scenario of AIM at the binary NEA

(65803) Didymos [105] and the on-asteroid activities phase of its lander, MASCOT2, on Didymoon [106]. It is also demonstrated that the sequence of asteroids to be visited can be changed easily and on a daily basis for any given launch date and even *after* launch and between rendezvous. [71] [72]

Therefore, a sailcraft carrying a set of five MASCOT landers based on a common design but differently equipped with science instruments and landing or mobility related systems appears desirable. Which lander is used can be decided after arrival at and initial study of the respective target asteroid, considering the expectations for the targets still to come. Many features of the MASCOT lander design can be shared with the core sailcraft and its four boom-sail deployment units (BSDU). Excluding their more extensive and for a realistic sailcraft also more voluminous suite of mechanisms, all these sub-spacecraft of the launch configuration are MASCOT-scale spacecraft of their own, 'nano' at heart, i.e., employing design features which are commonly associated with Earth-orbiting nanosatellites such as card module based integrated electronics in a common housing (E-Box). Indeed, this sharing of design elements and heritage has been done already, for the GOSSAMER-1 QM BSDU which was developed in parallel to MASCOT. This approach was carried on for the structurally similar ROBEX lunar-analog demonstration mission scientific Remote Units (RU) design. [107] The economy of scale becomes immediately obvious considering that one such mission would already consist of 10 independent sub-spacecraft physically connected at launch but to be separated step-by-step throughout the mission. The initial connection also enables resource-sharing between all initially connected as well as those still connected throughout cruise.

3. SEE FIVE – THE MNR MISSION SCENARIO

3.1 Overview of MNR mission scenario building blocks and options

In continuation of the earlier work on solar sails up to the GOSSAMER Roadmap, including its Science Working Groups, and on the background of the surging interest in small solar system bodies in several fields, we use the most mature system elements available to us to create the most cost-effective interplanetary exploration mission scenario addressing the most reasonable next step in small solar system body exploration. These elements include the latest MNR trajectory design optimizations addressing missions of a reasonable duration of 10 years at near-term sail performance, the GOSSAMER solar sail design concept using multiple sub-spacecraft which easily incorporates a wide variation of configurations, and the small solar system body lander designs evolved from PHILAE to MASCOT and further on which easily integrate to small and very small carrier spacecraft. In the following sections, these three core elements are presented.
The flexibility of the resulting MNR mission design is demonstrated by its application to the fictional Earth impactor exercise scenarios which are a regular activity at the Planetary Defense Conferences.

3.2 The MNR reference mission

Peloni et al. [71] set a benchmark MNR objective: to study at least 5 NEAs by a rendezvous of at least 100 days, each, in a mission duration of less than 10 years, and presented a multiple-NEA rendezvous mission through solar sailing. Table 1

shows the mission parameters for the sequence shown in the reference paper. The characteristic acceleration of 0.2 mm/s² assumed in this paper was shown to be within the capability of current and near-term sailcraft technology by Seefeldt et al. [108].

Table 1 – Mission parameters for the considered sequence. (For parameters passed from sequence-search algorithm to optimizer see [71]).

Object	Stay time [days]		Start	End	Time of flight [days]
Earth	//		10 May 2025	26 Feb 2027	657
2000 SG$_{344}$	123		29 Jun 2027	06 Sep 2028	436
2015 JD$_3$	164		18 Feb 2029	24 Sep 2030	584
2012 KB$_4$	160		04 Mar 2031	29 Sep 2032	576
2008 EV$_5$	171		20 Mar 2033	30 Sep 2034	560
2014 MP	//				

It is worthwhile to note that the arrival at 2014 MP after 3431 days or nearly 9.4 years is not necessarily the end of the mission, nor is it the 222-day stay there still within the 10-year trajectory design goal. The visit at 2014 MP may well be followed by another departure and more journeys to and stays at other NEAs, as long as the sailcraft remains flightworthy. The duration of the mission does not depend on a finite amount of fuel aboard. It only depends on the creativity and attention to detail of the spacecraft designers, the skill and care of the hardware integrators, the means put at their disposal by 'programmatics', the ingenuity and patience of the operators on the ground to get smarter, faster than the sailcraft mechanisms wear out and age in space, and the will to pay them a while longer for their effort.

For one, Pioneer 6 was designed to last about 6 months counting from its launch on December 16th, 1965 into a NEA-like heliocentric orbit. It was last operated on December 8th, 2000 – 35 years later. In 1997, three of its instruments still worked well. Two of its three companions fared similarly well; Pioneer 7 successfully participated in the Halley campaign of 1986 and in 1995 one of its instruments was still working, as for Pioneer 8 in 1996. Only Pioneer 9 is known to have failed in 1983. Thereafter, we only know that Earth did not call any of them again, yet. [109]

Table 2 – Orbital parameters, size and other properties of the bodies in the MNR sequences [110] [111] [112]

Object	Earth	2000 SG$_{344}$	2015 JD$_3$	2012 KB$_4$	(341843) 2008 EV$_5$	2014 MP
Orbital type	-	Aten	Amor	Amor	Aten	Amor
Semi-major axis [AU]	1	0.977	1.059	1.093	0.958	1.050
Eccentricity	0	0.067	0.008	0.061	0.083	0.029
Inclination [deg]	0	0.112	2.719	6.328	7.437	9.559

Absolute magnitude [mag]	-	24.7	25.6	25.3	20.00	26.0
Estimated size [m]	-	35 – 75	20 – 50	20 – 50	260 – 590 *400 ±50*	17 – 37
geometric albedo					*0.137*	
EMOID [AU]	-	0.00085	0.054	0.072	0.0132	0.0187
PHA	-	no	no	no	yes	no
NHATS	-	yes	yes	yes	yes	yes
taxonomic type	-				C;X	
albedo	0.367				0.104	
rotation period [h]	23.93				3.725	
lightcurve amplitude [mag]	-				0.05	
radar observation	-				Y	
spectral observation	-				Y	
IR observation	-				Y	
Ascending node Earth separation [AU]	-	-0.03197	0.06224	0.09177	0.01535	0.08022
Descending node Earth separation [AU]	-	-0.02184	0.05451	0.08589	-0.10839	0.01890

The asteroids selected by the sequence-search algorithm do tend to have fairly Earth-like orbits. However, the catalog was here restricted to NHATS-listed asteroids and PHAs of which a larger fraction populates this region. MNR missions or solar sails are not at all restricted to targets near the ecliptic or near 1 AU. In earlier studies, the capabilities of solar sails in closely Earth-co-orbital [104], very high heliocentric inclination [103], and even fully retrograde orbits [113] [114] [115], for similarly demanding ≈10-year missions have been demonstrated for near-term sails. Thus, the combination of micro spacecraft solar sail and nano-lander makes every small solar system body accessible within reasonable mission duration, at least out to the orbit of Jupiter.

Solar sailing has the advantage of continuous target asteroid flexibility. For each launch date, hundreds of accessible NEA target sequences exist even within the restricted database of targets. The targets do not have to be selected before launch and they can be changed en-route, for example when scientific or commercial interest changes over the years of the mission or when a new target of particular interest appears.

3.2.1 The Unknown Unknowns

It is worth noting how little is known about all the asteroids mentioned above that would be of use to a highly optimized spacecraft design. Presently, 2008 EV₅ is the

only one for which a shape model is available [116] which can be used together with the other few known parameters [117] to calculate a likely asteroid thermal environment, see Figure 4.
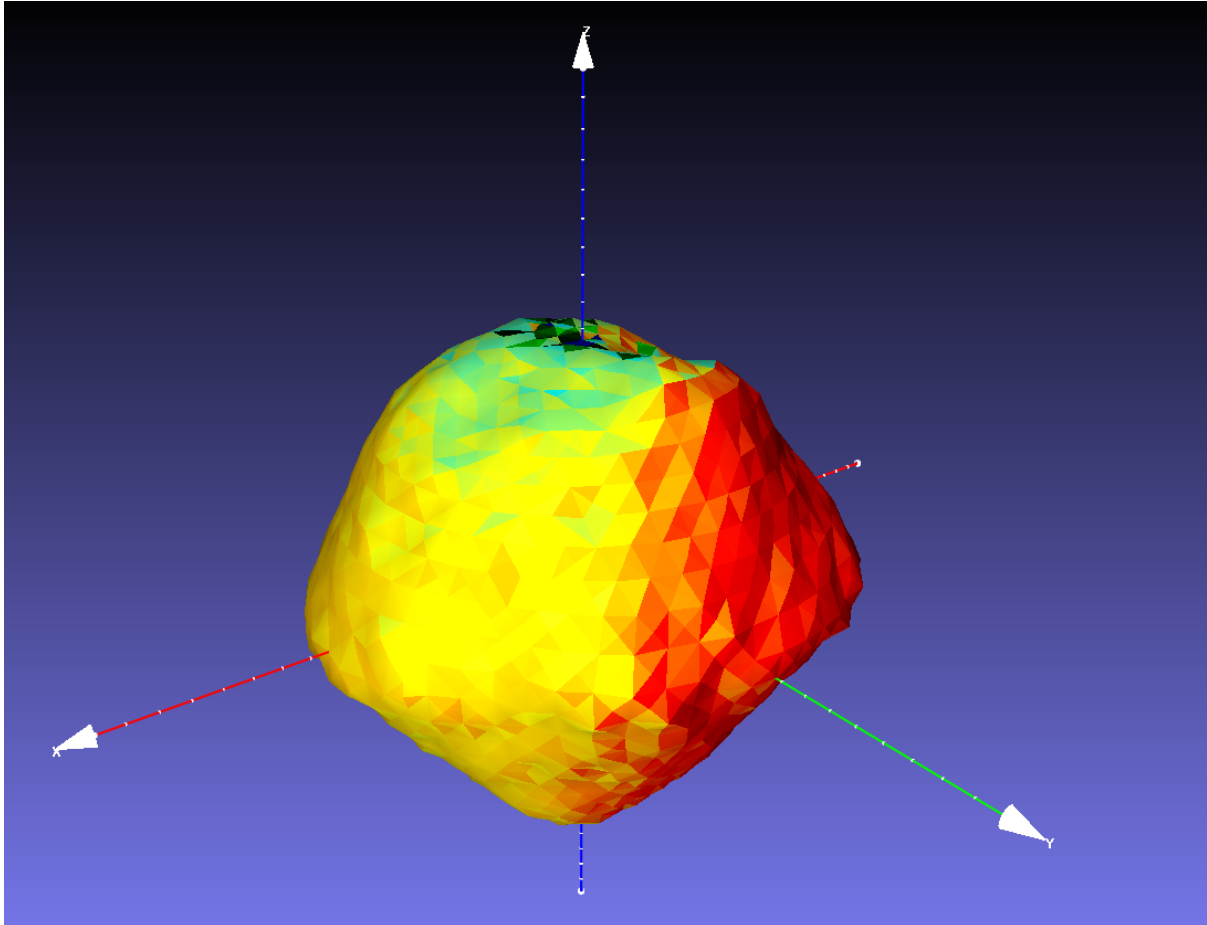

Figure 4 – Asteroid surface thermal model of (341843) 2008 EV$_5$ with temperatures on March 4th, 2031, 0[h], ranging from 121 K to 364 K (blue to red). Rotation period 3.725 h, assumed TI = 450 and PM = 0. Shape model from [116], asteroid parameters from [117], methods from [118] with adapted parameters.

Since the purpose of the MNR mission is to expand the knowledge on NEAs and potentially discover objects with unexpected properties, the design of the spacecraft, and in particular the landers, needs to anticipate a very wide variation of the conditions on the ground, and be very robust in this respect. This is the case for MASCOT as the rather strong seasonal variations on Ryugu were taken into account to enable the use of as many landing windows as possible.

3.3 Going For The One – On the Return Leg

To study the potential for a multiple NEA sample return mission, the last leg to 2014 MP has been removed and substituted with a return leg to the Earth. The same methodology described in Peloni et al. [71] was used to compute the return leg to the Earth. The total mission duration is now 4131 days, about 11.3 years – far from a significant increase in terms of technology requirements. The complete trajectory of

the overall sequence is shown in Figures 5 and 6, whereas Table 3 shows the updated mission parameters.

Table 3 – Mission parameters for the considered sequence with the last leg to the Earth.

Object	Stay time [days]		Start	End	Time of flight [days]
Earth	//		10 May 2025	26 Feb 2027	657
2000 SG₃₄₄	123		29 Jun 2027	06 Sep 2028	436
2015 JD₃	164		18 Feb 2029	24 Sep 2030	584
2012 KB₄	160		04 Mar 2031	29 Sep 2032	576
2008 EV₅	*160*		*18 Mar 2033*	*22 May 2036*	*1161*
Earth	∞				

It is important to note that the sequence still contains 2008 EV$_5$, which is classified as a PHA and was selected as one of the candidate targets for the ARRM mission by NASA [119]. Also, although departure from it comes 11 days earlier, the stay time at 2008 EV$_5$ remains well beyond 100 days and among the longest of this particular sequence of asteroids.
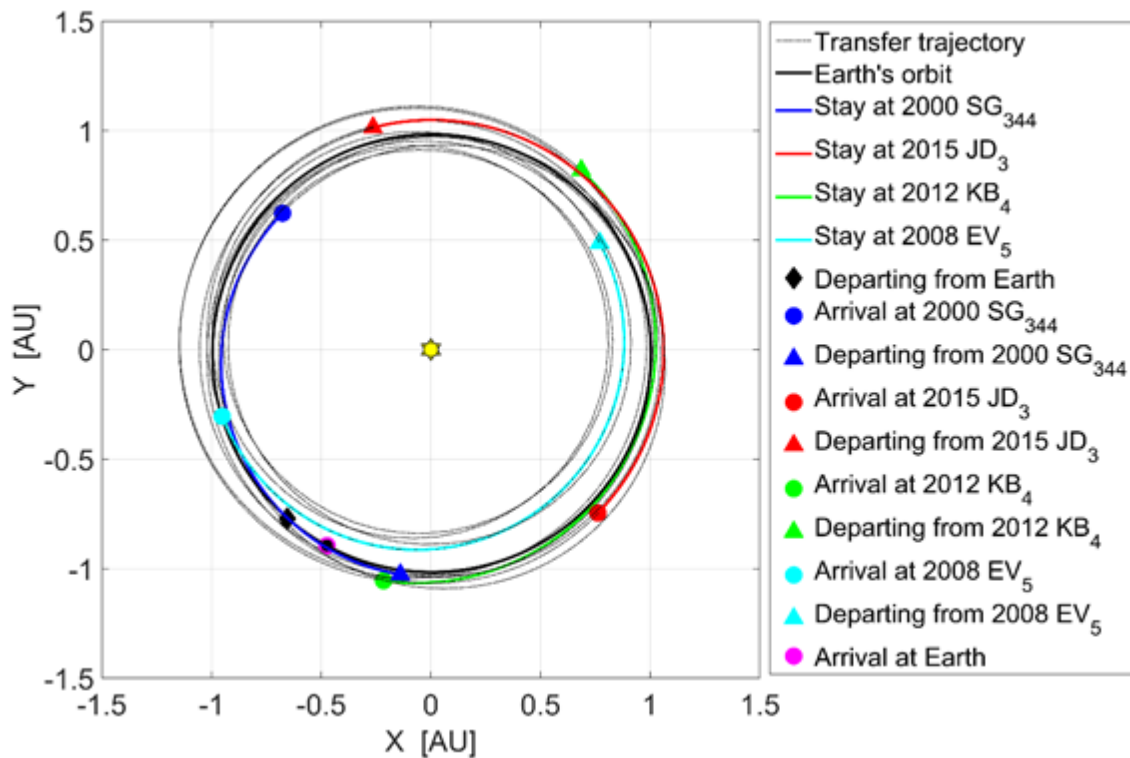
Figure 5 – Heliocentric view of the complete three-dimensional trajectory of the considered sequence.
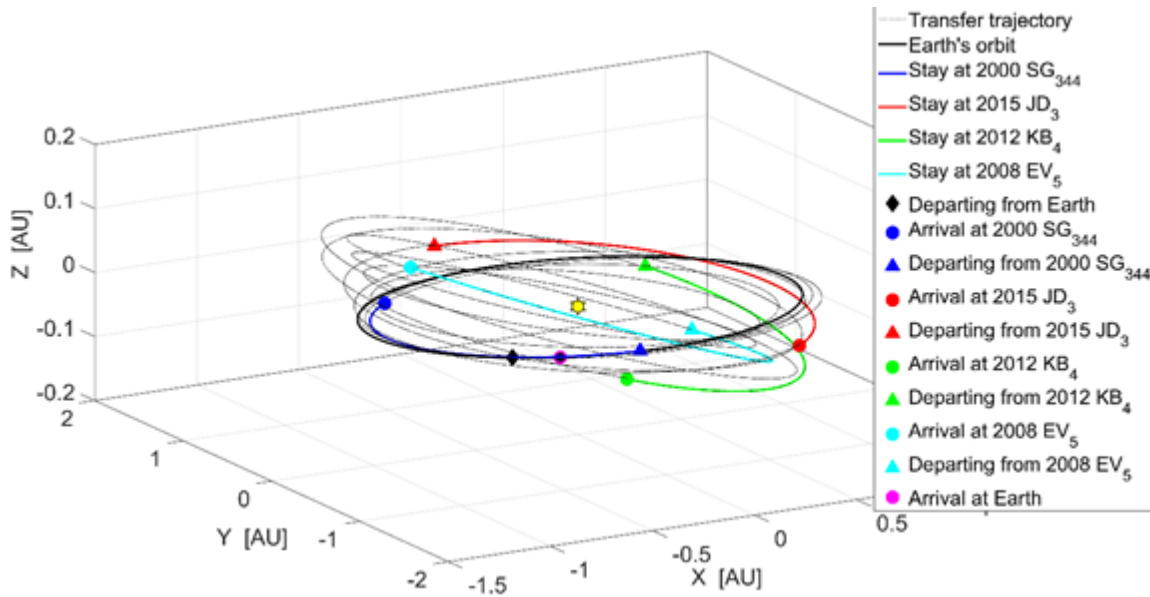

Figure 6 – Three-dimensional view of the complete three-dimensional trajectory of the considered sequence.

4. FLY FIVE – THE GOSSAMER PRINCIPLE OF SAILCRAFT DESIGN

The DLR GOSSAMER solar sail design is based on a crossed boom configuration with triangular sail segments made of a membrane manufactured from aluminized polyimide foil. A specifically designed combination of folding and coiling ensures that the deployed sail area can be held taut between the partly deployed booms.
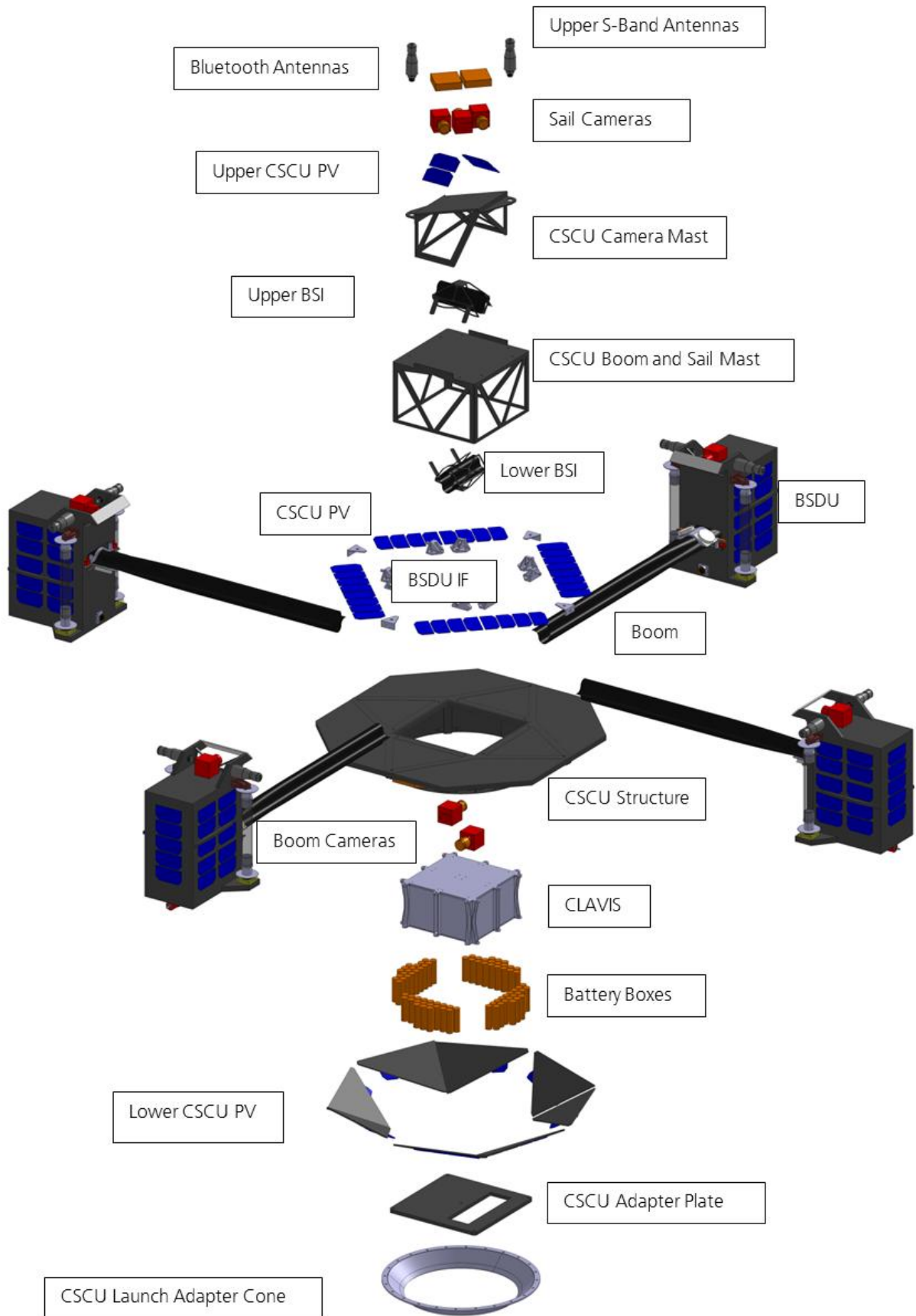
Figure 7 – GOSSAMER-1 PFM final design exploded view

A key design feature of the GOSSAMER solar sail is the Boom Sail Deployment Unit (BSDU) which is moving away from the Central Sailcraft Unit (CSCU) to uncoil the booms and unroll and unfold the sail segments. During deployment, four BSDUs synchronously move away from the central bus unit, each with two spools on which one half of either adjacent sail is stowed. (For a detailed discussion see [73] [74] [108] [120] [121] [122] and references therein.)
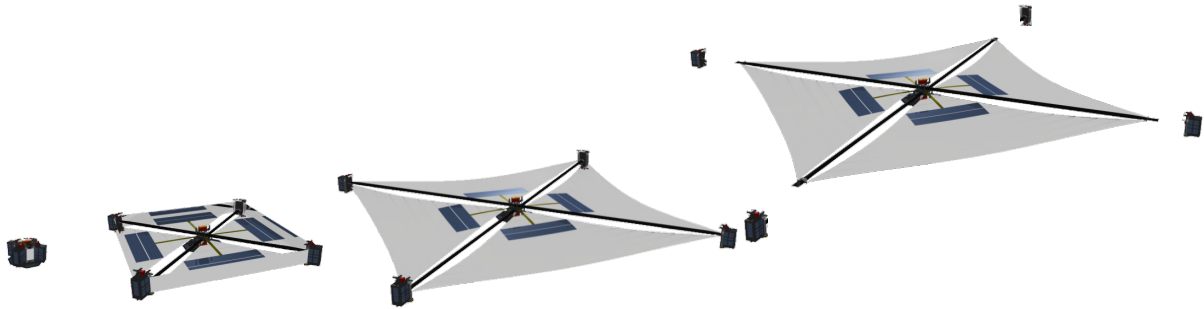

Figure 8 - GOSSAMER deployment sequence with BSDU separation

The BSDUs communicate through a wired interface while attached to the CSCU. After the connections are separated, the 5 sub-spacecraft communicate in a wireless network. The Umbilical connector and other harness technologies were jointly developed with the MASCOT project, the wireless communication concept and much of the BSDU electronics were re-used in the ROBEX project's Remote Unit.
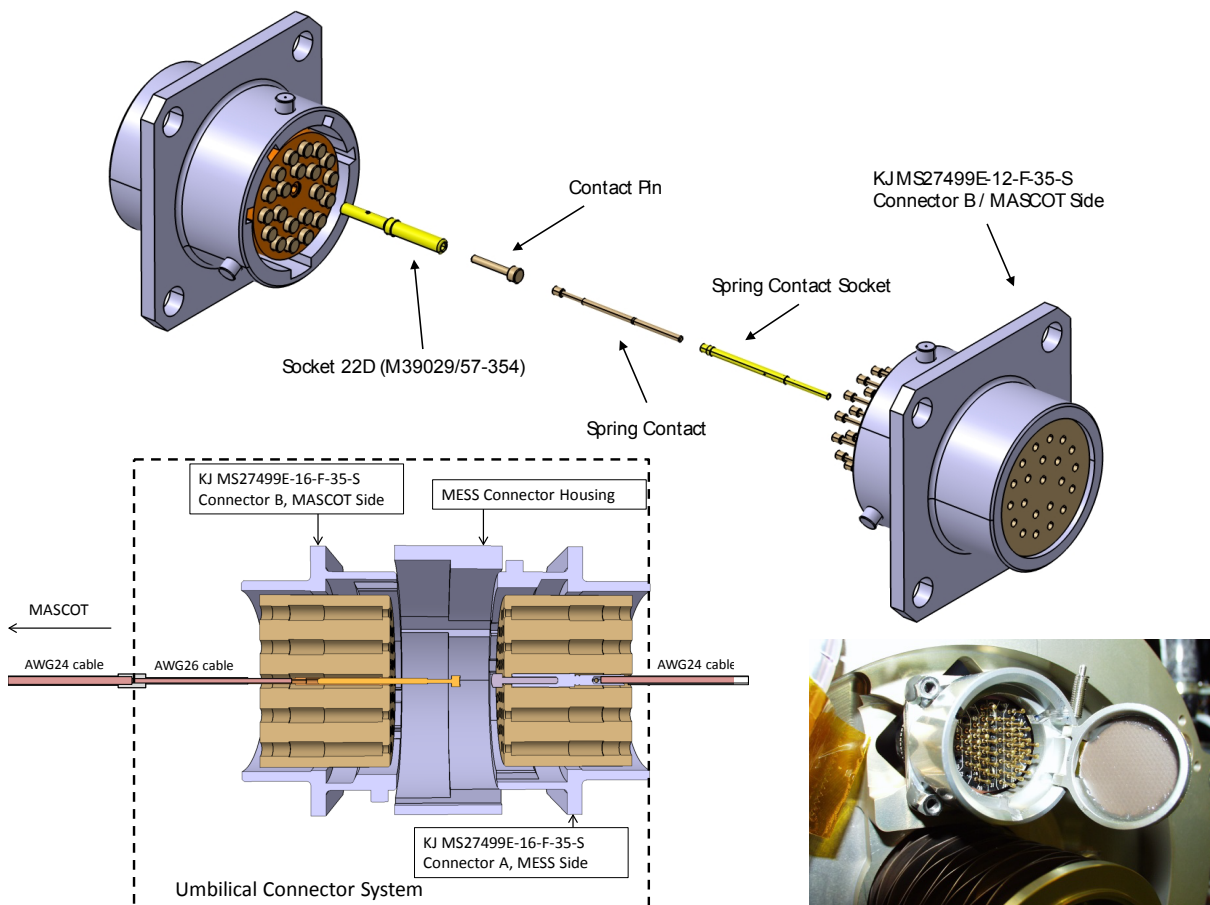

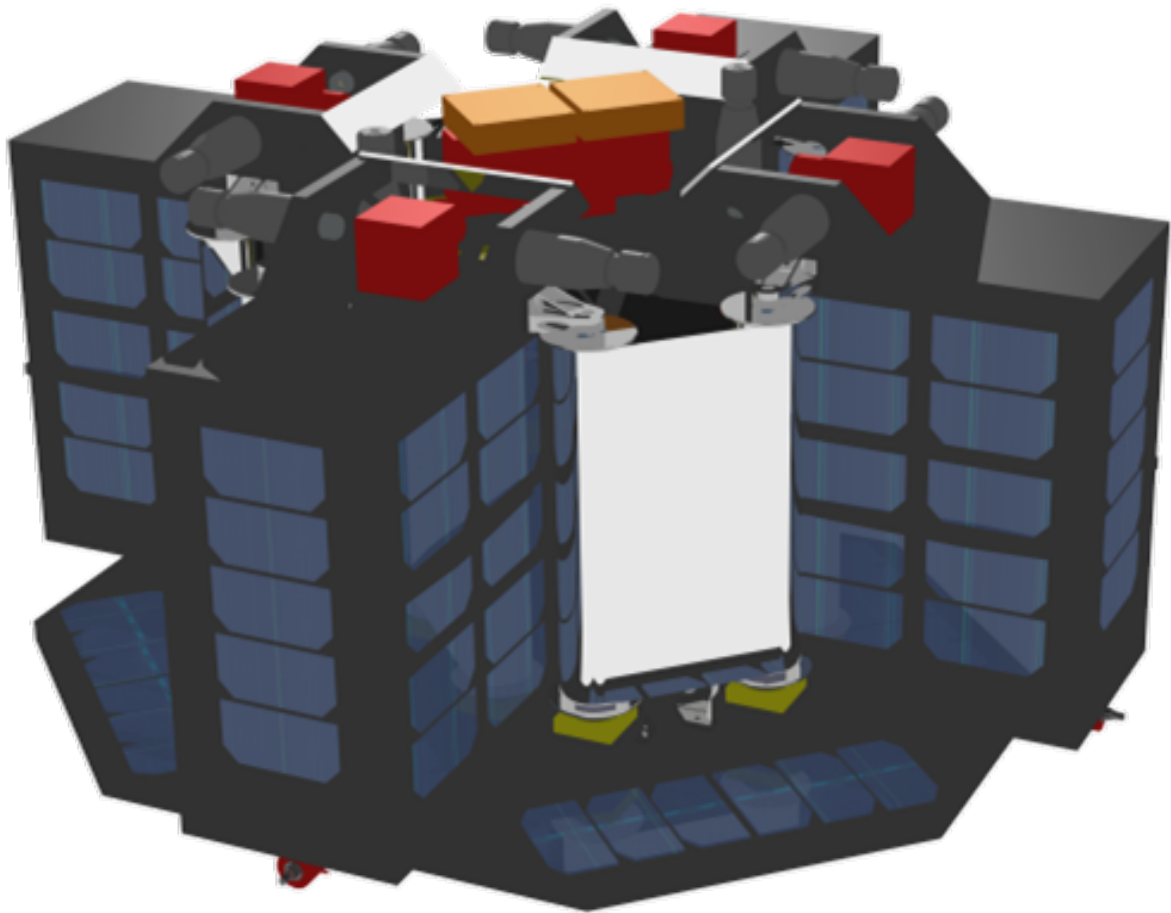Figure 9 – Umbilical connector: PHILAE and MASCOT heritage

Figure 10 – GOSSAMER-1 independent free-flyer design launch configuration (CAD view of final PFM design status)

4.1 *Un pour tous, tous pour un* – shared resources multi-sub-spacecraft design

The controlled GOSSAMER deployment concept [108] [123] requires synchronized operation of the four BSDUs moving away from the CSCU, and thus coordinated communication of all five elements. After separation of the BSDUs, a wireless network is used. [124] [125] [126] [127]

Before separation, communication is also possible via wired connection through umbilical connectors from each BSDU to the CSCU. This interface between sub-spacecraft also supports power transfer from each BSDU to the CSCU. Either sub-spacecraft can provide power to the other and receive power from it. At the same time, it is in control of its own energy budget through control of the switch in the Power Distribution (PD) unit which feeds power to the Charging Network (CN).
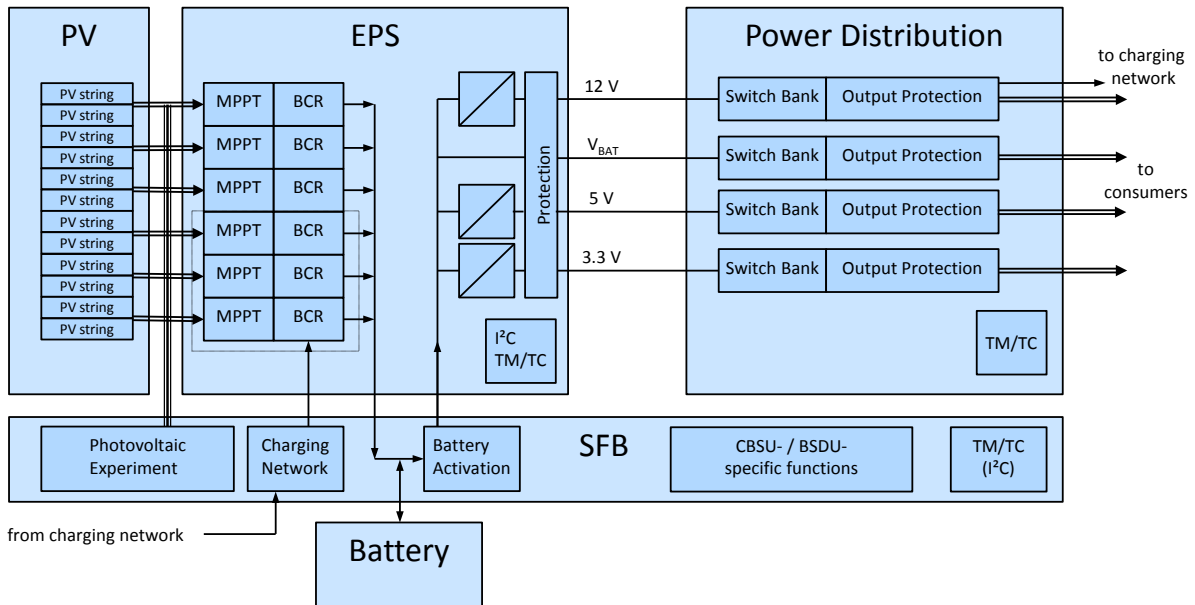
Figure 11 – GOSSAMER-1 common Electrical Power Subsystem (EPS) architecture of CSCU and BSDUs with Charging Network (CN) interfaces routed through Power Distribution (PD) units and a Special Functions Board (SFB) connecting to Photovoltaic arrays (PV) and the battery (Bat.)

The power receiving interface connects through a Special Function Board (SFB) to the same Battery Charge Regulator(s) (BCR) fed by the Photovoltaic (PV) arrays on the surface of each unit, similar to a maintenance charging connection from the Electrical Ground Support Equipment (EGSE) or the launch vehicle (LV). Each side of either interface is protected in a fail-safe manner, against energy loss and deep discharge of the feeding side's battery as well as against complete loss of energy flow.

The charging network effectively creates one spacecraft power subsystem from the energy generation, storage and distribution units of five self-sufficient spacecraft with their own complete and independent power subsystems and control units. This concept grew from the secondary passenger ("piggy-back") launch envisaged for GOSSAMER-1 with the QB50 project and the mission objectives assigned to it in the GOSSAMER Roadmap. For secondary passengers, a pre-determined separation attitude cannot always be provided. Note that in the Roadmap context, GOSSAMER-1 only had to demonstrate membrane deployment which does not require attitude control.
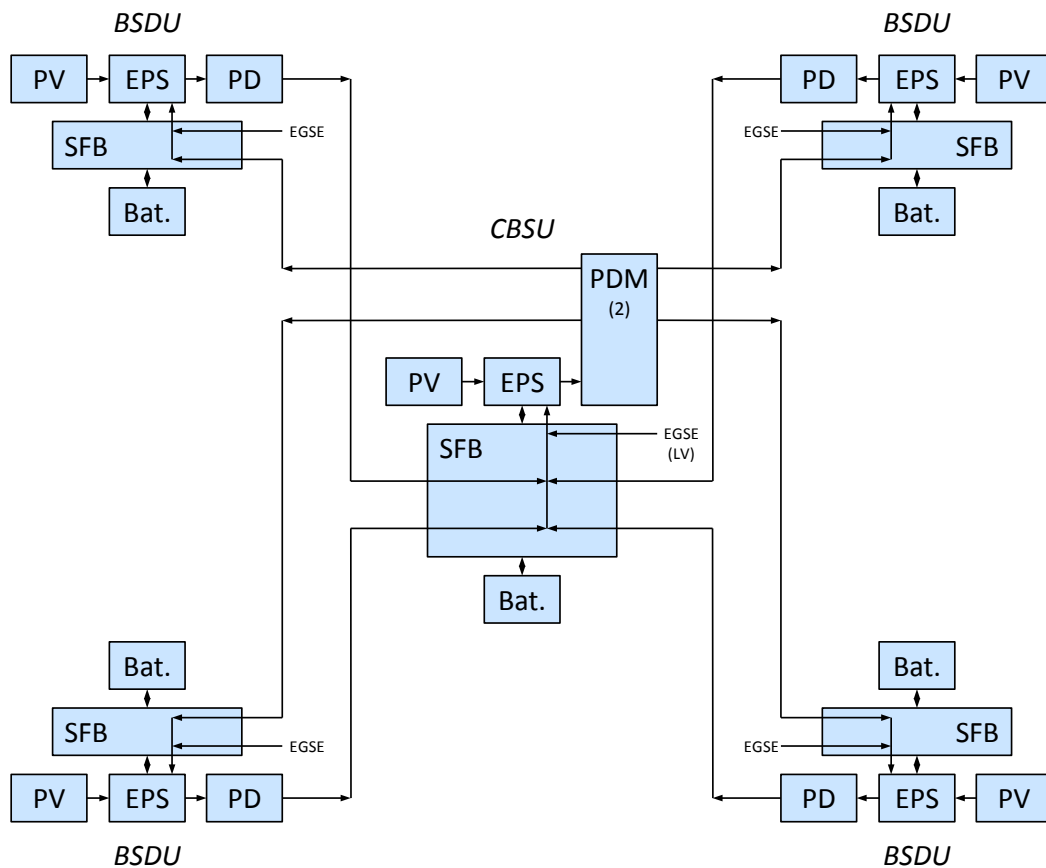
Figure 12 – GOSSAMER-1 Charging Network (CN) architecture with central Launch Vehicle (LV) interface, separate Electrical Ground Support Equipment (EGSE) interfaces to each unit

Thus, it was entirely possible that GOSSAMER-1 was deployed by the launcher such that e.g. only one BSDU is fully illuminated by the Sun. Even in this case, sufficient power supply for deployment could be achieved without the need to carry an excessively large and fully pre-charged battery.

4.2 Size Matters – Mission Design for a Realistic Near-Term Sail

The MNR mission scenario by Peloni et al. [71] is feasible using near-term solar sails with a characteristic acceleration of only a_c = 0.2 mm/s. In currently available technology such as introduced by GOSSAMER-1, this corresponds approximately to a (50 m)² sail, i.e. one of square shape and 50 m side length, carrying a science payload of approximately 20 kg, or a (70 m)² sail carrying about 60 kg. This science payload could be composed of heritage remote sensing instruments such as flown on conventional planetary science missions like ROSETTA or CASSINI.
However, the current state of small body science demands in-situ measurements for significant progress. Sailcraft, due to their huge size and inherent agility limits can not as easily land or even perform a touch & go like HAYABUSA on an asteroid. But applying recent technology and MASCOT-style integration concepts, a combination of approximately 10 kg 'orbiter' science payload and one or, respectively, five MASCOT landers of approximately 10 kg, each, appears feasible. By this combination, the gap between sail and soil can be closed, and the access frequency of asteroids to landers dramatically increased. Sail-based sample-return missions

have also been studied for many years, recently with focus on JAXA's Solar Power Sail with its PHILAE-sized lander. [128]
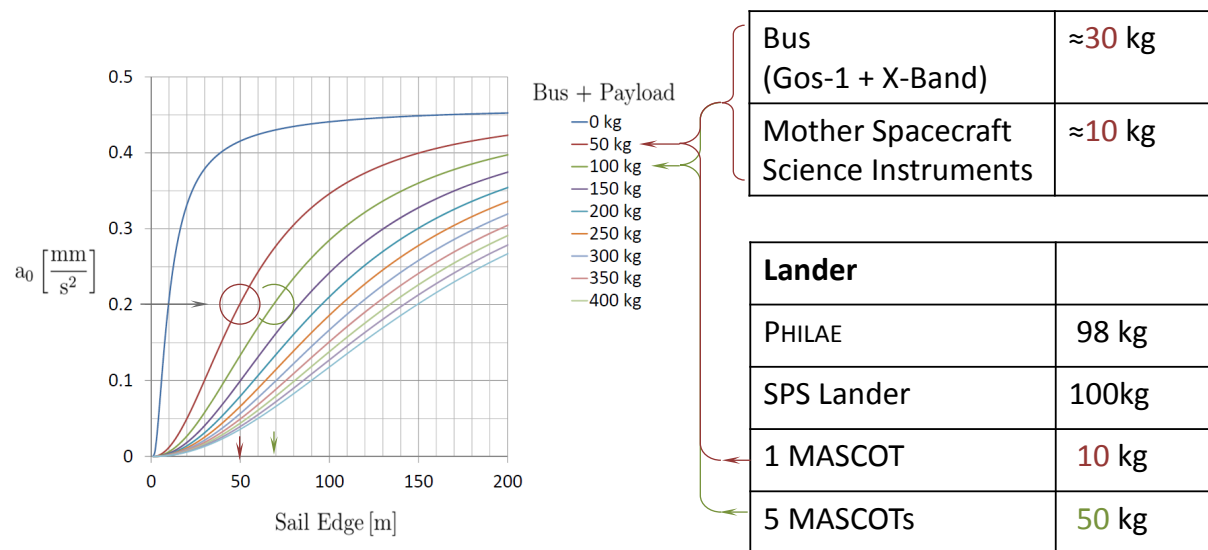

Bus (Gos-1 + X-Band)	≈30 kg
Mother Spacecraft Science Instruments	≈10 kg

Lander	
PHILAE	98 kg
SPS Lander	100kg
1 MASCOT	10 kg
5 MASCOTs	50 kg

Figure 13 – Payload performance of near-term solar sails based on GOSSAMER-1 technology [128] and approximate size at a_c = 0.2 mm/s² in relation to micro- and nanolander payloads for near-term missions. Note that a larger set of MASCOT-like nanolanders requires a dedicated carrier structure of approx. 10 kg while one nanolander can be accommodated on an existing structural panel.

4.3 Critical Technology Development for Membranes in Space

Solar sail membranes are mostly made of thin polyimide foils covered on one or both sides with metallic layers. Depending on mission scenario, the material is subjected to different kinds of harsh space environmental conditions. Obviously, the one which brings the most risk to any space mission is impact caused by particles of space debris or micro-meteorites. However, those events are not the only ones which can harm the sail or even cause the entire mission to fail. Near the Earth, and up to an altitude of about 800 km, the photo-dissociated oxygen atoms (ATOX) hit permanently the sail surface. Any foil defect made during folding and stowing of the sail material, e.g. a folding line, is a potential "hot-spot" for further sail-failures. A folding line, when permanently exposed to ATOX events together with UV/VUV-light, degrade by cracking and in consequence the sail membrane can tear in parts. Therefore, anti-crack propagation mechanisms present on the sail material are necessary in order to prevent such events [129].

Above 800 km the influence of the ATOX events is negligible compared to the magnitude of the charged particle flux such as electrons and protons. The energy spectrum of the particles varies from eV to MeV range [130]. The electrons can cause membrane material charging. Protons stuck within the foil can degrade the polyimide part of the foil by breaking its molecular bonds causing delamination of the metallic surface. Protons stuck within the metallic surface layer recombine with its electrons forming hydrogen atoms [131] [132] [133]. The atoms agglomerate into small hydrogen voids to ultimately form molecular hydrogen blisters on the foil surface [134] [135]. A foil exposed to a flux of 2.5 keV protons is shown in Figure 14. The material is 7.5 µm thick Upilex-S film covered on both sides with 100 nm

vacuum deposited Aluminum layers. The upper picture presents the spot area – the place where the protons hit the surface – in light gray color. The bottom picture shows an electron microscope picture of the spot. One can recognize a number of small blisters present on the surface.
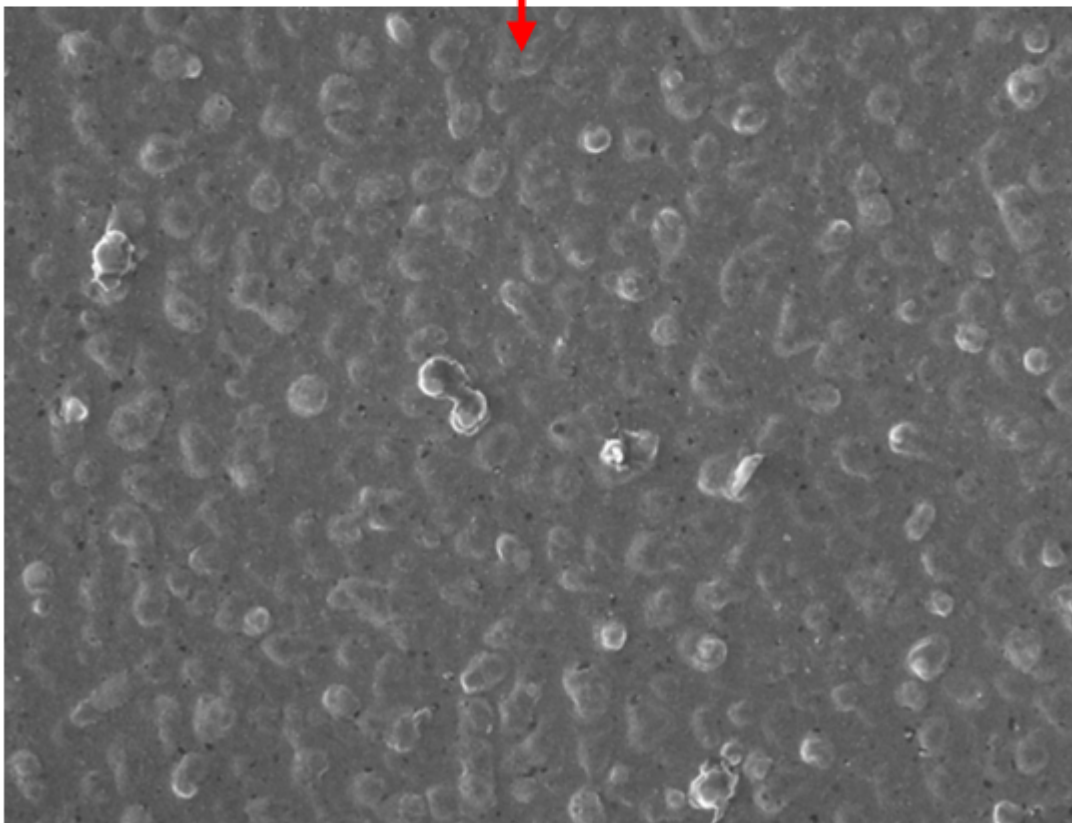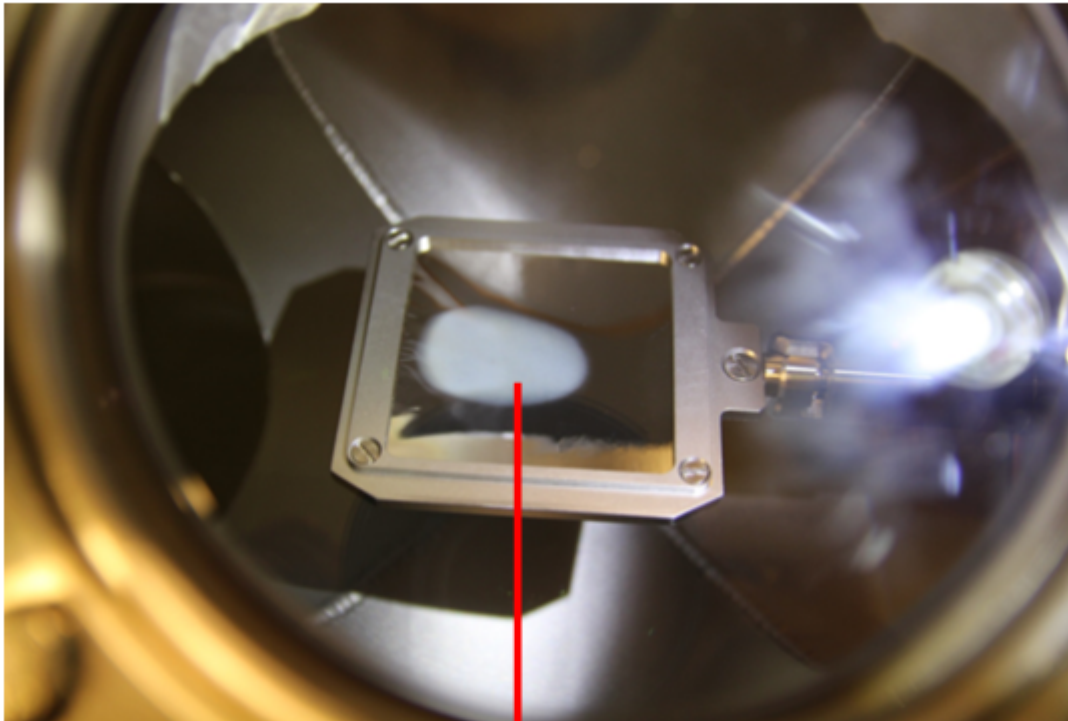
⊢— 3 µm —⊣

Figure 14 – Irradiated Spot area – light gray area (top) and electron microscope picture of the spot of the Aluminum surface (bottom)

All of the materials planned for space applications have to be evaluated for their behavior under particle and electromagnetic radiation [136] [137]. They can be examined in terrestrial laboratories under conditions which mimic those present at destination orbit of the sail. DLR in Bremen has a facility which can simulate such conditions. The Complex Irradiation Facility (CIF) was designed and commissioned with the aim to perform material investigations under simultaneous irradiation of both corpuscular and electromagnetic radiation. The complete facility has been built in Ultra High Vacuum (UHV) technology. The differential pumping system achieves a final pressure in the 10^{-10} mbar range.

The CIF is equipped with electron and proton linear accelerators. The kinetic energy of both species can be set separately within a range of 1 keV to 100 keV. The minimum achievable current is 1 nA while the maximum current is 100 µA. Also three electromagnetic sources are available: an argon VUV source, a deuterium lamp, and a Xenon lamp. All three working simultaneously cover wide wavelength range from 40 nm to 2150 nm [138]. The facility can examine not only thin solar-sail films but also solid or granular structures such as meteorite samples. The facility is presented in Figure 15.
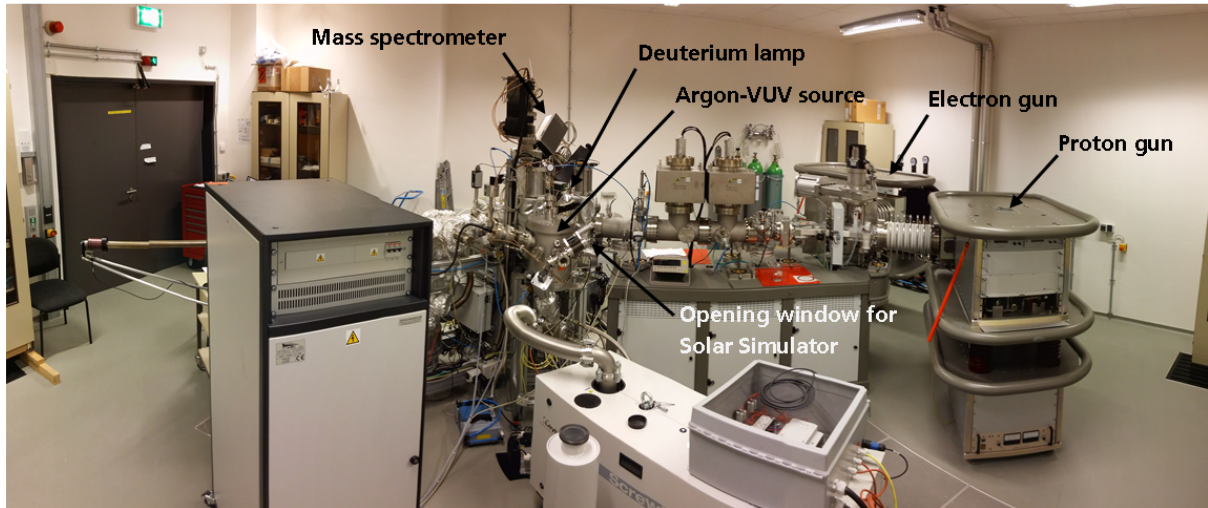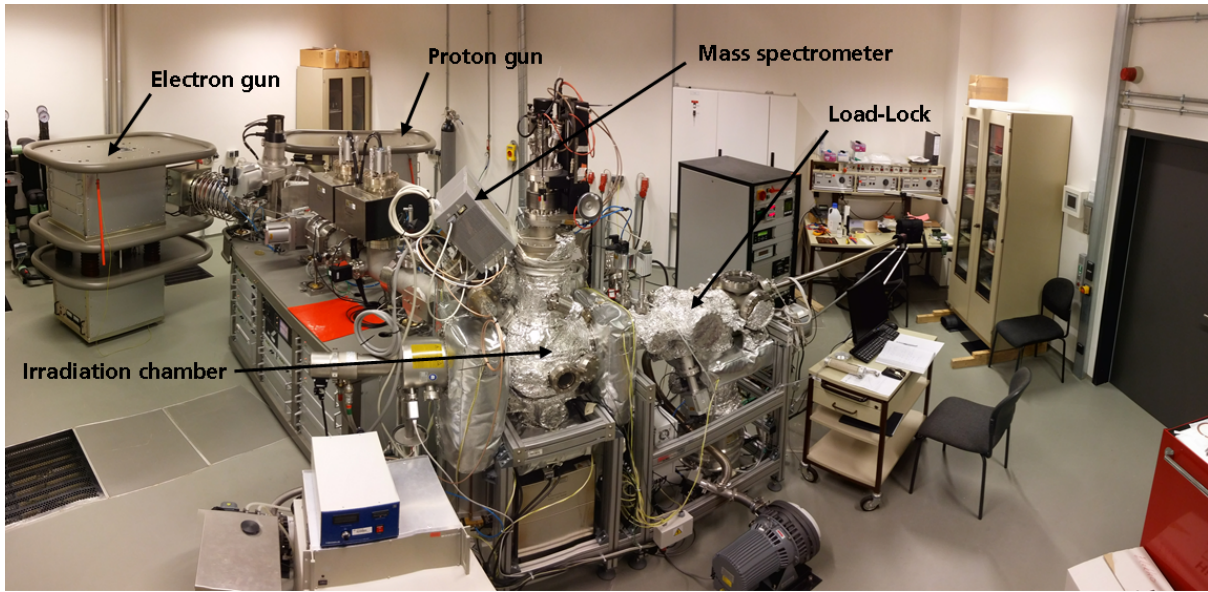
Figure 15 – The Complex Irradiation Facility at DLR Bremen

The work on membrane materials degradation properties and mitigation continues after the end of the GOSSAMER project for the deployable large-scale photovoltaics project, GOSOLAR. Both share the same technologies, materials and challenges in this respect, albeit with a different weighting.

The CIF is also suitable for the investigation of space weathering of natural materials. It can irradiate materials in UHV with a wide range of temperatures. From the sample's irradiated α/ε equilibrium temperature, they can be artificially heated by halogen lamps to 450°C or cooled down to the LN$_2$ level of -193°C. Low-energy corpuscular and high-energy electromagnetic radiation interacts at the immediate surface of regolith grains where the spectrum of reflected sunlight is formed which is used to infer asteroid composition from a distance. By irradiating suitable mineral or rock samples compatible with the UHV conditions inside the facility, the CIF can thus help to improve the connection between the spectral classification of asteroids performed by Earth-based telescopes and the inferred composition. The wide ranges of irradiation and thermal parameters that can be set and changed during an irradiation campaign enable space weathering experiments simulating different

heliocentric distances and other conditions at the surface of celestial bodies e.g. related to the day-night cycle. [139] [140]

5. UP AND AWAY – LAUNCHING A SMALL SPACECRAFT TO ESCAPE VELOCITY

Due to the stringent mass requirements of solar sailing and the need to deploy very large structures, anyway, the resulting spacecraft launch configuration can be very compact and lightweight. A typical MNR design would fit the current standard 'micro-payload' secondary passenger slots of launch vehicles flying to GTO or other high altitude orbits, e.g. ASAP on European or ESPA on U.S. launchers. From Navsat-MEO, GEO or other high and moderately eccentric orbits, the sail could comfortably depart from Earth under its own thrust. With the high frequency of GTO launches, a reliable and affordable access to Earth departure becomes available at the expense of a small propulsion module for substantial perigee-lifting for easy spiral-out from Earth orbit or direct escape from GTO to $c_3 > 0$ which offers the advantage of less time spent in the radiation belts.

5.1 Kickstart – small spacecraft on heavy launchers

Dedicated launches would be an option in the case of missions requiring an extremely high c_3 and/or reduced flight time to target. Based on the current performance of Ariane 5 ECA [141], the performance for a maximum velocity escape trajectory has been calculated. For a dedicated launch, unnecessary standard equipment units such as the double launch adapter Sylda are removed. The performance for different c_3 values and an inclination of 6°, in case of launches from the Kourou spaceport are plotted in Figure 16. Payloads of 500 kg, 250 kg, and 50 kg, respectively, can be injected on escape trajectories with a c_3 of up to approximately 56 km²/s², 60 km²/s², and 64 km²/s².
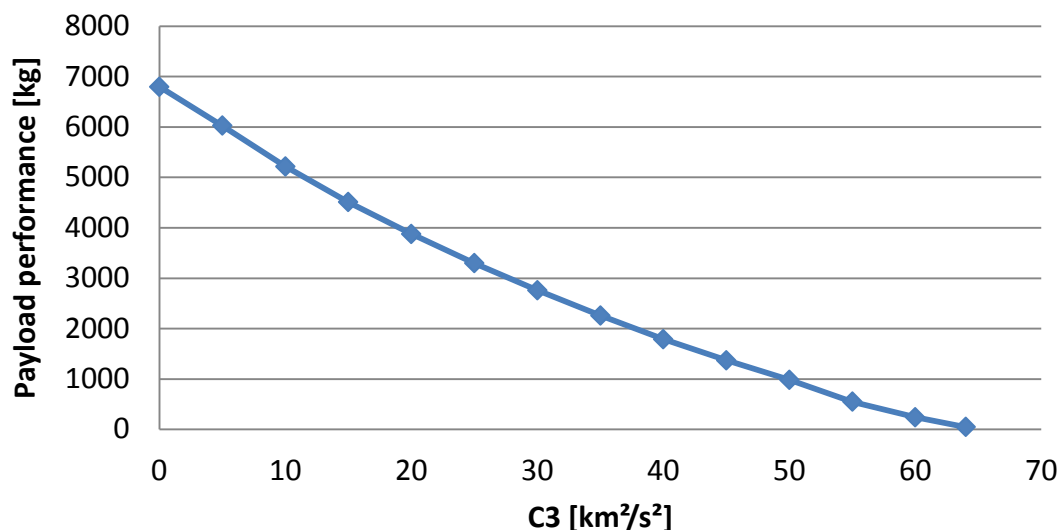

Figure 16 – Payload performance of Ariane 5 ECA for different C_3 values and an inclination of 6°

The payload masses of 500 kg, 250 kg, and 50 kg, respectively, correspond approximately to a dual MNR launch (or a NEW HORIZONS or HAYABUSA2 reflight), a single MNR launch (or a DEEP IMPACT Bus reflight), and a minimum sailcraft e.g. similar to NEAscout [83] or ACS3-based solar sails [88] (or a MASCOT-style high-density design chemical propulsion flyby spacecraft) with minimum deep space communication equipment added.

It is noteworthy that even this entirely unoptimized configuration based on off-the-shelf launcher hardware, when combined with a 'small' payload, achieves a performance level comparable to that of the hyper-giant launch vehicles which were thought to be required for entry-level planetary exploration beyond one-way missions to Venus or Mars, prior to the discovery of gravity-assist trajectories. [25] And that this discovery in turn fostered the advanced technologies making this scenario possible today.

The addition of further small upper stages as part of the standard launch vehicle's payload such as the off-the-shelf Star-37 or Star-48 solid rocket motors used for PIONEER-10 and 11 (258 kg) and NEW HORIZONS (478 kg), respectively, can further increase c_3 performance. However, solid rocket motors are less accurate than liquid propulsion stages. Recently, LISA Pathfinder (LPF, 480 kg) was kicked from a low Earth parking orbit of 200 x 1600 km to its Lissajous orbit around the Sun-Earth Lagrange point L_1 by a liquid-fuelled Propulsion Module (LPF PRM, 1420 kg wet). [142]

6. LANDERS

It is assumed that landers are separated from the carrying sailcraft like MASCOT from HAYABUSA2, by a pre-set spring force. [34] [98] [143] The solar sail trajectory is modified such for lander separation that the initial state vector relative to the asteroid ensures that the separated lander hits its mark, similar to MASCOT2 and AIM. [106] The sail may be in very slow fly-by, or in a stable solar-radiation-pressure displaced orbit or station-keeping. [144] [145] [146]

6.1 Close-in Sailcraft Operation

While reasonably stable orbits of and station-keeping near asteroids appears generally feasible, [144] [145] [146] genuine proximity operations with a solar sail close to a real asteroid likely pose significant challenges. Any such manoeuvres depend critically on the efficiency and agility and glitch if not failure tolerance of sail attitude control methods and mechanisms which are yet to be proven in flight. Should in practice only gross motor skills be feasible within the lightweight design requirements of solar sailing or if the control methods were found to be physically challenged, it may be best to have a self-propelled spacecraft attached to a solar sail for cruise flight between targets. At the asteroid, the sail would be parked at a safe distance and detach the self-propelled spacecraft for all proximity operations. The JAXA Solar Power Sail also follows this concept as it is based on a spinning sail-like photovoltaic membrane design. In this case, however, the rendezvous and re-docking after the proximity operations introduce additional challenges but could also build on experience from space station operations as well as small spacecraft dockings [147] [148] [149] [150]. Another solution would be to un-deploy the solar

sail, but it remains to be seen how (un)realistic this is even in terms of the most basic feasibility.

6.2 Deployment Conditions and Constraints for Sail-Deployed Ballistic Landers

Though the deployment of landers to asteroid surfaces poses many challenges, it should be first noted that it is orders of magnitude easier than lander deployment to any large planetary body in terms of obstacles to overcome. It is specifically this relative ease that makes their inclusion on a small-body bound spacecraft a real advantage to the mission. However, most asteroid or comet landers are designed to operate on a specific body, whose size and mass is known to some degree before the mission hardware is built. A specifically optimized design allows tuning of the deployment mechanism and strategy prior to the mission, identifying the best strategy to deploy one given lander to one (or several) given asteroid(s).

A most notable exception is PHILAE, which was designed to land on a broad range of comets – fortunately, as it turned out: a launch delay forced a change of target from 46P/Wirtanen to 67P/Churyumov-Gerasimenko.

The strength of a MNR sailcraft lies on the genericity of its design and the possibility to alter course as desired. Therefore, the task at hand is to design a strategy allowing the deployment of a lander to *any* asteroid.

The two main challenges resting on the deployment of a lander to a small body are:
1) guarantee that the lander reaches the surface.
2) guarantee that the lander remains at the surface.

Note that there is an absolute and a gradual element in either challenge.

For the first challenge, the location at which the surface is reached can be important as well as the time it takes to get there. For example, communication between lander and sailcraft is temporarily lost at the most critical phase if contact with the surface is first achieved only on the far side of the target asteroid e.g. out of a near-parabolic trajectory. Also, if the lander reaches the surface out of a bound but unstable orbit, the duration required for natural disturbances to perturb the orbit into a surface intercept may be a significant fraction of the duration of the rendezvous of the MNR sailcraft with the asteroid.

For the second challenge, similarly the distance covered while bouncing to dissipate the residual kinetic energy and the duration required to reach an at-rest state may be of importance, beyond its ultimate achievement. Long bouncing, although usually a random walk, may also lead the lander to the far side of the target asteroid.

6.2.1 1st Challenge: Guarantee that the lander reaches the surface

Two strategies can be adopted: passive or active descent.

With a ballistic descent, the lander does not control its trajectory. Simply put, the lander must be thrown at the surface on release. The direction on which to deploy the lander depends on the characteristics of the dynamical system and on the trajectory of the spacecraft itself. All small-body landing packages have been on ballistic descents from MINERVA (aboard HAYABUSA) to PHILAE, to the next generation of asteroid landers aboard HAYABUSA2 (the MINERVAs and MASCOT).

A controlled descent means the landers controls, at least in part, its descent after release. This descent requires the lander to have actuators (e.g. thrusters) as well as sensors (e.g. vision) and a GNC system, essentially making it a small spacecraft. Landing spacecraft, like HAYABUSA or OSIRIS-REx, use controlled descent.

6.2.2 2nd Challenge: Guarantee that the lander remains on the surface

Here again, passive or active options are possible.

The problem of remaining on the surface is that the lander is generally deployed in an energy state where it could, should it not find the ground, escape the asteroid system to infinity. [151] [152] It is also possible that the lander is initially deployed with less energy than needed to escape but, because it impacts on a rotating surface, it gains at impact the energy necessary to escape. [153] A passive lander will therefore try to minimize its energy at deployment, keeping it as low as possible and hoping that the first impact [154] will dissipate enough energy to guarantee a bound state with respect to the asteroid. Passive damping mechanisms (e.g. crushable surfaces) are also possible. An example of a passive lander is MASCOT. Note that this strategy will generally be poor at guaranteeing a definite landing zone since no matter how accurate the first impact is, the subsequent bounces will create a highly randomized trajectory, potentially yielding wide landing zones. However, MASCOT-like landers can later relocate to the preferred operation location, as was planned for MASCOT2 on AIM.

The effective coefficient of restitution (CoR), the ratio of the norms of velocities before and after impact, is dependent on the lander design and the local properties of the asteroid surface at the point of impact. The worst case is a rigid surface with a CoR close to 1 (ideally elastic), e.g. a bare large boulder, on which the combined effective CoR becomes that of the lander structure or landing gear. The structural CoR of MASCOT is approximately 0.6. [155] PHILAE and the surface of 67P combined achieved a CoR of approximately 0.3 at the first vertical-touch-down with damping element activation. All later bounces had no damping unit involvement and achieved about 0.7, presumably of some elastic structural element like the magnetometer boom with a brittle comet surface material. [12] During the bouncing phase, energy is also exchanged with the rotation of the lander. Grazing contact with friction can remove energy out of the linear motion or the rotation, also without much affecting the respective other. Asymmetric contact, e.g. with only 1 or 2 of 3 landing gear feet, will induce rotation at the expense of linear velocity, reducing the effective CoR beyond structural response which can be highly elastic, particularly at right angles to the expected direction of motion or damper action. Conversely, in the extreme, an effective CoR >1 can appear when a fast rotation is heavily slowed down in a way that transfers the rotational energy into linear motion. (also cf. [156] [157] [158] [159])

Conversely an active strategy would be for the lander to anchor itself to the ground as soon as it impacts. An example of active lander was PHILAE's design: it would anchor itself to the ground with two harpoons, it would activate downward thrusters and it would screw its feet to the ground. This strategy reduces the landing ellipse to the first impact ellipse. But, the lander then requires some GNC capability with associated actuators and sensors, thus adding complexity, mass and cost.

6.2.3 Possible strategies

Considering the two options of each problem, only three types of landers appear sensible:
1) The passive lander, e.g. MASCOT or MINERVA. The lander travels on a ballistic arc to the surface and dissipates its energy by bouncing on the ground.
2) The anchoring lander, e.g. PHILAE. The lander travels on a ballistic arc to the surface but it is able to anchor itself to the ground immediately at first impact. [160] [161]
3) The controlled lander, e.g. the JAXA Solar Power Sail Lander or the MMX spacecraft. The lander controls its descent to the surface with thrusters and remains on the ground after a very soft touchdown, possibly anchoring itself to guarantee stability.

Generally speaking, a passive lander is the least onerous option but is also limited in its allowed range of asteroids. A controlled lander can go anywhere but is conversely a much more expensive option. We define here 3 broad strategies by which each type of lander can reach its trajectory:
1) the ballistic low-energy trajectory, fitting best the passive lander on a slowly rotating asteroid. The lander is deployed on an elliptic arc, or any other low energy trajectory, that impacts the asteroid surface. The nominal deployment can be optimized to minimize the energy at impact [153] [152].
2) the ballistic high energy trajectory, fitting best the anchoring lander. The lander is deployed on a high speed (1 m/s or above). The nominal trajectory aims directly at center of the small body. Upon this high velocity impact, the lander anchors itself immediately. A passive lander would bounce and likely fail to remain bound to the asteroid with such a strategy unless the combined CoR of lander and surface is very low.
3) the controlled descent, that only fits the controlled lander as it is the only one with the means of achieving a controlled descent. A controlled descent could start as any of the two previous trajectories.

6.2.4 Constraints on the deployment

To be employed, these strategies add constraints to the deployment. Although the controlled descent can theoretically adapt to any situation (since the lander controls its trajectory), the two ballistic trajectories need the mothership sailcraft to guarantee impact with the surface. Previous analyses show that the main factor weighing on this capability is the accuracy of the deployment velocity [162]. The deployment velocity is the combination of the velocity imparted to the lander by the deployment mechanism (with respect to the spacecraft) and the velocity of the spacecraft (with respect to the asteroid center of mass). Uncertainty on the former stems from the deployment mechanism imperfection (e.g. spring elasticity uncertainty, thermal variations, collision at release with bounding box). Uncertainty on the latter stems from the spacecraft GNC system.

Considering this combined error, noted ΔV, as a parameter, the two strategies (ballistic high-energy and ballistic low-energy) can be tested for their feasibility. We can indeed define ΔV threshold accuracies that render each of them unfeasible.

The low-energy ballistic trajectory must at least be able to deploy the lander such that the periapse remains below the radius R of the asteroid. Denoting the asteroid density ρ and the height of deployment h, we can then compute this maximum allowable ΔV as:

$$\Delta V_{low} = \sqrt{\frac{8}{3}\pi G\rho \frac{R^4}{(R+h)(2R+h)}}$$

For the high-energy ballistic trajectory, one can obtain a very simple worst-case first approximation by neglecting the effects of gravity on such a trajectory – which is valid for the smallest targets. Denoting V as the nominal deployment speed, aimed directly at the center of the asteroid, the maximum allowable ΔV guaranteeing not to miss the small body is:

$$\Delta V_{high} = \frac{R}{R+h}V$$

In general, it should be expected that h will be the minimum value guaranteeing the safety of the spacecraft. Previous missions, like HAYABUSA and HAYABUSA2, as well as concept missions, have rarely considered less than 50 m for deployments. In the case of a solar sail or large dimensions, 100 m seems like a prudent minimal value. Larger values, such as 300 to 1000 m, seem more likely in the context of a surveyor spacecraft whose missions requires survival over many asteroid encounters. This value is also dependent on the radius of the targeted body: 100 m altitude does not carry the same risks above a 1 m rock than above a 1 km body.

For the low-energy ballistic trajectory, the density ρ of the asteroid is an essential parameter. Past missions have shown that small solar system bodies can exhibit rubble pile structures of very high porosity. This density parameter would likely be between 1 to 3 g/cm³ for NEOs. Note however that lower values have been observed on comets (e.g. 67P by ROSETTA, slightly lower than 0.5 g/cm³) and higher values on main-belt asteroids (e.g. Lutetia by ROSETTA, around 3.4 g/cm³), and it is not unlikely that still higher density objects exist up to the density of pure non-porous NiFe, approximately 8 g/cm³.

For the high-energy ballistic trajectory, since, for smaller targets, the increase in speed due to gravity is negligible, one can assume the deployment speed equals the impact speed. It can be assumed that impacts up to 2 m/s pose little risk to the payload of the lander, especially as the lander is equipped with a damping landing gear. For instance, PHILAE impacted slightly over 1 m/s. Future technological developments in landing gears could also increase this value.

We have plotted on Figure 17 the ΔV thresholds of each trajectory, each for three likely values of their main parameter, respectively asteroid density and deployment velocity, assuming deployment occurs at a fixed altitude of 500 m. As one decreases the asteroid diameter, the challenge increases and forces the mission designer to consider an anchoring lander rather than a passive lander, and even a controlled lander rather than an anchoring lander. Conversely any development that improves the accuracy on velocity extends the realm of use of an anchoring lander or of a passive lander. Note that this analysis does not include the effects of rotation, which can be very important to consider [153]: all but the largest fast rotators would be

impossible targets for a passive lander. It appears that there is a threshold size of about 200 m diameter above which almost all objects are slow rotators whereas smaller objects are mostly fast rotators, probably related to the internal cohesion of the asteroid. [163] [164] It may be inferred that larger objects are nearly cohesion-less rubble piles while smaller objects may also be in some way monolithic. This natural size threshold is slightly above the 140 m minimum diameter defined as one criterion for PHA status. Thus, a velocity accuracy of about 1 cm/s is required for a passive landers which can be sent to any such object.
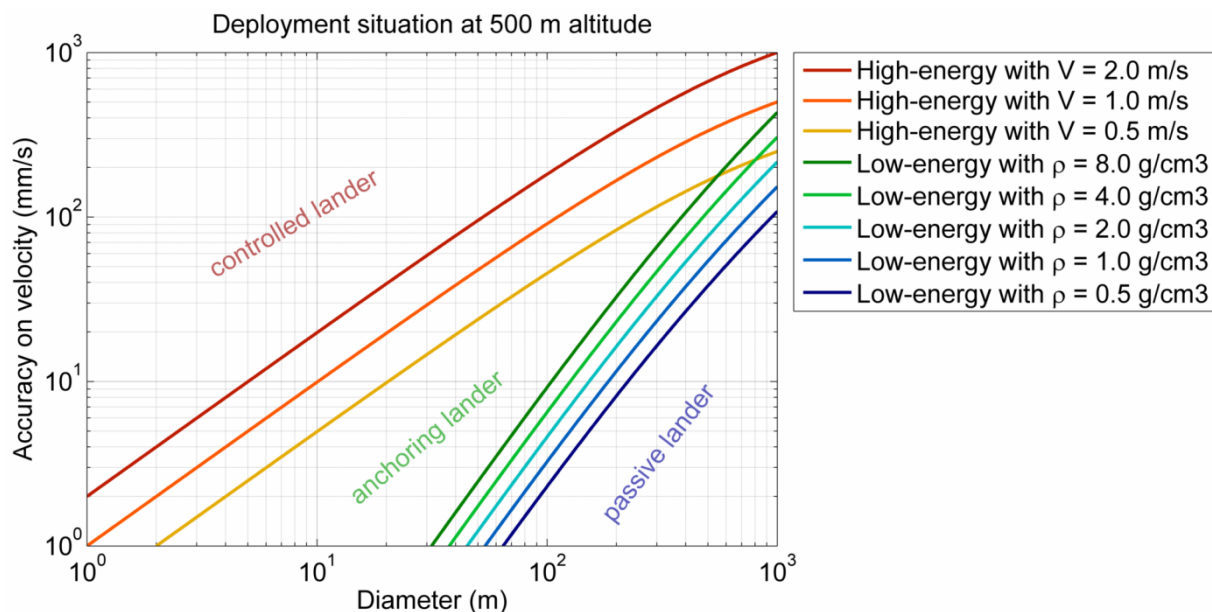

Figure 17 – Accuracy requirements on the delivery velocity of ballistic landers delineating the regions of feasibility for passive, anchoring (semi-active), and fully controlled (active) landers.

Separation velocities and accuracies of the orders of magnitude covered in Figure 17 have been achieved in small solar system body missions. However, it should be noted that a spacecraft does not have a single "score" on its accuracy. The performance of the carrier spacecraft's GNC reflected in numbers like the accuracy on velocity shown in Figure 17 are very situation dependent. Depending on where the spacecraft was and what it was doing, the numbers can vary widely. Moreover, there is a difference between the known velocity a posteriori, the known velocity in real-time e.g. as observable in live telemetry based analysis, and the real-time velocity as used on board in a closed-loop guidance function. Comparatively, the deployment mechanism accuracy is easier to ascertain because it doesn't depend on the situation or the performance or design of the software.

6.2.5 Technological developments

It should be noted from Figure 17 that the high-energy ballistic trajectory seems feasible for almost any asteroid if the initial velocity (hence close to touchdown velocity) is 1 m/s. As the anchoring lander can provide much more capability over a passive lander, notably the capability to handle fast rotators, it could be relevant to focus on the technological gaps remaining for the development of such a lander. Notably, one will note the need to devise anchoring devices with both high reliability

and adaptability to any asteroid terrain (i.e. soft regolith or hard rocky surfaces) as well as the actuators, sensors and flight software able to adjust attitude and detect impact.

The calculations summed up on Figure 17 are only applicable or useful for the smaller targets, less than 1 km in diameter. Beyond this size, the body presents, at this altitude, a strong enough gravity field and a large enough surface: bringing a lander to the surface is not as challenging. But, in the case of a large asteroid, one may wish to direct a lander to a precise landing zone comparable in size to the smaller targets presented in Figure 17, which would then show very similar curves. Moreover, one would probably find that 500 m is too low an altitude and would deploy from much farther away, once again recreating similar curves. In addition, fast rotators, regardless of their mass, would still present the issue of remaining on the surface which would make them very hard targets for passive landers, forcing them to land and stay at the poles. In any case, the situation remains that larger (and slowly spinning) asteroids and higher GNC accuracy allow for lightweight passive lander, while more challenging bodies or coarser GNC will require a more capable lander. The development of a fully automated lander would allow to land anywhere with very few impositions on the spacecraft GNC. Conversely, developing better GNC and release mechanisms would to enable passive or anchoring landers to be used on a wider range of targets.

At the other end of the asteroid size scale, it is obvious that any database of asteroids will be dominated by the smallest objects the NEA surveys are capable of detecting with some measure of efficiency. Their sheer number outruns the reduction of discovery efficiency towards smaller sized objects until the detection range becomes so small that the volume covered by the survey instrument shrinks so much that it becomes the dominant factor in discovery rate. [165] The database and algorithms used in [71] [72] do not apply any filter on asteroid properties other than those a priori applied by the NHATS, LCDB and PHA catalogues. So it may appear at first glance that MNR trajectory searches turn up mostly sequences composed of small objects not suited for passive landers like MASCOT. Still, even without filtering or rating sequences by their targets, MNR sequences do appear which contain multiple objects that should be easily accessible for MASCOT-like landers. For example, the sequence Earth – 2003 WT_{153} – (65679) 1989 UQ – (401954) 2002 RW_{25} discussed in [72] contains two large, almost km-sized PHAs most likely well suitable for MASCOT-like landers, after a very small first target which could be of interest to ARRM-like missions [119]. The total ΔV for this sequence of only 3 targets is 52.1 km/s which is considered not feasible with current or near-tern high-performing electric-propulsion technology [72]. The sequence Earth – 2011 CG_2 – 2004 VJ_1 – 2005 TG_{50} – 2015 JF_{11} also discussed in [72] contains two relatively large objects most likely suitable for MASCOT-like landers, and two moderately small targets.

6.2.6 Head-on Sailcraft Operation – Kinetic Impactor Delivery

Beyond rendezvous operations for science, exploration, characterization and prospection, a detachable self-propelled spacecraft would also be a necessary development for a sail-delivered kinetic impactor since extreme agility is required to hit a threatening asteroid, most likely smaller than 200 m diameter, at relative velocities likely to exceed 50 km/s. It is unlikely that the required combination of

timely precision and agility can be achieved in the foreseeable future with a hoisted solar sail. However, the most extreme relative velocities possible within the solar system can *only* be achieved by solar sail. It has been demonstrated by Dachwald et al. [113] [114] [115] that a kinetic impactor payload can be delivered by solar sail with realistic performance (a_c = 0.5 mm/s²) to a head-on orbit with a relative velocity exceeding 80 km/s relative to the incoming asteroid if the perihelion is sufficiently interior to Earth's orbit. This puts an entirely small spacecraft based approach towards asteroid mitigation within reach (cf. [166]).

6.4 MASCOT – the Mobile AsteroidSurface Scout

DLR in collaboration with the French space agency, CNES, has developed the Mobile Asteroid Surface Scout, MASCOT, a small asteroid lander which packs four full-scale science instruments (Figure 18) and relocation capability into a shoebox-sized 10 kg spacecraft. [34] [98] [143] It carries the near-IR soil microscope, MicrOmega (MMEGA), [167] a high dynamic range black-and-white camera with night-time multicolour illumination (MasCAM), [168] a 6-channel thermal IR radiometer (MARA), [169] and a fluxgate magnetometer (MasMAG). [170]

MMEGA is a near-infrared imaging spectrometer/microscope for the study of mineralogy and composition at grain scale. During operations the instrument optical head touches the asteroid surface. MMEGA acquires 3D (x,y,λ) microscopic image-cubes of an area approximately (3 mm)² in size with a spatial sampling of 25 μm² in 128² px images. For each pixel, the spectrum is acquired in contiguous spectral channels covering the range 0.99 to 3.55 μm. The spectral range is chosen as to include diagnostic features of most potential constituents of the surface: minerals, both pristine and altered, in particular by water; frosts and ices; organics. The spectral sampling is better than 40 cm^{-1} typically with a signal-to-noise ratio of 100, over the entire spectral range. Image-cubes are built by illuminating the samples with monochromatic light, using an AOTF-based dispersive system. Images are acquired onto a 2D HgCdTe array, cooled by a dedicated cryocooler. Measurements are performed both during day and night, at least one, each, per location. [167]

MasCAM uses a clear filter 1 Mpixel Si-CMOS sensor with high dynamic range imaging capability covering a (60°)² field of view, pointed slightly down to image an area in front of the lander. Multiple observations during the day are used for detailed studies of the reflection and scattering properties of the surface. During daytime, images are black-and-white. At night, colour images are taken using 4-channel IR-RGB LED illumination. [168]

MARA is a 6-band multispectral thermal infrared radiometer, covering wavelengths from 5 to 100 μm. In addition to a clear filter, the remaining channels are narrow-band filtered and can be adapted to a thermal infrared instrument aboard the orbiter such as TIR aboard HAYABUSA2. Observations over at least one complete rotation of the asteroid are used to determine thermal inertia of the landing site.

MasMAG is a vector compensated three-axis fluxgate magnetometer consisting of a digital electronics board and a sensor head developed at the Institute for Geophysics and Extraterrestrial Physics (IGeP) of the Technical University of Braunschweig (TUBS). It has a long heritage at IGeP from previous space missions such as THEMIS, VENUS EXPRESS, ROSETTA, EQUATOR-S, and BEPICOLOMBO. Due to the extreme conditions the design covered in these missions, the sensors can be mounted outside of the temperature controlled compartment.

The MASCOT Flight Model (FM) was delivered to JAXA mid-June 2014 and was launched aboard the HAYABUSA2 space probe on December 3rd, 2014, to asteroid (162173) Ryugu (formerly 1999 JU$_3$, [171]) During the cruise phase, HAYABUSA2 uses a combination of Earth gravity-assist and solar-electric propulsion. MASCOT is an organically integrated high-density constraints-driven design. [34] [58] [59] [172] [173] [174] [175] Its structure is a highly integrated and ultra-lightweight truss-frame made from a CFRP and Rohacell® foam sandwich. [176] [177] It has three internal mechanisms: i) the Preload Release Mechanism (PRM) to release a controlled kN-range preload in the structure across the separation interface which mitigates launch vibrations; ii) the Separation Mechanism to realize a gentle push-off of MASCOT at ~5 cm/s out of the Mechanical Support Structure (MESS) recessed inside the HAYABUSA2 envelope; and iii) the Mobility Mechanism for self-righting and hopping across the asteroid surface over distances from less than a metre up to 220 m. [178] MASCOT uses a semi-passive thermal control concept, with two heatpipes, a radiator, and Multi-Layer Insulation (MLI) for heat rejection during active phases, supported by a heater for thermal control of the battery and the main electronics during passive phases. [179] During its on-asteroid operational phase, it uses a primary battery as power supply. During cruise, it is supplied by HAYABUSA2. The Power Conversion and Distribution Unit (PCDU) applies a mixed isolating/non-isolating conversion concept adapted to grounding within a nonconductive structure. [11] All housekeeping and scientific data is sent to Earth via a relay link with the HAYABUSA2 main spacecraft using redundant UHF-Band transceivers inherited from JAXA's MINERVA rovers and two patch antennae on either side of the lander, with omnidirectional coverage. The MASCOT On-Board Computer (OBC) is a redundant system providing data storage, instrument interfacing, command and data handling, as well as autonomous surface operation functions. The operational redundancy mode is configurable in a four module set of two CPUs and two I/O and mass memory boards to optimize power consumption and robustness on the background of an exclusively primary battery powered mission. Knowledge of the landers attitude on the asteroid is key to the success of its self-righting and hopping function. The attitude is determined by a threefold set of sensors: optical proximity sensors (OPS), photo electric cells (PEC) and auxiliary as well as experimental thermal sensors. The surface temperature is recorded near the PEC sensors. While these readouts are mainly for operational purposes, it is expected that some additional information can be derived on the immediate environment of the lander on the sides not in the field of view of the science instruments.
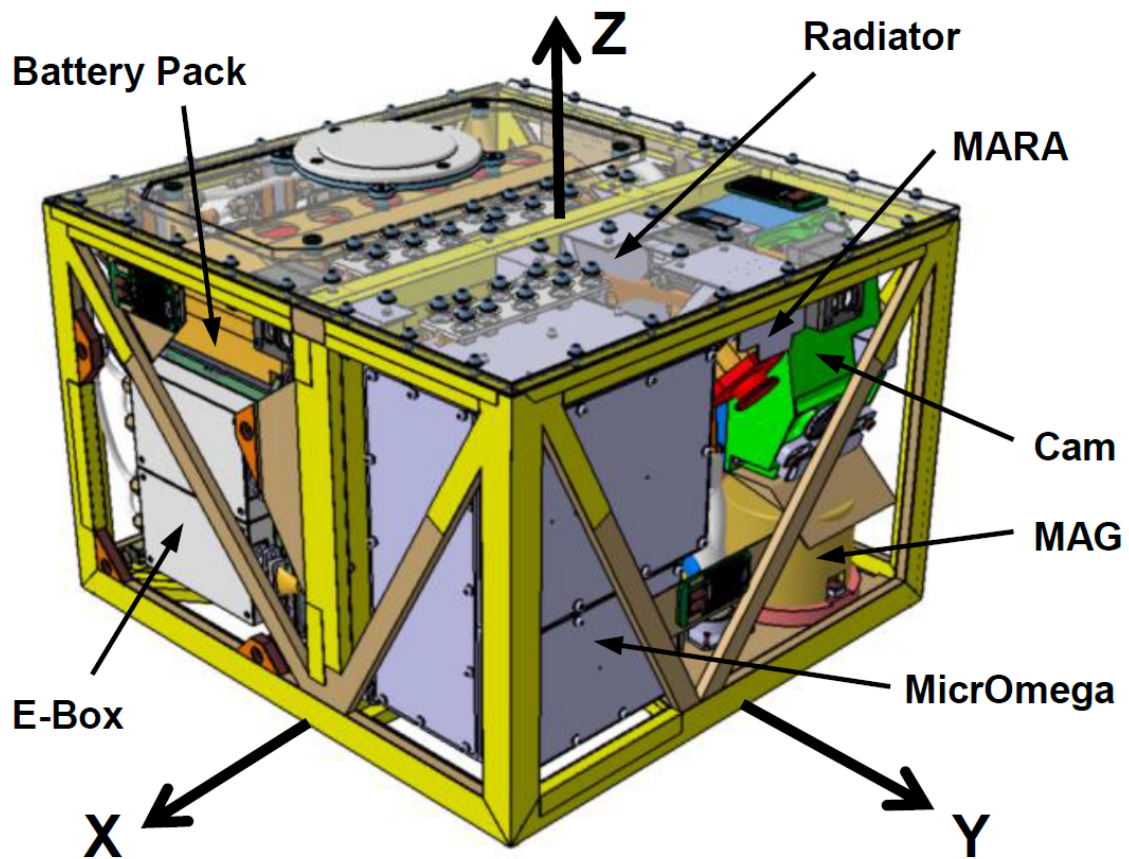
Figure 18 – MASCOT Landing Module

6.4.1 MASCOT2

MASCOT2 [98] [106] was a nanolander based on the design of MASCOT [34] [143] for ESA's AIM spacecraft [180] of the joint NASA-ESA AIDA mission [181] [182] which also includes the DART kinetic impactor test spacecraft [183]. It is designed to operate for several months on the asteroid surface and provide detailed information about the asteroid's interior, its landing site and key physical properties of the surface material. The lander's main instrument is a bistatic, Low Frequency Radar (LFR) to sound the interior structure of the asteroid. [184] [185] [186] It is supported by the same suite of camera (MasCAM) [168], radiometer (MARA) [169], and magnetometer (MasMAG) [170] as already carried on MASCOT. The second new instrument is an accelerometer, DACC.

MASCOT2 is slightly enlarged (Figure 19) to accommodate deployable LFR antennae for descent, and on-surface operations and a deployable photovoltaic top panel to enhance power generation for the long continuous runs required by LFR. The deployables are released once MASCOT2 has arrived at the optimal site for LFR operations. The deployment mechanisms have been studied in detail.

The LFR is a bistatic radar using nearly identical units aboard the lander and the orbiter, AIM, which transmit and receive mutually in a synchronized manner in the HF to VHF range where radio signals can propagate through a small asteroid. Its

spatial resolution for deep internal structure sounding is <30m. Its signal is also used for precise mass determination of the secondary by tracking during descent via a small auxiliary antenna. LFR builds on the heritage of CONSERT aboard PHILAE/ROSETTA. [187] It supplements the high-frequency radar (HFR) onboard the orbiter which resolves the top meters of the surface in high resolution.

The triaxial accelerometer, DACC, is used to observe the interaction of MASCOT2 with the surface during touch-down, bouncing, self-righting and in reaction to motion during deployment operations. It will be attempted to observe the DART impact shock wave.

For navigation, MASCOT2 uses the same set of Optical Proximity Sensors (OPS), Photoelectric Cells (PEC) and temperature sensors on each face of the lander as MASCOT. Additionally, means to aid the localization of MASCOT2 by AIM are provided.

The MASCOT Mobility hopping mechanism has been adapted to the specific needs of MASCOT2 by a dual-axis implementation. [106] Utilizing sensors as well as predictions, those actuators could in a further development be used to implement anti-bouncing control schemes, by counteracting with the lander's rotation. Furthermore, by introducing sudden jerk into the lander by utilization of the mobility, layers of loose regolith can be swirled up for sampling.
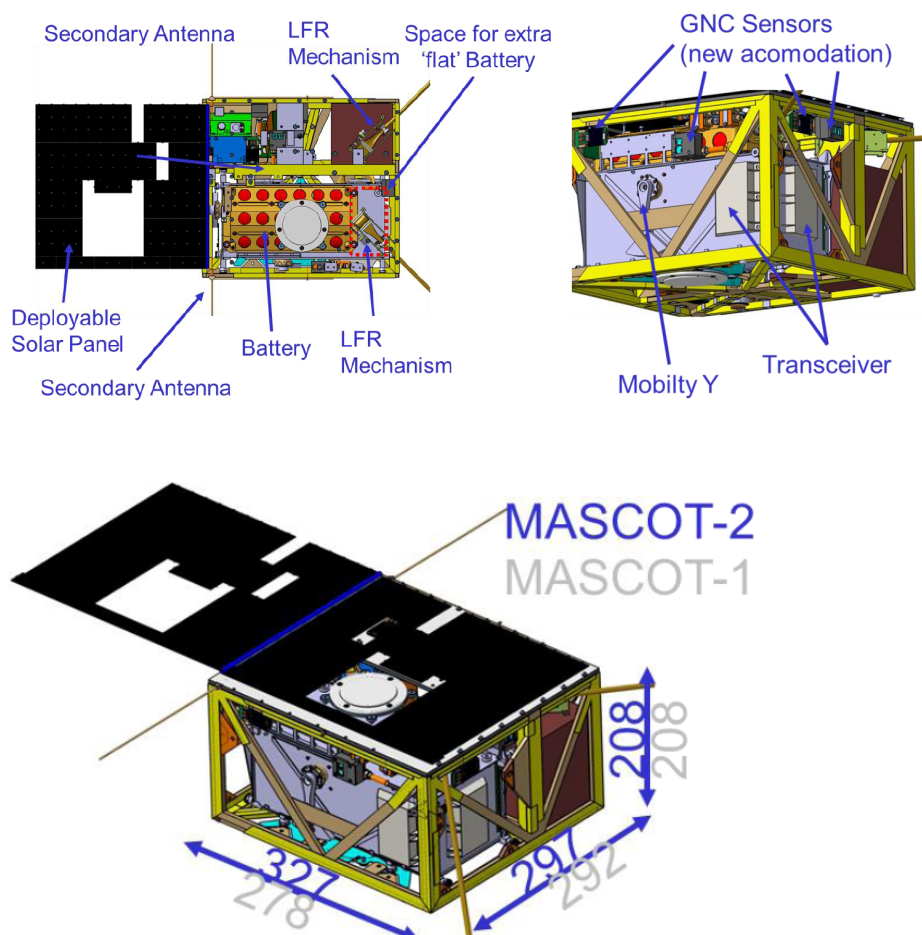

Figure 19 – The MASCOT2 lander for ESA's AIM mission

6.4.2 Multiple MASCOTs

Since the delivery of MASCOT for HAYABUSA2, several studies for MASCOT-style landers on other small solar system bodies have been conducted. [128] [188] Also, there have been precursor studies for the development of MASCOT aboard MARCOPOLO, including payload concepts similar to MASCOT2. [189] Over time, these studies have created a wide repertoire for variation of the science instruments carried as well as overall mission scenarios. Lander instrumentation can be adjusted e.g. for regolith investigations (MASCOT), radar tomography (MASCOT2), mineralogy, thermal surface properties characterization related to the Yarkovsky and YORP effects, etc.

With a suite of differently instrumented landers aboard, it is then possible to select the lander most appropriate for the currently rendezvoused asteroid when it has been characterized remotely on or after arrival of the sailcraft.

Akin to the HAYABUSA2 MINERVA landers, it is also possible to divide the payload mass down further, e.g. for CubeSat format landers or Mini-MASCOTs for very much reduced tasks. A typical planetary defence related minimum science payload could consist of a planetary radar beacon, a miniature camera similar to those qualified for GOSSAMER-1 [190] [191] [192], and a version of MARA [169] [193] adapted to the direct requirements.

6.5 Design Robustness to the Asteroid Environment

Obviously, the possibilities of adapting to the properties of the surface of an unknown celestial body are limited before launch. From telescope observations in the visual and near-infrared, only, the volume of a small asteroidal body can be determined prior to rendezvous to somewhat better than an order of magnitude. Composition and porosity at the surface can be inferred with the help of infrared observations which also constrain the size much better. [194] Although some constraints can be inferred, the interior composition and porosity can not be determined unless the object is a binary and very high resolution radar observations are possible. [195]

In the absence of such fortunate circumstance, it is difficult to determine whether the object is – in the extremes – a fluffball possibly filling its entire Roche lobe like Saturn's moon Methone [196] with zero gravity all over its surface or a solid block of nickel-iron thinly veiled by a layer of different regolith akin to (16) Psyche [197]. Further, almost all asteroids <200m are fast rotators, i.e. spin faster than the period of a circular orbit at their equator radius, [163] [164] and faceted objects apparently free of regolith like 2017 BQ_6 have been observed by planetary radar [198].

Thus, a worst-case design has to be pursued, including flexibility for operational adjustments which can only be made once a first characterization of the target orbit has been made by the carrier sailcraft early in the respective rendezvous.

The heatpipe-based thermal design of MASCOT accommodates a broad range of asteroid environments regarding the variation of albedo and surface thermal inertia, from fluffball (low thermal inertia) to bare rock (high thermal inertia) on dark bodies like Ryugu and higher albedo objects like Didymoon.

6.6 Sample-Return Landers

NEA samples of the five asteroids visited can be returned by one larger lander shuttling between the NEA surfaces and the sailcraft. A reasonable design goal

would be to pick up at least 2 samples per NEA and transfer them to a re-entry capsule aboard the sail. The technology to pick up and transfer asteroid samples already exists in several forms. It was demonstrated by the HAYABUSA mission, and has been further developed for HAYABUSA2 and OSIRIS-REx.

6.6.1 Solar Power Sail Lander Derivate

We evolve our design from the lander design for the JAXA Solar Power Sail mission to pick up samples from a Jupiter Trojan asteroid. [199] [200] This design emphasizes in-situ analysis of samples due to the very long duration return journey from the orbit of Jupiter.
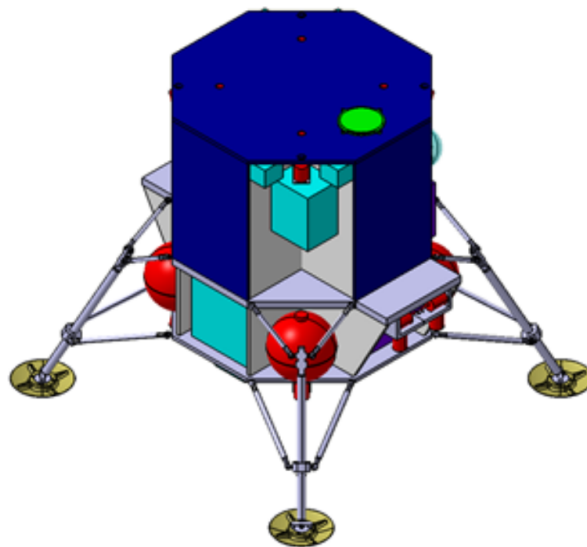

Figure 20 – 100 kg Trojan Asteroid Lander investigated as part of the JAXA Solar Power Sail (SPS) mission.

For the MNR scenario, a reduced in-situ suite of instruments can be considered due to shorter mission duration facilitating sample return to Earth.
To account for the added mass of a system capable of collecting a larger amount of samples multiple times, the original Trojan lander science suite is modified in order to remain within mass constraints.
- the in-situ science suite is cut down, reducing science payload mass, making it available for the sample collection and transfer system
- the collection of sub-surface samples is dropped, as this piece of hardware is the main mass-driver of the sampling/science suite. Subsurface sampling requires counter-thrusting systems, as well as being heavy on its own.

Samples would be collected and stored on the Lander and either transferred to the solar sail after each NEA rendezvous, or as a final package at the end of the multi-rendezvous mission. Both options have their advantages, resulting in a trade between simple systems (one-time transfer) and mission success / safety against failure during one of the NEA encounters (individual transfer after each mission).

The propulsion system is reevaluated for the multi-encounter mission and the lower gravity of the asteroids, compared to a 20 to 30km Trojan asteroid.

Based on the asteroid data listed in Table 4, a first estimate of the delta-v and thrust requirements is performed. Results are listed in Table 5, based on the worst-case assumption of parameters, as little information is available on the proposed asteroids; the targets may also change in the course of the mission design, or even during its execution. By using worst case assumptions, and adding sufficient margins (100%), the Lander allows for mission flexibility.

Table 4: Asteroid Data. In most cases rotation rate is unknown (assumed = 0.1 h). Gravity is based on worst case assumptions for albedo and density. Where unknown, an albedo range of 0.04 to 0.4 and a density of 4000 kg/m³ is assumed.

asteroid	absolute magnitude H [mag]	diameter [m]	μ [m³/s²]	rotation period [s]	gravity [m/s²]
2000SG344	24.7	24 - 77	6.38E-02	360	5.36E-05
2015JD3	25.6	16 - 51	1.85E-02	360	3.51E-05
2012KB4	25.3	19 - 59	2.87E-02	360	4.25E-05
2008EV5	20.0	205 - 245	2.06E+00	13410	1.37E-04
2014MP	26.0	13 - 43	1.11E-02	360	3.08E-05
test			6.38E-02		5.36E-05

Table 5: delta-v budget for 5 asteroid landings and sample-retrievals. The fifth is added as additional margin. All delta-v are estimated according to the worst case scenario for horizontal and vertical velocity. Included are three 10-m-hops per asteroid. The total margin added is 100% to increase system flexibility for large asteroids and faster rotating targets.

asteroid	Hopping (10 m arc)	Descent & ascent	total [m/s] (incl. 100% Margin)
2000SG344	0.20	1.51	3.42
2015JD3	0.16	0.99	2.30
2012KB4	0.18	1.12	2.59
2008EV5	0.32	0.61	1.85
2014MP	0.15	0.80	1.89
TOTAL			12.05

The ΔV requirements include for every asteroid the ΔV to cancel out horizontal and vertical velocity from a release position at 5000 m altitude to the landing site of the asteroid, as well as the reverse transfer to return to the solar sail. Also included is the ΔV to perform a number of hops (three times) on the asteroid surface with a distance of ≈10m.

Due to the multi-rendezvous mission duration, propulsion system leakage becomes an issue. The use of isolation valves during cruise phase allowed for low leakage in a high-pressure cold gas system on the Trojan SPS mission. However, if multiple landings are performed at different times throughout the entire mission duration, this approach is not possible. The use of liquid propellant systems is one alternative to reduce leak-rates, as liquid stored propellants are more suited for long-term storage (cf. PHILAE).

An analysis of propellants is performed trading propellant mass, volume, and power requirements. Power requirements are based on the heating enthalpy of the liquid and the mass-flow rate needed to provide sufficient thrust for both hovering and ascent from the asteroid surface. Thrust is designed according to the maximum gravity asteroid (in this case 2008 EV$_5$); including sufficient margin, a thrust of 40 mN is sufficient to provide two times the gravitational acceleration of the largest target asteroid (2008 EV$_5$) for a 100 kg lander system.

Propellant mass is traded with propellant volume and power requirements for a number of potential propellants.
Different options can be considered as best suited for use as propellant in the NEA Lander.
Propellants such as Hexafluoroethane (R116) or Sulfurhexafluoride offer low power and storage volume, with reasonable propellant mass requirements. Lower propellant mass is available by taking higher heating power requirements into account (see Table 6 for comparison of a number of suitable propellant options).

Table 6 – Propellant-dependent parameters.

	Carbon Dioxide	Sulfur Hexa-fluoride	Nitrous Oxide	N-Butane	R116	R134a
operating pressure (gas) [bar]	21.37	1.27	18.11	0.1	6.6	0.1
operating pressure (liquid) [bar]	91.15	51.3	89.66	51.76	43.53	54.65
ISP [sec]	52.76	45.04	55.11	72.23	44.37	53.32
liq. Propellant density [kg/m³]	844.71	1471.47	841.96	586.24	1013.38	1249.73
maximum heating temperature [K]	352.73	346.13	356.99	423	328.8	393.02
ideal heating power [W]	19.91	8.52	19.02	21.43	7.41	15.39
propellant mass [kg]	2.30	2.69	2.21	1.69	2.73	2.28
propellant volume	2725.82	1829.35	2619.41	2877.90	2695.85	1823.29
propellant heating energy [Wh]	164.72	70.35	157.43	177.85	61.17	127.34
propellant mass fraction [%]	2.30	2.69	2.21	1.69	2.73	2.28

Based on these results and an adapted propulsion system design of the Trojan lander for use with liquid stored propellants is considered (Figure 21). The selected propellant is Sulfurhexafluoride due to low volume and heating power requirements. However, other options such as R116, R134a and n-Butane are not that different.
Operating pressure is low, at 51 bar at a nominal operating temperature range around 10°C for the liquid stored propellant, and 1.3 bar on the generated gas side of the system.
The required propellant mass of 2.69 kg easily fits into the 100-kg lander mass budget. The total propulsion system dry mass is 10.0 kg, including propellant tanks, valves, tubing and battery for heating the propellant. Tank Volume is 1830 cm³, including 100 cm³ of buffer tank volume. Power requirements (considering a conservative 70% system efficiency) are 12 W (100 Wh total energy). This can be handled by the on-board battery without issues, especially when considering the use of low power solenoid valves is possible at these lower operating pressures.
The main reason for these low power requirements is the low gravity and therefore thrust requirements needed to allow the lander to operate around the targeted NEAs.

Figure 21: Schematic of a liquid propellant based lander propulsion system operating at vapor-liquid equilibrium pressure.

This system provides an alternative to the N_2 system considered for the Trojan SPS Lander, with the added benefits of low pressure and reduced leakage risk, at the price of additional heating power. The system mass is reduced to 13 kg, compared to the 26 kg needed in the SPS Trojan mission.

While the Trojan lander had to trade descent/ascent times with propellant usage for powered descent, this lander can rely on solar power for operation due to its orbit in proximity to 1 AU; not 5.2 AU.

6.7 Resource Sharing of Lander(s) and Sailcraft

Following the BSDU-CSCU concept of GOSSAMER-1, many resources can be shared with the CSCU in cruise and the CSCU-BSDUs before sail deployment.

Landers which have to expect rough terrain and unexpected shadowed areas (cf. PHILAE) require a relatively large battery while a deployed sailcraft operating in deep space in almost all cases of nominal operation only needs a relatively small capacity battery to buffer brief high-power peaks caused e.g. by actuator activations. Thus, the batteries of the still-attached lander(s) can support the CSCU during deployment of the sail membrane and booms when the BSDUs have already separated from it. Similarly, the sailcraft can generate its power after deployment from ultra-lightweight membrane-mounted photovoltaics similar to the GOSSAMER-1 Photovoltaics Experiment (PVX) or the GOSOLAR technology currently under development. [69] These thin-film CIGS photovoltaic cells have a lower efficiency, currently ≈12%, than rigid triple-junction photovoltaic cells which are currently approaching 30%. Thus, thin-film generators, although still significantly lighter, require about three times the

array area for a given power output. Rigid triple-junction photovoltaic cells are therefore used for the pre-deployment photovoltaic generators of high-density small spacecraft design GOSSAMER-style sailcraft for secondary payload flight opportunities. Area-efficient photovoltaics are also required for mobile asteroid landers. The landers' photovoltaics generators exposed to the outside in launch configuration and after BSDU separation can therefore be used as a significant part of the pre-deployment, respectively in-deploment photovoltaics of the CSCU.
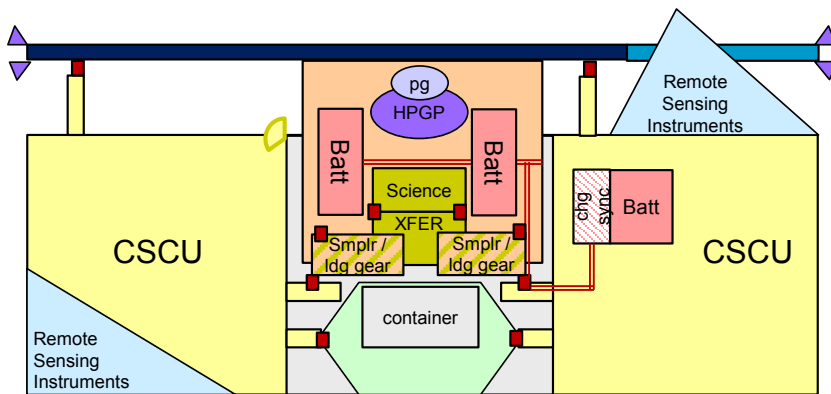

Figure 22 – Notional accommodation of a multiple sample-return microlander aboard an advanced minisailcraft with shared use of CSCU pre-deployment photovoltaics, battery, and lander propulsion
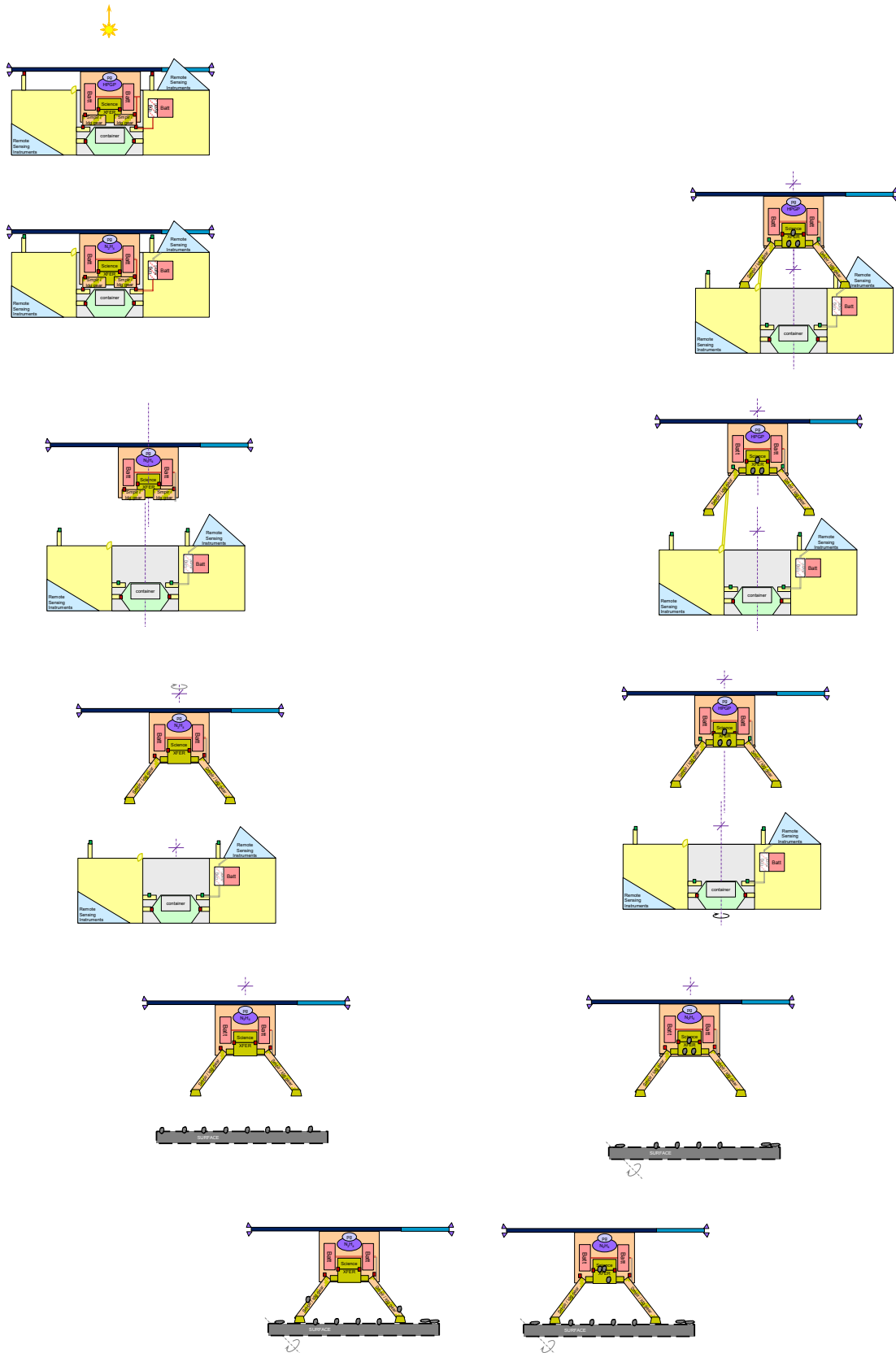
Figure 23 – Concept of operation of a multiple sample-return microlander aboard an advanced minisailcraft showing the first deployment and sample delivery to the sailcraft by berthing

Science instruments of the landers, in particular panoramic cameras and thermal infrared sensors, can provide services on an operational spacecraft which are normally only designed into demonstrator spacecraft to monitor sail deployment and membrane ageing, [73] [74] [88] [201] [202].
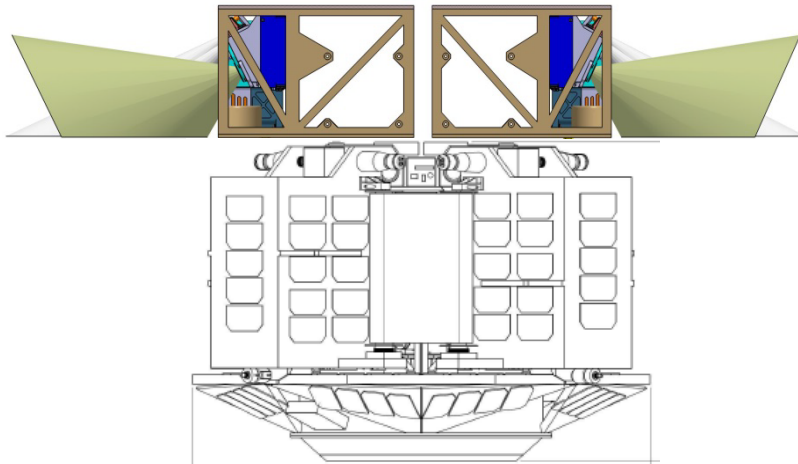

Figure 24- – Notional accommodation of MASCOT-style nanolanders aboard a GOSSAMER-style microsailcraft to provide the synergetic capability of membrane deployment and ageing monitoring using lander instruments with a similar field of view as MasCAM and MARA on MASCOT, as well as additional area for pre-deployment photovoltaics

Suitably designed and/or oriented instruments of the landers still attached can also double as 'orbiter' instruments, e.g. to monitor the asteroid in the vicinity of the sailcraft without the need to turn it for the pointing of a boresighted sailcraft camera.

These and more opportunities for resource sharing can be used to adapt lander designs similar to MASCOT, PHILAE, or the Solar Power Sail Trojan lander into GOSSAMER-style-integrated sub-spacecraft performing a common mission.
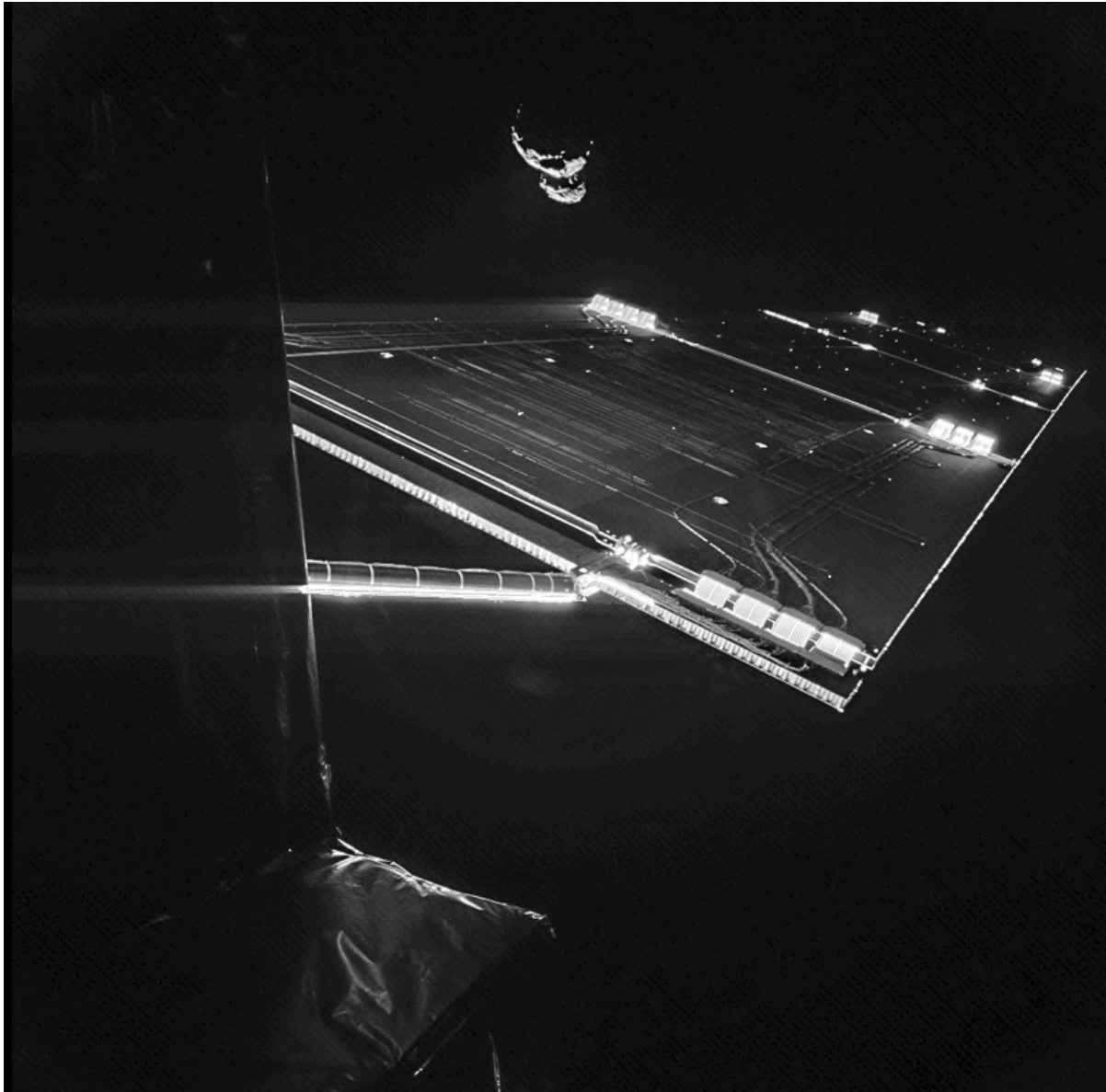
Figure 25 – Carrier spacecraft hardware monitoring and rendezvous target tracking imagery example: 67P seen from the still attached Pʜɪʟᴀᴇ lander along the photovoltaic panels of Rᴏsᴇᴛᴛᴀ – image credit: ÇIVA/Pʜɪʟᴀᴇ/Rᴏsᴇᴛᴛᴀ

7. EXERCISE

7.1 Solar Sail – Online Change of the Mission

7.1.1 Diversion to fly-by or rendezvous

Due to its early impact in 2027, this PDC's fictitious impactor 2017PDC requires more extensive modifications of the MNR sequence presented above, which we for

now have to relegate to future work. However, the asteroid 2011 AG$_5$ used for the PDC'13 exercise [203] more easily matches the existing 5-NEA-sequence. [71] The modified sequence also demonstrates the target change flexibility unique to solar sailing.

The last leg to 2014 MP shown in Table 1 has again been removed to add a leg to the potentially hazardous asteroid 2011 AG$_5$, which was one of the two case studies considered during the Planetary Defense Conference 2013. At the time of the conference, the potential impact was expected to occur on February 3rd, 2040. Table 7 shows the properties of all the encountered bodies of the new considered sequence.

Table 7 – Properties of all the encounters of the new considered sequence.

Object	2000 SG$_{344}$	2015 JD$_3$	2012 KB$_4$	(341843) 2008 EV$_5$	(367789) 2011 AG$_5$
Orbital type	Aten	Amor	Amor	Aten	Apollo
Semi-major axis [AU]	0.977	1.059	1.093	0.958	1.431
Eccentricity	0.067	0.008	0.061	0.083	0.390
Inclination [deg]	0.112	2.719	6.328	7.437	3.682
Absolute magnitude [mag]	24.7	25.6	25.3	20.00	21.8
Estimated size [m]	35 – 75	20 – 50	20 – 50	260 – 590 *400 ±50*	110– 240
geometric albedo				*0.137*	
EMOID [AU]	0.00085	0.054	0.072	0.0132	0.00039
PHA	no	no	no	yes	yes
NHATS	yes	yes	yes	yes	no
Taxonomic type				C;X	
Albedo				0.104	
Rotation period [h]				3.725	
Light-curve amplitude [mag]				0.05	
Radar observation				Y	
Spectral observation				Y	
IR observation				Y	
Ascending node Earth separation [AU]	-0.03197	0.06224	0.09177	0.01535	-0.00166
Descending node Earth separation [AU]	-0.02184	0.05451	0.08589	-0.10839	0.56452

A methodology similar to the one described in Sullo et al. [204] [205] has been used for this study to compute the leg to 2011 AG$_5$. First, a constant-mass low-thrust transfer between 2008 EV$_5$ and 2011 AG$_5$ has been computed by means of the indirect optimization approach. The time of flight and the initial values of the costates have been determined through a particle swarm optimization (PSO) [206]. For this

scenario, the orbits of both objects are considered coplanar. That is, the orbital plane of 2011 AG$_5$ has been rotated and projected onto the one of 2008 EV$_5$. Moreover, the maximum acceleration given by the propulsion system was set to a_{max} = 1 mm/s². Starting from the low-thrust solution, the homotopy-continuation approach described in [204] has been used to find a coplanar solar-sail transfer with a_c = 0.2 mm/s². Then, the Automated Trajectory Optimiser for Solar Sailing (ATOSS) [207] [208] has been used to find the final three-dimensional (3-D) trajectory by first changing the orientation of the orbital plane and then changing its inclination.

The total mission duration is now 4398 days, about 12 years, and the sailcraft arrives at the final target object on 25 May 2037, about 3 years before the potential impact. The complete trajectory of the overall sequence is shown in Figure 26, whereas Figure 27 shows only the last transfer leg between 2008 EV$_5$ and 2011 AG$_5$. Figure 28 shows the acceleration history in the orbital reference frame needed during this last leg, whereas Table 8 shows the updated mission parameters. It is important to note that the sequence still contains 2008 EV$_5$, which is classified as a PHA and was selected as one of the candidate targets for the ARRM mission by NASA [119].

Table 8 – Mission parameters for the considered sequence with the last leg to 2011 AG$_5$.

Object	Stay time [days]		Start	End	Time of flight [days]
Earth	//		10 May 2025	26 Feb 2027	657
2000 SG$_{344}$	123		29 Jun 2027	06 Sep 2028	436
2015 JD$_3$	164		18 Feb 2029	24 Sep 2030	584
2012 KB$_4$	160		04 Mar 2031	29 Sep 2032	576
2008 EV$_5$	7.5		*07 Oct 2032*	*25 May 2037*	*1691*
2011 AG$_5$	*987 to* $\oplus$				
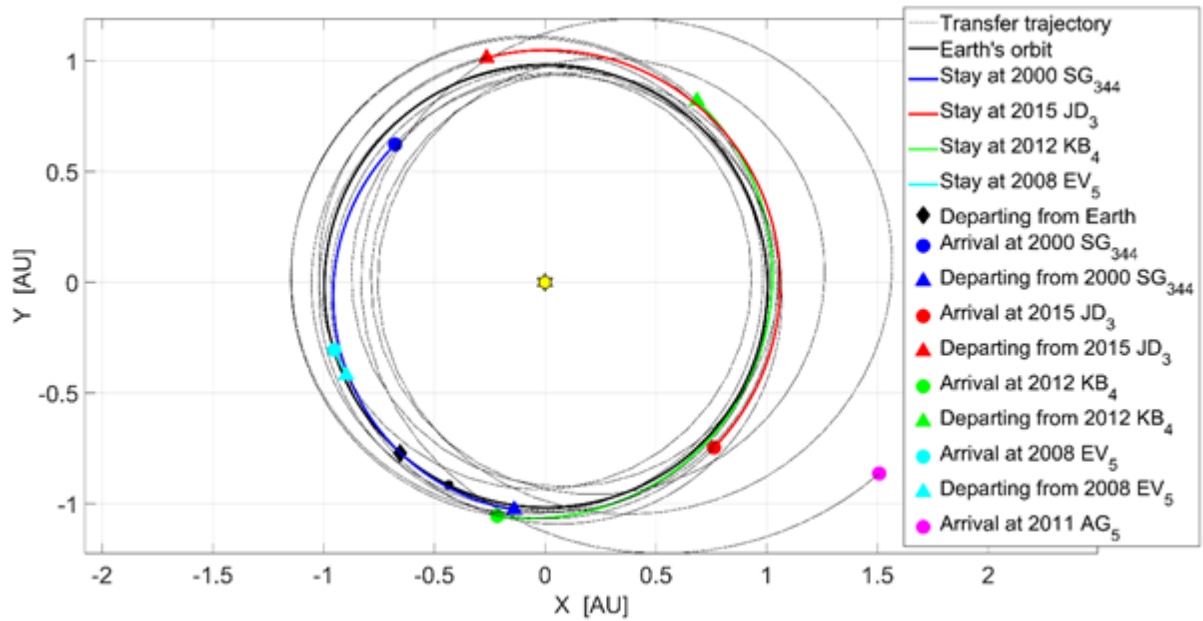
Figure 26 – Heliocentric view of the complete three-dimensional trajectory of the considered sequence. Ecliptic-plane view.
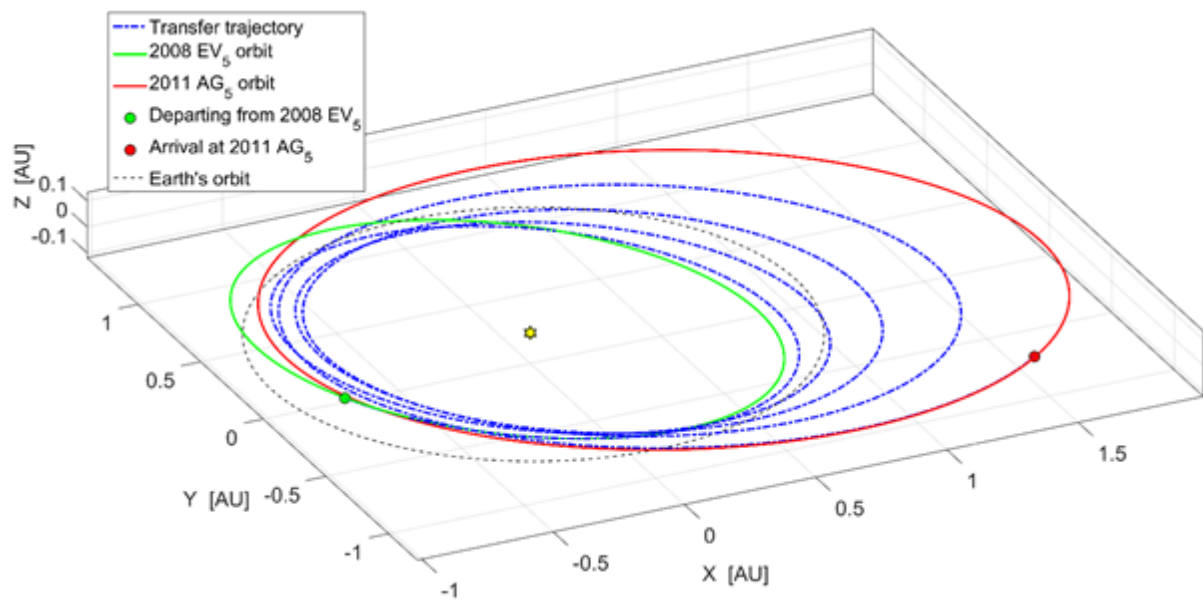
Figure 27 – Heliocentric view of the last transfer leg between 2008 EV$_5$ and 2011 AG$_5$.
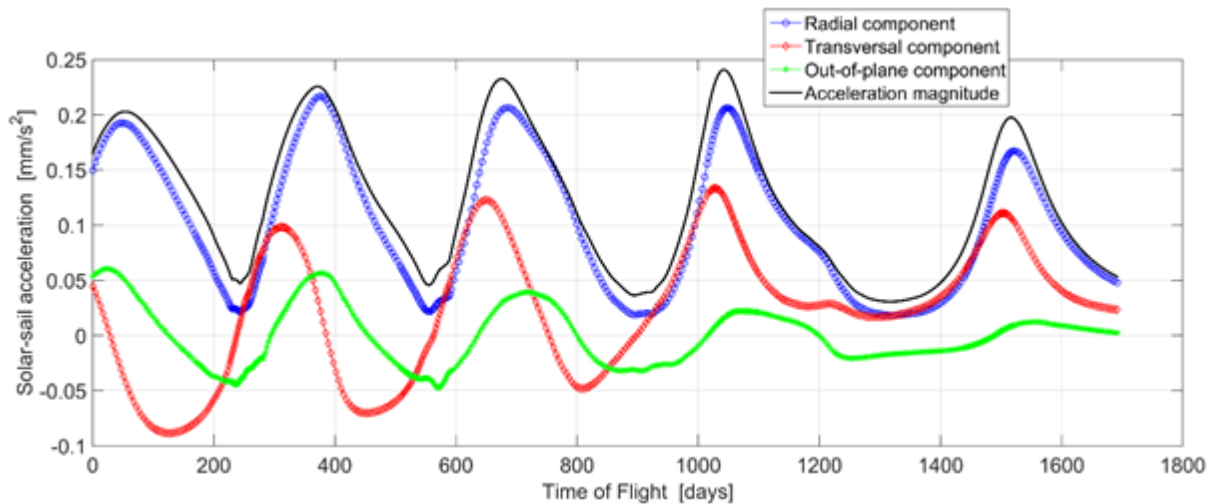
Figure 28 – Acceleration history during the last transfer leg between 2008 EV$_5$ and 2011 AG$_5$.

7.2 PDC Exercise 2017 Fictitious Impactor

7.2.1 Rendezvous

A second case study is considered which targets the fictitious potentially-hazardous asteroid 2017 PDC introduced at the Planetary Defense Conference 2017. The potential impact of this fictitious object is arranged to be in July 2027 [209]. Table 9 shows the ephemerides of 2017 PDC.

Table 9 – Ephemerides of 2017 PDC.

Object	2017 PDC
Semi-major axis [AU]	2.24
Eccentricity	0.607
Inclination [deg]	6.297
Right ascension of the ascending node [deg]	298
Argument of periapsis [deg]	312
Mean anomaly [deg]	332
Epoch [MJD]	57940
Absolute magnitude [mag]	21.9
Estimated size [m]	110 – 240

Because of the date of impact, the multiple-NEA rendezvous mission presented in [71] is not a good candidate. Therefore, from the same study presented in [71], a different sequence has been optimized and considered as a potential starting point for a leg to 2017 PDC. Table 10 shows the mission parameters for such sequence.

Table 10 – Mission parameters for the original sequence for 2017 PDC case study.

Object	Stay time [days]		Start	End	Time of flight [days]
Earth	//		13 Aug 2020	26 Apr 2022	621
2005 TG$_{50}$	128		02 Sep 2022	13 Jan 2024	498
2015 JF$_{11}$	104		25 Apr 2024	10 Jun 2026	776
2012 BB$_{14}$	139		28 Oct 2026	02 Aug 2028	644
2014 YN	//				

Table 11 – Properties of all the encounters of the original sequence for 2017 PDC case study.

Object	2005 TG$_{50}$	2015 JF$_{11}$	2012 BB$_{14}$	2014 YN
Orbital type	Aten	Aten	Apollo	Aten
Semi-major axis [AU]	0.92348	0.99547	1.0644	0.89227
Eccentricity	0.134504	0.16669	0.0994	0.13429
Inclination [deg]	2.401	9.317	2.645	1.208
Absolute magnitude [mag]	24.8	20.8	25.0	25.7
Estimated size [m]	19-85	120-538	17-78	13-56
EMOID [AU]	0.01240	0.1143	0.01712	0.00497
PHA	No	No	No	No
NHATS	Yes	Yes	Yes	Yes
Ascending node Earth separation [AU]	0.02879	0.13308	0.06773	-0.2359
Descending node Earth separation [AU]	-0.18638	-0.15138	0.04104	0.01767

As for the previous case study, the mission is changed after the second leg to go towards 2017 PDC. The same methodology to find a transfer leg from 2015 JF$_{11}$ to 2017 PDC has been used in this case, starting from a low-thrust solution with a_{max} = 2 mm/s². Nevertheless, this time the orbit of the target asteroid is too different from the one of the departing object and no good solution has been found for this case study. In fact, a solar-sail transfer leg with a_c = 0.73 mm/s², considering the orbit of 2017 PDC coplanar with the one of 2015 JF$_{11}$, needs more than 2000 days to be performed. That is, a sailcraft with a much larger characteristic acceleration than the one considered in this study would arrive at the target asteroid on 21 August 2030, which is about three years after the predicted impact with the Earth. Figure 29 shows the aforementioned transfer leg with the non dimensional acceleration vector.
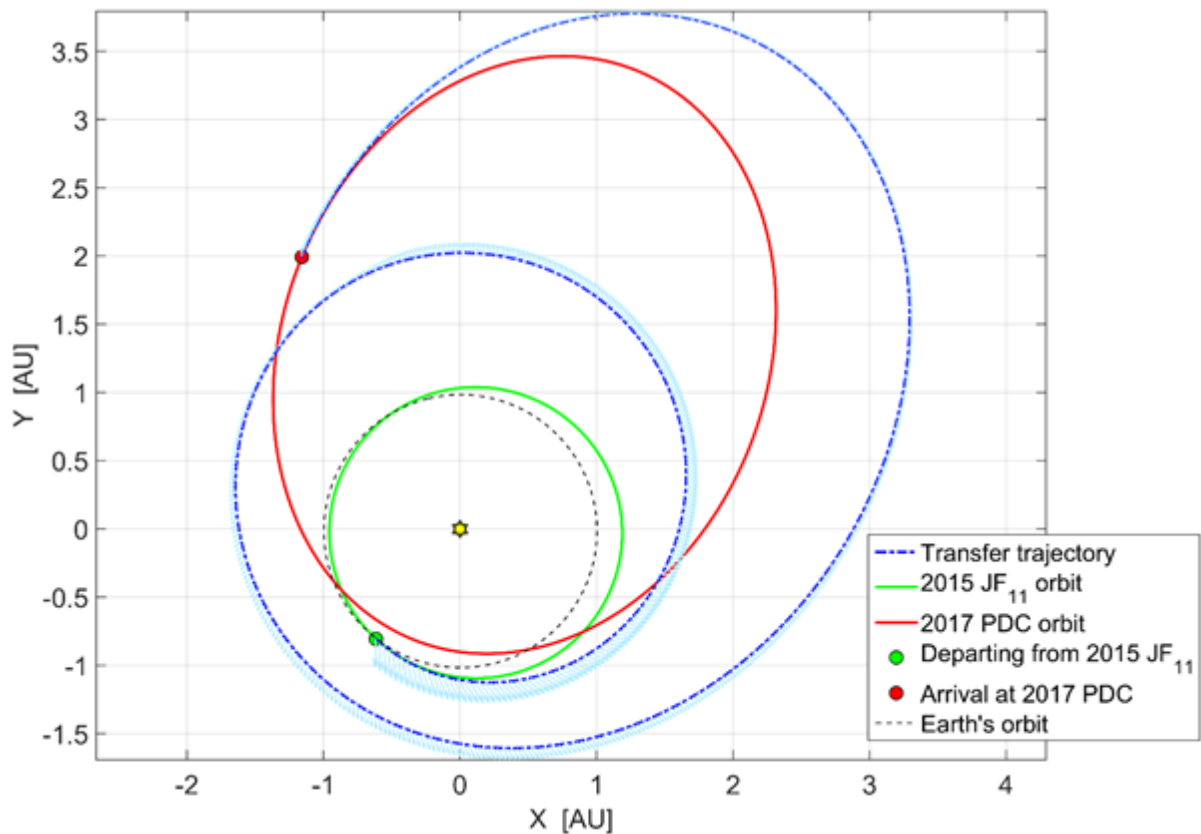
Figure 29 – Heliocentric view of the coplanar leg between 2015 JF$_{11}$ and 2017 PDC. Characteristic acceleration $a_c = 0.73$ mm/s^2.

In the case of an actual deflection, such a mission could still be useful to study the effects of the deflection method on the asteroid, particularly if a rendezvous was not feasible before the averted impact and a fast encounter method was used for deflection. It can also be used to monitor the object and refine its trajectory, particularly if a beacon is part of the suite of landers or a configuration can be found that enables or rather retro-fits radio science.

The environmental effects on the sailcraft and its landers on the way to 2017 PDC are significant. Receding from the Sun to nearly 4 AU from a sequence of fairly Earth-like orbits for which the spacecraft was designed, it will need more power to stay warm while less photovoltaic input is available. However, with most MASCOT-like landers or a shuttling lander still attached after only two of the planned five rendezvous completed, normally surplus photovoltaic generator area is still available and connected to the GOSSAMER-style charging network, and more power-consuming units could be turned on to warm up by activity. This concept was also applied on MASCOT2, to minimize the amount of dedicated thermal control hardware where functional subsystems could be used instead. Also, the relatively large photovoltaic array required to power the long runs of LFR worked in this direction to extend the envelope of operability towards Didymos' aphelion. A serendipitous survey of the asteroid belt from the inside might be a worthwhile task for the cameras required to operate as their own heaters, delivering much data to the OBC to warm up its CPUs by moving object detection algorithms.

7.2.2 Fly-By

Due to the short lead time to impact, a rendezvous with 2017 PDC is very difficult. In the assumed scenario of an already flying sailcraft diverting from the multiple-NEA rendezvous mission after having visited the second object to target 2017 PDC, a rendezvous can not be achieved. However, it can still be used to target 2017 PDC for a fast flyby.

Since the second leg of the original MNR mission ended on January 13th, 2024, we only have 3 years to reach the object before the impact with the Earth (if any), a challenge for a first-generation sail with a characteristic acceleration of $a_c = 0.2$ mm/s². Therefore, we cannot expect the already flying sail to contribute to or perform a pre-deflection characterization mission by rendezvous. That said, the following plots show the trajectory to reach 2017 PDC for a fast flyby on 14 April 2027, which is about 3 months before the expected impact. If the deflection missions were successful, then the orbit of 2017 PDC will be slightly different to the original one which was the one considered for this calculation. However, the resulting post-deflection orbit will not be significantly different from the original one. Therefore, if the deflection missions were successful, the sailcraft trajectory could be online adjusted with the new target orbit. Localization of 2017 PDC relative to the sail by navigation images could help to confirm or refine the post-deflection orbit, and possibly provide early warning of fragments lingering close to the main mass after deflection.
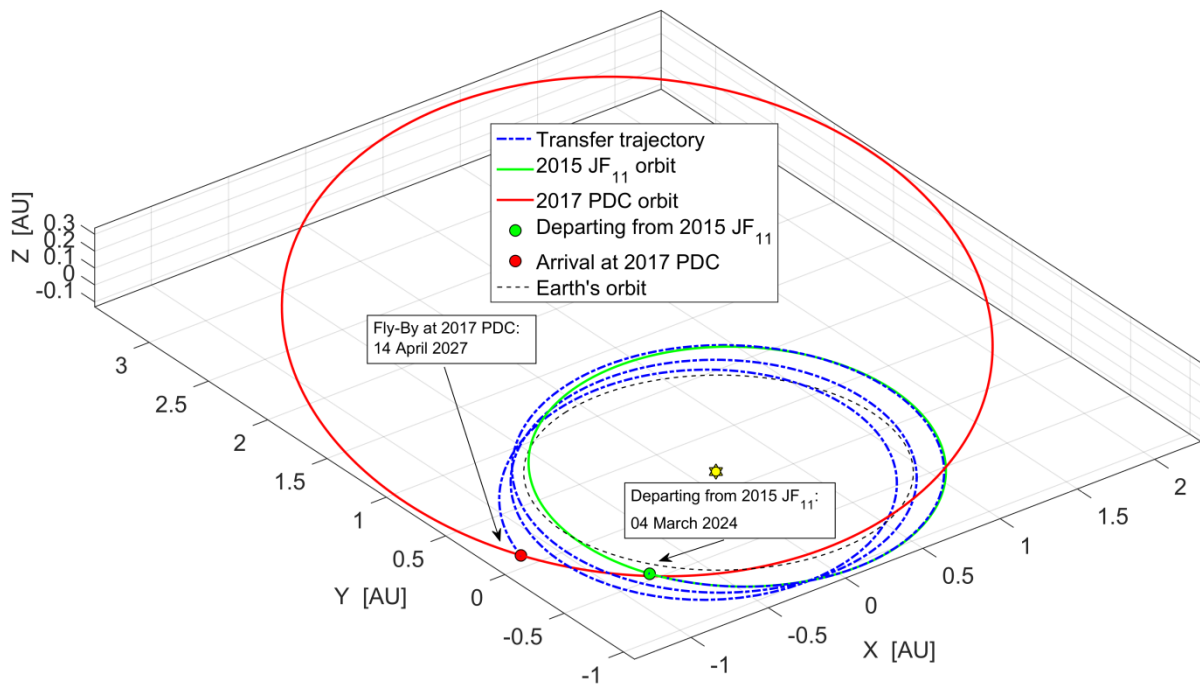
Figure 30 – 3D view of the fast fly-by leg from 2015 JF$_{11}$ to 2017 PDC

If the MNR mission still carries MASCOT-like landers at this point, it may be worthwhile to sacrifice one or more of them in an attempt to get imagery of side of 2017 PDC not seen by the sailcraft, from the landers tumbling away into deep space after a directed separation, although the chances of catching a useful image will be small. If a shuttling sample-return lander is carried, it can use its propulsion system

to achieve a near-synchronous flyby of both elements of the MNR mission with 2017 PDC sandwiched in-between, by slowly departing at a right angle from the near-collision course. With propulsion, it can aim its cameras at the target although they would not be optimized for this use. If the fly-by is sufficiently close, it can return to the sail as if from an asteroid surface or the sail can return to its lander to minimize the ΔV required by manoeuvring in to meet it.

In this extension of the MNR scenario, the use of landers as far-side remote sensing platforms is an example of operational improvisation in the extreme. However, dedicated derivatives of the lander platforms discussed could perform such tasks as their nominal mission, as well. Propelled sub-spacecraft not unlike the Solar Power Sail Lander can carry extensive suites of remote-sensing instruments on temporarily slightly diverging interplanetary trajectories for close-up all-round investigations on multiple asteroid fly-by missions such as CASTAway [210] [211] or Lucy [212]. For missions containing only a single fly-by and requiring only a short-term pointing capability e.g. for the few minutes of closest approach, a MASCOT-like 'one-way' platform with an added active GNC elements would suffice. Such missions include planetary exploration missions en-route to other targets but passing by an asteroid in cruise such as Galileo [213] [214] [215], or Rosetta [38] [216], but also non-rendezvous missions to one comet or asteroid like Stardust/NExT [217], Deep Impact/EPOXI [218], DART [183], or NEOTωIST [156] [157] [158] [159]. Missions with single or very few but due to main mission requirements distant fly-bys such as Cassini [219] or New Horizons [220] might be able to benefit from an intermediate solution, combining simplified propulsion and one-way elements.

7.3 Summary of the MNR mission scenarios studied

By the compilation of its catalogue of target objects from the NHATS and PHA sets of asteroids, the original MNR sequences of Peloni et al. [71] address a reasonable and likely collection of near-term MNR asteroid science missions to NEAs which are also easily accessible for larger dedicated single-target missions such as asteroid sample-return or even human exploration (NHATS) and/or are members of the only asteroid population which humans might one day be forced to interact with directly and promptly (PHAs). The MNR mission would in this case have a pathfinder character, down-selecting potential targets for a much more expensive future mission. In-situ resurce utilization applictions of MNR might follow a similar two- or three-stage approach consisting of a relatively large number of asteroid rendezvous followed by a few sample-returns leading up to a major resouce extraction effort.

Considering that hundreds of MNR sequences exist per launch day and many of these are related in a family tree like manner (cf. Figures 7 and 8 in [71]) already within a limited subset of asteroids it is obvious that an extreme flexibilty in the sequence of targets exists, even after launch and including the first target in the sequence. With the addition of more targets to the catalogue, whether by lifting restrictions on the selection or by adding new discoveries, this flexibility can only increase and broaden.

In the Planetary Defence Conference exercise cases we tested the degree of flexibility by forcing an already launched MNR spacecraft, which can therefore no longer be adapted to the specific mission, to reach one specific target which was not part of the initial catalogue and therefore not within a set of five asteroids yielding a well optimized trajectory. In the diversion to 2011 AG$_5$, this asteroid replaced 2014 MP in the same way as Earth had previously replaced it for a sample-return variation

of MNR, at the moderate expense of about 2 years longer total duration of the mission. In the case of fictitious object 2017 PDC which was designed as a hard to access target on purpose for the exercise, another sequence from the repertoire created in [71] had to be selected – this is up to this point equivalent to selecting another MNR spacecraft currently in space. The target was ultimately reached for rendezvous, however on a trajectory requiring a much higher performance sail and more time than the PDC scenario had till the fictitious impact. However, the original near-term performance sail was able to achieve a fast fly-by of the same fictitious impactor just prior to impact. While this as yet fictitious MNR small sailcraft with its modest near-term performance level could be diverted in flight from a completely unrelated mission to investigate one specific object, all other spacecraft called upon in the exercise at the PDC 2017 were dedicated designs requiring dedicated launches stretching present-day launch capabilities and still struggled to reach the asteroid in time.

In most reasonable scenarios related to new objects or changing interest after the launch of a MNR science mission there will likely be many objects fitting the updated selection criteria and NEA surveys will continuously expand this reservoir, turning target flexibilty to much more plain sailing than in the extreme cases here presented.

8. FUTURE WORK

We have here collected the building bricks required to begin a wider exploration of our neighbourhood by surveying the members of the solar system nearest to Earth for planetary science, planetary defence and planetary resources.

The development of MNR trajectories has reached a point where it enables rendezvous with NEAs for 100-day in-situ investigations comparable to currently proposed conventional SSSB science missions every 2 years per spacecraft, using solar sail propulsion alone from the rim of Earth's gravity well. [71] Small spacecraft technology enables shoebox-sized one-way landers [34] and at launch fridge-sized sailcraft [108] able to perform these MNR trajectories. By a modest increase in size, samples can be returned to Earth using the same basic technologies. [128] Current large launch vehicles can carry half a dozen or more of these lander-equipped sailcraft at once in their performance margins to geostationary transfer orbit from where only a small push is required to escape Earth, on a mass-available basis. [97] [96] By adding just one stage, the same class of launch vehicles can accelerate one such small spacecraft directly to a solar escape trajectory, if in the ecliptic plane. But thanks to the discovery of gravity-assist trajectories [23], most exploration missions start at Venus, Earth, or – now rarely – Jupiter, and don't require this kind of kickstart. [20]

So far, these bricks stand largely independent of each other.

MNR trajectory design does not ask for the little extra in c_3 that might still be in the tanks of a launcher after dropping a lighter primary passenger into GTO. Small spacecraft technology is struggling to find follow-on uses, even direct re-uses, or just ways to achieve the qualification level to become acceptable in the world of conventional mission development lines. Earth escape capable launch vehicles are rigidly optimized to cater best for these major service-providing missions.

In most cases, the reason is simply that any one of these tasks alone is already difficult enough – spaceflight is not done because it is easy, but because it is hard, a

challenge. But there is also the historical reason that the exploration of the solar system using the methods devised in the early 1960s has so far worked well and achieved brilliant results. The same applies to space-based services; communication, weather, navigation.

But some bricks are getting connected, gravity-assist sequencing begins to ask for low-thrust propulsion, and vice-versa, to widen the tight and sometimes rare launch windows or to give a boost to calmly spiraling trajectories. [221] [222] [223] [224] The resulting system-level trade works favourably for the missions which enter such negotiations. [29] [31] The tools for much more complex trades connecting many domain models are created by the development of Model-Based System Engineering. [98] [225]

It appears that a much easier access to the solar system as well as near-Earth space, much less constrained by launch windows or payload to target or thrust limitations, can be achieved by connecting all these bricks – small spacecraft technology, solar sail propulsion, solar-electric propulsion, high-energy escape launch systems – by comprehensive modelling, simulation, optimization, and most importantly practice in flight. The MNR mission in its applications for planetary science, planetary defence and planetary resources contains all these elements, and based on very near-term small spacecraft solar sails and "now-term" small spacecraft landers it is at a most affordable entry level to practice their connection into one system.

This future work can start now.

9. CONCLUSIONS

We outlined a synergetic development path of small spacecraft solar sails and nano- and micro-scale asteroid landers enabling a substantial increase in the number of NEAs studied by planetary science in a dynamic manner which allows in-flight adjustment of the choice of rendezvous targets. The capability to change targets in flight also allows a mission already in flight to respond to extreme events such as a probable Earth impactor being discovered. It may also follow changing commercial interest in this manner. Within the capabilities of near-term first-generation sailcraft technology, the small spacecraft design concepts of GOSSAMER-1 and MASCOT enable a sailcraft performance sufficient to achieve 5 NEA rendezvous of at least 100 days, each, in 10 years by one spacecraft. Each rendezvous includes a target-adapted one-way nano-lander delivery or a sample pick-up at each target by a larger shuttling lander.

The small spacecraft approach enables the use of surplus launcher payload capability in the geostationary and high Earth orbit market with a potential of 10's of launches per year. If the spacecraft concept here presented were serialized in a manner akin to similar-sized communication satellite constellation spacecraft, the number of NEAs visited and studied in-situ could be increased by orders of magnitude within a few decades. Beyond planetary science missions as we know them today, the exploration of our neighbourhood in the solar system could be advanced from the most direct and practicable pathfinding towards area surveys for classification and examination of the geological structure, minerals and other resources, and natural hazards of this domain.

On the other hand, the small mass of small spacecraft solar sails also enables very high launch energy missions based on available geostationary market launch

vehicles which can combine into fast, responsive and affordable missions to the most challenging targets of the solar system, including planetary defence scenarios.

Many of the technologies required for currently considered future large space infrastructure and flagship science mission scenarios such as high-thrust solar-electric space tugs or photovoltaic-powered missions to the outer planets can be developed, brought to maturity (i.e., TRL9) and first fielded at low cost by continuing their development in entry-level applications in small spacecraft. Small solar sails in combination with small lander modules as well as membrane-based deployable photovoltaics share the same critical technologies and challenges. They address reasonable planetary science and resources and situational awareness missions using near-term, even mostly "now-term" technology in an affordable and cost-effective manner.

Facilities commonly considered part of the engineering domain can also be used to advance natural materials science, particularly regarding the visible surface layers of asteroids. One example is the Complex Irradiation Facility designed to perform short-term terrestrial laboratory experiments devoted to degradation expertise of materials used in long term space missions. Such studies are feasible due to the fact that both the electromagnetic and corpuscular radiation sources have a pair of set parameters which effectively can increase or decrease radiation intensity.

REFERENCES

[1]   J. Kepler, De Cometis Libelli Tres, 1619.

[2]   J.C. Maxwell, A Treatise on Electricity and Magnetism (1st ed.), 2, 391, Oxford, 1873. (cf. [6])

[3]   A. Bartoli, Sopra I movementi prodotti della luce et dal calorie, Florence, Le Monnier, 1876; also Nuovo Cimento, 15, 193, 1884. (cf. [6])

[4]   John Perlin, A short summary of the evolution of photovoltaics, © 2015, http://californiasolarcenter.org/history-pv/, (accessed 15FEB2018).

[5]   P. Lebedev, Untersuchungen über die Druckkräfte des Lichtes, Annalen der Physik, 1901

[6]   E.F. Nichols, G.F. Hull, The Pressure due to Radiation, Phys. Rev. (Series I) 17, 91-104, 1903

[7]   C. Garner, B. Diederich, M. Leipold, A Summary of Solar Sail Technology Developments and Proposed Demonstration Missions. NASA/JPL/DLR, 1999,

[8]   H. Oberth, Die Rakete zu den Planetenräumen, 1923 – e.g. Michaels-Verlag, 1984, ISBN 3-89539-700-8.

[9]   N.N., Raumfahrt – Antrieb – Das Segelschiff, Der Spiegel 25/1958, 18JUN1958, http://magazin.spiegel.de/EpubDelivery/spiegel/pdf/41761638 via https://de.wikipedia.org/wiki/Richard_Garwin, also cf. http://www.nro.gov/history/csnr/leaders/Founders_of_Natl_Reconnaissance.pdf and e.g. https://en.wikipedia.org/wiki/Richard_Garwin; accessed 18NOV2016.

[10] N.N., Blast from The Past – Solar Powered radio from the 50's, www.ecofriend.com (accessed 2011), acopian.com/radio-news.html (accessed 08JAN2018).

[11] J.T. Grundmann, J. Biele, R. Findlay, S. Fredon, T.-M. Ho, C. Krause, S. Ulamec, C. Ziach, One Shot to an Asteroid – MASCOT and the Design of an Exclusively Primary Battery Powered Small Spacecraft in Hardware Design Examples and Operational Considerations, № 3051, European Space Power Conference 2014.

[12] J. Biele, S. Ulamec, M. Maibaum, R. Roll, L. Witte, E. Jurado, P. Muñoz, W. Arnold, H.-U. Auster, C. Casas, C. Faber, C. Fantinati, F. Finke, H.-H. Fischer, K. Geurts, C. Güttler, P. Heinisch, A. Herique, S. Hviid, G. Kargl, M. Knapmeyer, J. Knollenberg, W. Kofman, N. Kömle, E. Kührt, V. Lommatsch, S. Mottola, R. Pardo de Santayana, E. Remetean, F. Scholten, K.J. Seidensticker, H. Sierks, T. Spohn, The landing(s) of Philae and inferences about comet surface mechanical properties, Science, Vol.349, issue 6247, aaa9816-1 (2015).

[13] E. Hand, Comet lander's scientific harvest may be its last – Philae has fallen silent after fragmentary messages, Science, Vol.349, issue 6247, 459-460 (2015);

[14] M. Braun, K. Geurts, S. Ulamec, New command for Philae, http://www.dlr.de/dlr/en/desktopdefault.aspx/tabid-10081/151_read-16365/#/gallery/21643

[15] Wilson, A. (Ed.), Huygens: Science, Payload and Mission, ESA SP-1177.

[16]   http://exploration.esa.int/mars/47852-entry-descent-and-landing-demonstrator-module/, (accessed 08JAN2018).

[17]   Dwayne A. Day, John M. Logsdon and Brian Latell (ed), Eye in the Sky: The Story of the Corona Spy Satellites, Smithsonian Institution Press, 1998, ISBN 1-56098-830-4

[18]   Curtis Peebles, The Corona Project: America's First Spy Satellites, Naval Institute Press (U.S.A.) / Airlife Publishing (UK), 1997, ISBN 1-55750-688-4

[19]   Don P. Mitchell, Sputnik-3, © 2007, http://mentallandscape.com/S_Sputnik3.htm, (accessed 15FEB2018).

[20]   R.L. Dowling, W.J. Kosmann, M.A. Minovitch, R.W. Ridenoure, The Effect of Gravity-Propelled Interplanetary Space Travel on the Exploration of the Solar System: Historical Survey, 1961 to 2000, Proceedings of the 33rd Symposium of the IAA, Amsterdam, The Netherlands, 1999, AAS History Series Vol.28 / IAA History Symposia Vol.19, ISBN 978-0-87703-539-8, 2007, pp.337-432.

[21]   W. Hohmann, Die Erreichbarkeit der Himmelskörper, Oldenbourg Verlag, Munich, 1923; The Attainability of Celestial Bodies, NASA Technical Translation F-44, 1960, pp 79-89

[22]   G.A. Crocco, One-Year Exploration Trip Earth-Mars-Venus-Earth, Proceedings of the 7th IAC, Rome, 1956, pp. 227-252.

[23]   M.A. Minovitch, A Method For Determining Interplanetary Free-Fall Reconnaissance Trajectories, JPL Technical Memo #312-130, Aug. 23rd, 1961.

[24]   M.A. Minovitch, The Determination and Characteristics of Ballistic Interplanetary Trajectories Under the Influence of Multiple Planetary Attractions, JPL Technical Report No. 32-464, Oct. 31st, 1963.

[25]   R.L. Dowling, W.J. Kosmann, M.A. Minovitch, R.W. Ridenoure, The Origin of Gravity-Propelled Interplanetary Space Travel, Proceedings of the 24th History Symposium of the IAA, Dresden, Germany, 1990, AAS History Series Vol.19 / IAA History Symposia Vol.11, ISBN 0-87703-422-2, 1997, pp.63-102.

[26]   M.A. Minovitch, Utilizing Large Planetary Perturbations for the Design of Deep-Space, Solar-Probe, and Out-of-Ecliptic Trajectories, JPL Technical Report No. 32-849, Dec. 15th, 1965.

[27]   R.L. Dowling, W.J. Kosmann, M.A. Minovitch, R.W. Ridenoure, Gravity Propulsion Research at UCLA and JPL, 1962-1964, Proceedings of the 25th History Symposium of the IAA, Montreal, Canada, 1991, AAS History Series Vol.20 / IAA History Symposia Vol.12, ISBN 0-87703-424-9, 1997, pp.27-106.

[28]   G.A. Flandro, Fast Reconnaissance Missions to the Outer Solar System Utilizing Energy Derived from the Gravitational Field of Jupiter, Astronautica Acta Vol.12 No.4, April 18th, 1966, pp.329-337.

[29]   Y. Tsuda, S. Nakazawa, K. Kushiki, M. Yoshikawa, H. Kuninaka, S. Watanabe, Flight status of robotic asteroid sample return mission HAYABUSA2. Acta Astronautica 127, 702-9, 2016. doi: 10.1016/j.actaastro.2016.01.027.

[30]   J. Kawaguchi, A. Fujiwara, T. Uesugi, Hayabusa – Its technology and science accomplishment summary and Hayabusa-2, Acta Astronautica, Vol. 62, 639–647, 2008.

[31]   K. Berry, B. Sutter, A. May, et al., OSIRIS-REx Touch-And-Go (TAG) Mission Design and Analysis. 36th AAS Guidance and Control Conference, Breckenridge, CO, 2013.

[32]   Eldon C. Hall, Journey to the Moon - The History of the Apollo Guidance Computer, AIAA, 1996, ISBN 1-56347-185-X

[33] J.T. Grundmann, J. Biele, M. Drobczyk, C. Lange, S. Montenegro, F. Nohka, J.-C. Schröder, M. Wrasmann, The Ends of Small – Practical Engineering Constraints in the Design of Planetary Defence Missions, IAA-PDC13-04-05P

[34]   Tra-Mi Ho, Volodymyr Baturkin, Christian Grimm, Jan Thimo Grundmann, Catherin Hobbie, Eugen Ksenik, Caroline Lange, Kaname Sasaki, Markus Schlotterer, Maria Talapina, Nawarat Termtanasombat, Elisabet Wejmo, Lars Witte, Michael Wrasmann, Guido Wübbels, Johannes Rößler, Christian Ziach, Ross Findlay, Jens Biele, Christian Krause, Stephan Ulamec, Michael Lange, Olaf Mierheim, Roy Lichtenheldt, Maximilian Meier, Josef Reill, Hans-Jürgen Sedlmayr, Pierre Bousquet,   Anthony Bellion, Olivier Bompis, Céline Cenac-Morthe, Muriel Deleuze, Stéphane Fredon, Eric Jurado, Elisabet Canalias, Ralf Jaumann, Jean-Pierre Bibring, Karl Heinz Glassmeier, David Herčík, Matthias Grott, Luca Celotti, Federico Cordero, Jeffrey Hendrikse, Tatsuaki Okada; MASCOT - The Mobile Asteroid Surface Scout Onboard the HAYABUSA2 Mission; Space Science Reviews, 2016, DOI 10.1007/s11214-016-0251-6

[35] C. Ziach, V. Baturkin, T.-M. Ho, C. Grimm, J.T. Grundmann, C. Lange, N. Termtanasombat, R. Findlay, J. Reill, M. Lange, O. Mierheim, J. Biele, C. Krause, S. Ulamec, B. Borgs, M. Grott, R. Jaumann, M. Deleuze, J.-P. Bibring, H.-U. Auster, and the MASCOT Project Team, MASCOT, the Small Mobile Asteroid Landing

Package on its Piggyback Journey to 1999 JU3: Pre-Launch and Post-Launch Activities, IAC-15-A3.4.6

[36] Andrew Ging, Regaining 20 Watts for the Cassini Power System, 46th AIAA/ASME/SAE/ASEE Joint Propulsion Conference & Exhibit, Nashville, AIAA 2010-6916.

[37] NASA, Juno Mission to Jupiter, https://www.nasa.gov/pdf/316306main_JunoFactSheet_2009sm.pdf , also: JPL/NASA, Jupiter Orbit Insertion Press Kit Juno https://www.jpl.nasa.gov/news/press_kits/juno/pdf/juno-hires.pdf

[38] K.-H. Glassmeier, H. Boehnhardt, D. Koschny, E. Kührt, I. Richter, The Rosetta Mission: Flying Towards the Origin of the Solar System, Space Science Reviews (2006), DOI: 10.1007/s11214-006-9140-8

[39] G. Schwehm, ROSETTA – The comet rendezvous mission, ESA-SP-1179

[40] Michael F. Piszczor, Scott W. Benson, David A., Scheiman, Homer J. Fincannon, Steven R. Oleson, Geoffrey A. Landis, Advanced Solar Cell and Array Technology for NASA Deep Space Missions, 33rd Photovoltaic Specialists Conference, 2008.

[41] M.D. Rayman, The successful conclusion of the Deep Space 1 Mission: important results without a flashy title, Space Technology 23 (2): 185–196 (2003).

[42] D.M. Di Cara, D. Estublier, Smart-1: An analysis of flight data, Acta Astronautica 57 (2–8): 250–256 (2005).

[43] H. Yano, T. Kubota, H. Miyamoto, T. Okada, et al., Touchdown of the Hayabusa Spacecraft at the Muses Sea on Itokawa, Science Vol. 312 (2006), 1350-1353.

[44] http://isa.ifsi-roma.inaf.it/BepiColombo/BC1/BC1.html (accessed 21OCT2014)

[45] L. Johnson, R. Young, E. Montgomery, D. Alhorn, Status of solar sail technology within NASA, Advances in Space Research 48 (2011) 1687-1694.

[46] O. Mori, H. Sawada, R. Funase, T. Endo, M. Morimoto, T. Yamamoto, Y. Tsuda, Y. Kawakatsu, J. Kawaguchi, Development of First Solar Power Sail Demonstrator – IKAROS.

[47] M. Leipold, C.E. Garner, R. Freeland et al., ODISSEE - A Proposal for Demonstration of a Solar Sail in Earth Orbit, 3rd IAA International Conference on Low-Cost Planetary Missions, Laurel, Maryland, April 27 - May 01, 1998

[48] M. Leipold, M. Eiden, C.E. Garner et al., Solar Sail Technology Development and Demonstration, 4th IAA International Conference on Low-Cost Planetary Missions, Laurel, Maryland, May 2-5, 2000

[49] E.K. Jessberger, W. Seboldt, K.-H. Glassmeier, G. Neukum, M. Pätzold, G. Arnold, H.-U. Auster, D. deNiem, F. Guckenbiehl, B. Häusler, G. Hahn, N. Hanowski, A. Harris, H. Hirsch, E. Kührt, M. Leipold, E. Lorenz, H. Michaelis, D. Möhlmann, S. Mottola, D. Neuhaus, H. Palme, H. Rauer, M. Rezazad, L. Richter, D. Stöffler, R. Willnecker, J. Brückner, G. Klingelhöfer, T. Spohn, ENEAS – exploration of near-Earth asteroids with a sailcraft, Technical report, August 2000, Proposal for a Small Satellite Mission within the Space Sciences Program of DLR.

[50] B. Dachwald, W. Seboldt, Multiple near-Earth asteroid rendezvous and sample return using first generation solar sailcraft, Acta Astronautica, 57(11):864–875, 2005.

[51] W. Seboldt, M. Leipold, M. Rezazad, L. Herbeck, W. Unkenbold, D. Kassing, M. Eiden. Groundbased demonstration of solar sail technology. Rio de Janeiro, Brazil, 2000. 51st International Astronautical Congress, IAF-00-S.6.11

[52]   M. Macdonald, G.W. Huges, C.R. McInnes, et al., GEOSAIL: An Elegant Solar Sail Demonstration Mission, Journal of Spacecraft and Rockets, Vol. 44, No 4, pp 784 – 796, 2007

[53]   D. Agnolon, Study Overview of a Solar Sail Demonstrator: GEOSAIL, ESA, SCI-PA/2007/018/Geosail, date of issue: 09/01/2008

[54]   M. Leipold, M. Macdonald, C.R. McInnes, et al., GEOSAIL System Design for Demonstration of Solar Sailing in Earth Orbit, Proceedings of the Second International Symposium on Solar Sailing (ISSS 2010). The New York City College of technology of the City University of New York, July 2010

[55]   U. Geppert, B. Biering, F. Lura, J. Block, R. Reinhard, The 3-Step DLR-ESA GOSSAMER Road to Solar Sailing, ISSS, 2010

[56]   U. Geppert, B. Biering, F. Lura, J. Block, M. Straubel, R. Reinhard, The 3-Step DLR–ESA GOSSAMER road to solar sailing, Advances in Space Research 48 (2011) 1695-1701

[57]   European Code of Conduct for Space Debris Mitigation and Support to Implementation of the European Code of Conduct for Space Debris Mitigation, Issue 1.0 28JUN2004 – also: ISO24113 Space systems, 2011. Space Debris Mitigation Requirements. International Organization for Standardization

[58]   C.D. Grimm, J.T. Grundmann, J. Hendrikse, On Time, On Target – How the Small Asteroid Lander MASCOT Caught a Ride Aboard HAYABUSA-2 in 3 Years, 1 Week and 48 Hours, IAA-PDC15-P-66, Planetary Defence Conference 2015.

[59] J.T. Grundmann, V. Baturkin, et al., "You've got 2 Years, 6 Months, 1 Week and 48 Hours!" – the Ongoing Engineering Adventure of MASCOT and its Implications for Planetary Defence Missions, IAA-PDC13-04-06P.

[60]   Masahiro Umesato, Takakazu Okahashi, Sailing Into Space – Two Men in a Race Against Time, http://www.nec.com/en/global/ad/cosmos/ikaros/.

[61]   P. Seefeldt, T. Spröwitz, Qualification Testing of the GOSSAMER-1 Deployment Technology, Proceedings of the 14th European Conference on Spacecraft Structures, Materials and Environmental Testing (ECSSMET), 2016, #56220.

[62]   J.C. Mankins, Technology Readiness Levels – A White Paper, Advanced Concepts Office, Office of Space Access and Technology, NASA, 1995

[63]   Technology Readiness Levels Handbook for Space Applications, TEC-SHS/5551/MG/ap ed.1, rev.6, Sep.2008

[64]   Technology Readiness Levels (TRL), in: Horizon 2020 Work Programme, General Annexes, Commission Decision C(2014)4995, Part 19

[65]   DoD Interim Defense Acquisition Guidebook, October 30, 2002, formerly DoD 5000.2-R.

[66]   Nolte, Technology Readiness Calculator, AFRL, 2003. http://www.dtic.mil/ndia/2003/systems/nolte2.pdf , accessed 29APR2017.

[67] P. Spietz, J.T. Grundmann, P. Seefeldt, T. Spröwitz, GOSOLAR: Large-scale Deployable Photovoltaics for Planetary Defence and Small Solar System Body Applications using GOSSAMER Deployment Technologies, this conference, IAA-PDC17-05-P24

[68] P. Seefeldt, W. Bauer, B. Dachwald, J.T. Grundmann, M. Straubel, M. Sznajder, N. Toth, M.E. Zander, Large Lightweight Deployable Structures for Planetary Defence: Solar Sail Propulsion, Solar Concentrator Payloads, Large-scale Photovoltaic Power, IAA-PDC-15-P-20

[69]   P. Spietz, J.T. Grundmann, P. Seefeldt, T. Spröwitz, GOSOLAR: Large-scale Deployable Photovoltaics for Planetary Defence and Small Solar System Body

Applications using GOSSAMER Deployment Technologies, *this conference*, IAA-PDC-17-05-P24

[70]   J.T. Grundmann, P. Spietz, P. Seefeldt, T. Spröwitz, GOSSAMER Deployment Systems for Flexible Photovoltaics, Proceedings of the 67th International Astronautical Congress (IAC), Guadalajara, Mexico, 26-30 September 2016, ISBN 9781510835825, IAC-16-C3.3.6

[71]   A. Peloni, M. Ceriotti, B. Dachwald, Solar-Sail Trajectory Design for a Multiple Near-Earth-Asteroid Rendezvous Mission, Journal of Guidance, Control, and Dynamics, Vol. 39, No. 12, 2016, pp. 2712-2724, DOI: 10.2514/1.G000470

[72]   Peloni, A., Dachwald, B. and Ceriotti, M., "Multiple Near-Earth Asteroid Rendezvous Mission: Solar-Sailing Options", Advances in Space Research (accepted for publication). DOI: 10.1016/j.asr.2017.10.017.

[73]   P. Seefeldt, T. Spröwitz, P. Spietz, J.T. Grundmann, R. Jahnke, E. Mikulz, S. Reershemius, K. Sasaki, N. Tóth, Qualification Tested Technologies of the GOSSAMER-1 Solar Sail Deployment Demonstrator for Planetary Defence and Small Solar System Body Science and Applications, *this conference*, IAA-PDC-17-05-P23

[74]   Tom Spröwitz, Patric Seefeldt, Peter Spietz, Rico Jahnke, Jan Thimo Grundmann, Eugen Mikulz, Thomas Renger, Siebo Reershemius, Kaname Sasaki, Maciej Sznajder, Norbert Tóth, Membrane Deployment Technology Development at DLR for Solar Sails and Large-Scale Photovoltaics, 8.0618, ID:2867, IEEE Aerospace Conference 2018 (*accepted*).

[75]   Y. Tsuda, O. Mori, et al., Flight result and analysis of solar sail deployment experiment using S-310 sounding rocket, Space Technology, Vol. 26, 33-39, 2006.

[76]   O. Mori, Y. Shirasawa, H. Sawada, Y. Mimasu, Y. Tsuda, R. Funase, T. Saiki, T. Yamamoto, N. Motooka, Y. Kishino, J. Kawaguchi, IKAROS Extended Mission and Advanced Solar Power Sail Mission, 63rd IAC 2012, IAC-12,D1,1,3,x15786

[77]   S. Matunaga, S. Inagawa, T. Nishihara, S. Kimura, H. Sawada, O. Mori, K. Kitamura, Structure team of IKAROS, in: Proceedings of 28th International Symposium on Space Technology and Science, 2011-o-4-07v, 2011

[78]   T. Yamaguchi, Y. Mimasu, Y. Tsuda, R. Funase, H. Sawada, O. Mori, M.Y. Morimoto, H. Takeuchi, M. Yoshikawa, Trajectory Analysis of Solar Sail Spacecraft Considering the Large Uncertainty of Solar Radiation Pressure, ISSFD21, 2009.

[79]   H. Yano, O. Mori, S. Matsuura, R. Funase, R.Nakamura, F. Yoshida, E. Kokubo, N. Takato, IKAROS Team, JAXA Solar Power Sail Working Group, The Solar Power Sail Mission to Jupiter Trojans, 10th IAA LCPM 2013, S5

[80]   J. Kawaguchi, O. Mori, Y. Shirasawa, M. Yoshikawa, On the Trojan asteroid sample and return mission via solar-power sail – an innovative engineering demonstration, ACM2014.

[81]   O. Mori, H. Kato, J. Matsumoto, T. Saiki, Y. Tsuda, N. Ogawa, Y. Mimasu, J. Kawaguchi, K. Tanaka, H. Toyota, N. Okuizumi, F. Terui, A. Tomiki, S. Kawasaki, H. Kuninaka, K. Nishiyama, R. Tsukizaki, S. Hosoda, N. Bando, K. Yamada, T. Okada, T. Iwata, H. Yano, Y. Kebukawa, J. Aoki, M. Otsuki, R. Nakamura, C. Okamoto, S. Matsuura, D. Yonetoku, A. Matsuoka, R. Nomura, R. Boden, T. Chujo, Y. Oki, Y. Takao, K. Ikemoto, K. Koyama, H. Kinoshita, S. Kitao, T. Nakamura, H. Ishida, K. Umeda, S. Kashioka, M. Kadokura, M. Kurakawa, M. Watanabe, Direct Exploration of Jupiter Trojan Asteroid using Solar Power Sail, #17087, 4th International Symposium on Solar Sailing, Kyoto, 2017

[82]   J. Castillo-Rogez, L. Johnson, P. Abell, J. Bleacher, J. Boland, B. Farrell, L. Graham, D. Thompson and the NEAScout Team, Near Earth Asteroid Scout Mission, 2014

[83]   L. Johnson, J. Castillo-Rogez, J. Dervan, L. McNutt, Near Earth Asteroid (NEA) Scout, #17002, 4th International Symposium on Solar Sailing, Kyoto, 2017

[84]   T. Russel Lockett, A. Few, R. Wilson, Near Earth Asteroid Solar Sail Engineering Development Unit Test Program, #17054, 4th International Symposium on Solar Sailing, Kyoto, 2017

[85]   A. Heaton, N. Ahmad, K. Miller, Near Earth Asteroid Scout Solar Sail Thrust and Torque Model, #17055, 4th International Symposium on Solar Sailing, Kyoto, 2017

[86]   J. Orphee, B. Diederich, B. Stiltner, C. Becker, A. Heaton, Solar Sail Attitude Control System for the NASA Near Earth Asteroid Scout Mission, #17091, 4th International Symposium on Solar Sailing, Kyoto, 2017

[87]   O. Stohlman, E.Loper, T. Lockett, Temperature-Driven Shape Changes of the Near Earth Asteroid Scout Solar Sail, #17041, 4th International Symposium on Solar Sailing, Kyoto, 2017

[88]   J.M. Fernandez, G.K. Rose, O.R. Stohlman, C.J. Younger, G.D. Dean, J.E. Warren, J.H. Kang, R.G. Bryant, W.K. Wilkie, An Advanced Composites-Based Solar Sail System for Interplanetary Small Satellite Missions, AIAA Scitech 2018, Kissimmee, Florida, USA

[89] J.M. Fernandez, G.K. Rose C.J. Younger, G.D. Dean, J.E. Warren, O.R. Stohlman, W.K. Wilkie, NASA's advanced solar sail propulsion system for low-cost deep space exploration and science missions that uses high performance rollable composite booms, #17067, 4th International Symposium on Solar Sailing, Kyoto, 2017

[90]   J.M. Fernandez, Advanced Deployable Shell-Based Composite Booms For Small Satellite Structural Applications Including Solar Sails, #17089, 4th International Symposium on Solar Sailing, Kyoto, 2017

[91]   B. Doncaster, J. Shulman, 2016 Nano/Microsatellite Market Assessment Overview, http://www.spaceworksforecasts.com/docs/SpaceWorks_Nano_Microsatellite_Market_Forecast_2016.pdf

[92]   UNOOSA, ITU, Guidance on Space Object Registration and Frequency Management for Small and Very Small Satellites, http://www.unoosa.org/documents/pdf/psa/bsti/2015_Handout-on-Small-SatellitesE.pdf , p.2

[93]   P. Fortescue, G. Swinerd, J. Stark, Spacecraft Systems Engineering, chapter 18

[94]   E. Mabrouk, What are SmallSats and CubeSats, https://www.nasa.gov/content/what-are-smallsats-and-cubesats , Feb.26th, 2015, last updated Aug.4th, 2017

[95]   M. Swartwout, Twenty (plus) Years of University-Class Spacecraft: A Review of What Was, An Understanding of What Is, And a Look at What Should Be Next, SSC06-I-3, http://digitalcommons.usu.edu/cgi/viewcontent.cgi?article=1532&context=smallsat

[96]   J. Thiery, ASAP and VESPA: the access to space for Small Satellites, SSC09-IX-4

[97]   Evolved Expendable Launch Vehicle Rideshare User's Guide, May 2016, https://explorers.larc.nasa.gov/HPSMEX/SMEX/pdf_files/EELV-RideshareUsersGuide-v1-Signed[188].pdf

[98]   C. Lange, T.-M. Ho, C.D. Grimm, J.T. Grundmann, C. Ziach, R. Lichtenheld, Exploring Small Bodies: Nanolander and -spacecraft options derived from the Mobile Asteroid Surface Scout, Advances in Space Research, 2017 (*submitted*)

[99]   Lura, F. und Biering, Bernd und Lötzke, Horst Georg und Studemund, H. und Baturkin, Volodymyr (2007) BIRD Micro satellite Thermal Control System - 5 Years of Operation in Space. In: Small Satellites for Earth Observation. Selected Contribution Springer. Seiten 277-284. ISBN 978-1-4029-6942-0. http://elib.dlr.de/106278/

[100] Axmann, Robert und Gude, Julian und Mühlbauer, Peter (2011) TET-1 Satellite Operations Lessons Learned: Preparation of Mission, LEOP and Routine Operations of 11 Different Experiments. 62nd International Astronautical Congress, 03.-07.10.2011 , Cape Town, South Africa. http://elib.dlr.de/74418/1/IAC-11.D1.5.6.pdf

[101] Findlay, Ross und Eßmann, Olaf und Grundmann, Jan Thimo und Hoffmann, Harald und Kührt, Ekkehard und Messina, Gabriele und Michaelis, H. und Mottola, S. und Müller, H. und Pedersen, Jakob Fromm (2012) A space-based mission to characterize the IEO population. Acta Astronautica, 90 (1), Seiten 33-40. Elsevier. DOI: 10.1016/j.actaastro.2012.08.004 ISSN 0094-5765 http://elib.dlr.de/86965/

[102] B. Dachwald, H. Boehnhardt, U. Broj, U.R.M.E. Geppert, J.T. Grundmann, W. Seboldt, P. Seefeldt, P. Spietz, L. Johnson, E. Kührt, S. Mottola, M. Macdonald, C.R. McInnes, M. Vasile, R. Reinhard, Gossamer Roadmap Technology Reference Study for a Multiple NEO Rendezvous Mission, Advances in Solar Sailing, Springer Praxis 2014, pp 211-226.

[103] M. Macdonald, C. McGrath, T. Appourchaux, B. Dachwald, W. Finsterle, L. Gizon, P.C. Liewer, C.R. McInnes,G. Mengali, W. Seboldt, T. Sekii, S.K. Solanki, M. Velli, R.F. Wimmer-Schweingruber, P. Spietz, R. Reinhard, Gossamer Roadmap Technology Reference Study for a Solar Polar Mission, in: M. Macdonald (ed.), Advances in Solar Sailing, 2014 (3rd International Symposium on Solar Sailing)

[104] C.R. McInnes, V. Bothmer, B. Dachwald, U.R.M.E. Geppert, J. Heiligers, A. Hilgers, L. Johnson, M. Macdonald, R. Reinhard, W. Seboldt, P. Spietz, Gossamer Roadmap Technology Reference Study for a Sub-L1 Space Weather Mission, in: M. Macdonald (ed.), Advances in Solar Sailing, 2014 (3rd International Symposium on Solar Sailing)

[105] P. Michel, M. Kueppers, H. Sierks, et al., AIM-D2: Asteroid Impact Mission – Deflection Demonstration to the binary asteroid Didymos. Advances in Space Research, 2017 (*submitted*)

[106] J. Biele, S. Ulamec, C. Krause, B. Cozzoni, C. Lange, J.T. Grundmann, C. Grimm, T.-M. Ho, A. Herique, D. Plettemeier, H.-U. Auster, D. Herčík, I. Carnelli, A. Galvez, C. Philippe, M. Küppers, B. Grieger, J. Gil Fernandez, J. Grygorczuk, M. Tokarz, MASCOT2, a Lander to Characterize the Target of an Asteroid Kinetic Impactor Deflection Test Mission, *this conference*, IAA-PDC-17-05-P14

[107] Lange, C., Ho, T.-M., Ziach, C., Witte, L., Grimm, C.D., Grundmann, J.T., Rosta, R., (2015) Nanoscale landers and instrument carriers: enhancing larger mission's science return by investing in low cost solutions: the MASCOT‐1 to X and ROBEX examples. In: 11th Low Cost Planetary Missions Conference. 11th Low Cost Planetary Missions Conference, June 9-11, 2015, Berlin, Germany; also: http://www.robex-allianz.de/en/about-robex/demo-missions/   →   Space, http://www.robex-allianz.de/en/about-robex/topic-2000-system-infrastructure/

[108] Seefeldt, P., Spietz, P., Sproewitz, T., Grundmann, J.T., Hillebrandt, M., Hobbie, C., Ruffer, M., Straubel, M., Tóth, N., Zander, M., Gossamer-1: Mission

Concept and Technology for a Controlled Deployment of Gossamer Spacecraft, Advances in Space Research 59.1 (2017): 434-456, 2017, doi: http://dx.doi.org/10.1016/j.asr.2016.09.022

[109] https://en.wikipedia.org/wiki/Pioneer_6,_7,_8,_and_9 , https://de.wikipedia.org/wiki/Pioneer_6 (accessed 26APR2017)

[110] Data available online at https://cneos.jpl.nasa.gov/orbits/elements.html , retrieved 24FEB2018

[111] G. Hahn et al., Data Base of Physical and Dynamical Properties of Near Earth Asteroids (NEAs), http://earn.dlr.de/nea/, accessed 24FEB2018.

[112] NEODyS-2 Near Earth Objects - Dynamic Site, http://newton.dm.unipi.it/neodys/index.php (accessed 24FEB2018)

[113] B. Dachwald, R. Kahle, B. Wie, Solar Sailing Kinetic Energy Impactor (KEI) Mission Design Tradeoffs for Impacting and Deflecting Asteroid 99942 Apophis, AIAA/AAS Astrodynamics Specialist Conference and Exhibit, AIAA 2006-6178.

[114] B. Dachwald, R. Kahle, B. Wie, Head-On Impact Deflection of NEAs: A Case Study for 99942 Apophis, AIAA, Planetary Defense Conference 2007.

[115] B. Dachwald, B. Wie, Solar Sail Kinetic Energy Impactor Trajectory Optimization for an Asteroid-Deflection Mission, Journal of Spacecraft and Rockets, Vol. 44, No. 4, July–August 2007, DOI: 10.2514/1.22586.

[116] https://space.frieger.com/asteroids/asteroids/341843-2008-EV5

[117] M.W. Busch, S.J. Ostro, L.A.M. Benner, M. Brozovic, J.D. Giorgini, J.S. Jao, D.J. Scheeres, C. Magri, M.C. Nolan, E.S. Howell, P.A. Taylor, J.-L. Magot, W. Brisken, Radar observations and the shape of near-Earth asteroid 2008 EV5, Icraus 212 (2011) 649-660

[118] I. Pelivan, L. Drube, E. Kührt, J. Helbert, J. Biele, M. Maibaum, B. Cozzoni, V. Lommatsch, Thermophysical modeling of Didymos' moon for the Asteroid Impact Mission, Advances in Space Research, Apr. 2017, vol. 59, pp.1936-1949, doi: 10.1016/j.asr.2016.12.041, http://adsabs.harvard.edu/abs/2017AdSpR..59.1936P ..

[119] D.M. Reeves, D.D. Mazanek, B.D. Cichy, S.B. Broschart, K.D. Deweese, Asteroid Redirect Mission Proximity Operations for Reference Target Asteroid 2008 EV$_5$, 39th Annual AAS Guidance and Control Conference, AAS Paper 16-105, 2016.

[120] P. Seefeldt. A stowing and deployment strategy for large membrane space systems on the example of GOSSAMER-1. Advances in Space Research 60.6 (2017): 1345-1362, 2017

[121] P. Seefeldt, T. Spröwitz, P. Spietz, E. Mikulz, S. Reershemius, K. Sasaki, N. Tóth, R. Jahnke, Controlled Deployment of Gossamer Spacecraft. Proceedings of the Fourth International Symposium on Solar Sailing, 2017

[122] P. Seefeldt, T. Spröwitz, J.T. Grundmann, Verification Testing of the GOSSAMER-1 Deployment Demonstrator, Proceedings of the 67th International Astronautical Congress (IAC), Guadalajara, Mexico, 26-30 September 2016, ISBN 9781510835825, IAC-16-C3.3.6

[123] Seefeldt P. and Spietz, P., Raumfahrzeug-Membranentfaltungssystem und Verfahren zum Betrieb desselben, Patent 10 2016 101 430.3, Patent Filed 2016

[124] S. Montenegro, T. Walter, M. Faisal, N. Tóth, F. Dannemann, Wireless Avionics for a Solar Sailer, DASIA 2012 DAta Systems In Aerospace, May 14th to 16th, 2012, Dubrovnik, Croatia

[125] T. Mikschl S. Montenegro A. Hilgarth F. Kempf K. Schilling T. Tzschichholz, Resource sharing, communication and control for fractionated spacecraft (YETE), 10th Symposium on Small Satellites for Earth Observation, April 8 - 12, 2015, Berlin, Germany

[126] A. Hilgarth, T. Mikschl, S. Montenegro, K. Schilling, F. Kempf, A. Kheirkhah, T. Tzschichholz, YETE: Robuste, verteilte Systeme im Automotive- und Aerospacebereich durch eine modulare, flexible Echtzeitplattform, Deutscher Luft- und Raumfahrtkongress, 16. - 18. September 2014, Augsburg

[127] S. Montenegro, K. Schilling. YETE: Distributed, Networked Embedded Control Approaches for Efficient, Reliable Mobile Systems, embedded world Conference 2014, 25.-27.2.2014, Nuremberg, Germany

[128] J.T. Grundmann, J. Biele, B. Dachwald, C.D. Grimm, C. Lange, S. Ulamec, C. Ziach, T. Spröwitz, M. Ruffer, P. Seefeldt, P. Spietz, N. Tóth, J. Kawaguchi, O. Mori, A. Rittweger, J.-P. Bibring, A. Braukhane, R. Boden, T. Chujo, E. Dumont, S. Jahnke, M. Jetzschmann, H. Kato, H. Krüger, M. Lange, A. Martelo Gomez, D. Massonett, Y. Mimasu, T. Okada, M. Sagliano, K. Sasaki, S. Schröder, M. Sippel, T. Skoczylas, E. Wejmo, Small Landers and Separable Sub-Spacecraft for Near-term Solar Sails, #17094, 4th International Symposium on Solar Sailing, Kyoto, 2017

[129] Sinn T., et al. "ADEO passive de-orbit subsystem activity leading to a dragsail demonstrator: conclusions and next steps", Proceeding of 68th International Astronautical Congress (IAC), Adelaide, Australia, 25-29 Sept. 2017.

[130] N. V. Meyer, "Basics of the Solar Wind", Cambridge University Press, 2007.

[131] Eichler J., "Lectures in ion-atom collisions, from nonrelativistic to relativistic velocities", Chapter 10, Elsevier B.V., Amsterdam, 2005.

[132] Hagstrum H. D., "Theory of Auger Ejection of Electrons from Metals by Ions", Physical Review, Vol. 96, 1954, pp. 336-365

[133] Sols S., Flores F., "Charge transfer processes for light ions moving in metals", Physical Review B, vol. 30, 1984, pp. 4478-4880.

[134] Sznajder M., Geppert U., Dudek M., "Degradation of metallic surraces under space conditions, with particular emphasis on Hydrogen recombination processes", Advances in Space Research, vol. 56, 2015, pp. 71-84

[135] M. Sznajder, U. Geppert and M. R. Dudek, Hydrogen blistering under extreme radiation conditions npj Materials Degradation 2, 3 (2018). doi:10.1038/s41529-017-0024-z

[136] ECSS-Q-ST-70-06C, "Particle and UV radiation testing for space materials", 2008

[137] ASTM E512-94, "Standard particle for combined, simulated space environment testing of thermal control materials with electromagnetic and particular radiation", 2010.

[138] Renger T., Sznajder M., Witzke A., Geppert U., „The Complex Irradiation Facility at DLR-Bremen", Journal of Materials Science and Engineering A, vol. 4, 2014, pp. 1-9.

[139] M. Sznajder, J.T. Grundmann, T. Renger, Experimental Studies of Space Weathering Effects on Thin Membranes in Planetary Defence Applications and Asteroid Surface Materials by a Complex Irradiation Facility, *this conference*, IAA-PDC-17-05-P25

[140] M. Sznajder, U. Geppert, M. Marć, Degradation of thin solar-sail membrane films under interplanetary medium, , #17011, 4th International Symposium on Solar Sailing, Kyoto, 2017

[141] E. Dumont, E. David, Ariane 5 ECA VA212 and Ariane 5 Mea: Updated models (Status September 2013), 2013, SART-TN019-2013.

[142] eoPortal Directory, LPF (LISA Pathfinder) Mission , https://directory.eoportal.org/web/eoportal/satellite-missions/l/lisa-pathfinder (accessed 23FEB2018)

[143]   J.T. Grundmann, U. Auster, V. Baturkin, A. Bellion, J.-P. Bibring, J. Biele, O. Bompis, B. Borgs, P. Bousquet, E. Canalias, L. Celotti, C. Cenac-Morthe, F. Cordero, M. Deleuze, C. Evesque, R. Findlay, S. Fredon, K.-H. Glaßmeier, D. Granena, C.D. Grimm, M. Grott, V. Hamm, J. Hendrikse, D. Herčík, T.-M. Ho, R. Jaumann, C. Krause, R. Kroth, E. Ksenik, C. Lange, M. Lange, O. Mierheim, T. Okada, J. Reill, K. Sasaki, N. Schmitz, H.-J. Sedlmayr, M. Talapina, S. Tangruamsub, N. Termtanasombat, S. Ulamec, E. Wejmo, M. Wrasmann, T. Yoshimitsu, C. Ziach, and the MASCOT Team, Mobile Asteroid Surface Scout (MASCOT) – Design, Development and Delivery of a Small Asteroid Lander aboard HAYABUSA-2, IAA-PDC15-P-64

[144]   E. Morrow, D.J. Scheeres, D. Lubin, Solar Sail Orbits at Asteroids, AIAA Paper 2000-4420

[145]   E. Morrow, D.J. Scheeres, D. Lubin, Solar Sail Orbit Operations at Asteroids: Exploring the Coupled Effect of an Imperfectly Reflecting Sail and a Nonspherical Asteroid, AIAA/AAS Astrodynamics Specialist Conference and Exhibit, 5-8 August 2002, Monterey, California, AIAA 2002-4991

[146] A. Farrés, À. Jorba, J.-M. Mondelo, Orbital Dynamics for a Non-Perfectly Reflecting Solar Sail Close to an Asteroid, IAA-AAS-DyCoSS1 -11-09, 2009

[147] eoPortal Directory, PRISMA (Prototype Research Instruments and Space Mission technology Advancement), https://directory.eoportal.org/web/eoportal/satellite-missions/p/prisma-prototype (accessed 23FEB2018)

[148] JAXA, Engineering Test Satellite VII "KIKU-7" (ETS-VII), http://global.jaxa.jp/projects/sat/ets7/index.html (accessed 24FEB2018)

[149] Isao Kawano, Masaaki Mokuno, Hiroshi Horiguchi, Koichi Kibe, In-orbit demonstration of an unmanned automatic rendezvous and docking system by the Japanese engineering test satellite ETS-VII, https://doi.org/10.2514/6.1994-3648, AIAA-94-3648-CP, Guidance, Navigation, and Control Conference Scottsdale,AZ,U.S.A.

[150] M. Oda, Rendezvous docking and space robot experiments on NASDA's ETS-VII satellite -An overview of the project and experiment results-, https://pdfs.semanticscholar.org/b770/16385ec8b19ccb4af7820eec316eec03cdf8.pdf (accessed 24FEB2018)

[151] Tardivel, S., Michel, P., & Scheeres, D. J. (2013). Deployment of a lander on the binary asteroid (175706) 1996 FG3, potential target of the european MarcoPolo-R sample return mission. Acta Astronautica, 89, 60-70.

[152] Tardivel, S., Scheeres, D. J., & Michel, P. (2014). High-altitude deployment of landers to asteroid surfaces using natural manifolds. In 24th AAS/AIAA Space Flight Mechanics Meeting (No. 14-355).

[153] Tardivel, S., & Scheeres, D. J. (2014). Accurate Deployment of Landers to dynamically challenging asteroid. In 24th AAS/AIAA Space Flight Mechanics Meeting (No. 15-424).

[154] Tardivel, S., Scheeres, D. J., Michel, P., Van wal, S., & Sánchez, P. (2014). Contact motion on surface of asteroid. Journal of Spacecraft and Rockets, 51(6), 1857-1871.

[155] Biele, J., Kesseler, L., Grimm, C. D., Schröder, S., Mierheim, O., Lange, M., & Ho, T. M. (2017). Experimental Determination of the Structural Coefficient of Restitution of a Bouncing Asteroid Lander. arXiv preprint arXiv:1705.00701.

[156] Drube, Line & W. Harris, Alan & Engel, Kilian & Falke, Albert & Johann, Ulrich & Eggl, Siegfried & Cano, Juan & Martín Ávila, Javier & Schwartz, Stephen & Michel,

Patrick. (2016). The NEOTωIST mission (Near-Earth Object Transfer of angular momentum spin test). Acta Astronautica. 127. 10.1016/j.actaastro.2016.05.009.

[157] Eggl, Siegfried & Hestroffer, D & Cano, Juan & Martin Avila, Javier & Drube, Line & W. Harris, Alan & Falke, Albert & Johann, Ulrich & Engel, Kilian & Schwartz, Stephen & Michel, Patrick. (2016). Dealing with Uncertainties in Asteroid Deflection Demonstration Missions: NEOTwIST. Proceedings of the International Astronomical Union. 10. 10.1017/S1743921315008698.,

[158] A Engel, Kilian & Pugliatti, Mattia & Eggl, Siegfried & Hestroffer, D & Falke, Albert & Johann, Ulrich & Harris, Alan & Drube, Line & Cano, Juan. (2016). NEOTωIST -An Asteroid Impactor Mission Featuring Sub-spacecraft for Enhanced Mission Capability, IAC-16,B4,8,7,x34163, 67th International Astronautical Congress (IAC), Guadalajara, Mexico, 26-30 September 2016

[159] Weisenberger, Steffen & Drube, Line & Montenegro, Sergio. (2016). Instrumentation for an asteroid kinetic-impactor demonstration mission, Final Stardust Conference, 31st Oct - 4th Nov 2016, ESA-ESTEC, The Netherlands

[160] M. Thiel, J. Stöcker, C. Robe, N.I. Kömle, G. Kargl, O. Hillenmaier, P. Lell, The Rosetta Lander Anchoring System, 2003.

[161] M. Hilchenbach, Simulation of the Landing of Rosetta Philae on Comet 67P/Churyumov-Gerasimenko, SIMPACK User Meeting, 2004, p. 25.

[162] Tardivel, S. C. V. (2014). The deployment of scientific packages to asteroid surfaces (Doctoral dissertation, University of Colorado at Boulder).

[163] P. Pravec et al., Large Coherent Asteroid 2001 OE84, http://articles.adsabs.harvard.edu/cgi-bin/nph-iarticle_query?2002ESASP.500..743P&data_type=PDF_HIGH&whole_paper=YES&type=PRINTER&filetype=.pdf

[164] David Polishook, Nicholas Moskovitz, Audrey Thirouin, Amanda Bosh, Stephen Levine, Carlos Zuluaga, Stephen Tegler, Oded Aharonson, The fast spin of near-Earth asteroid (455213) 2001 OE84, revisited after 14 years: constraints on internal structure, https://arxiv.org/pdf/1707.01367.pdf

[165] A. Harris, NEA Population and Current Survey Status, *this conference*, IAA-PDC-17-02-01

[166] J.T. Grundmann, S. Mottola, M. Drentschew, M. Drobczyk, R. Findlay, A. Heidecker, R. Kahle, E. Kheiri, A. Koch, V. Maiwald, O. Mierheim, F. Nohka, D. Quantius, M. Siemer, P. Zabel, T. van Zoest, AsteroidSQUADS/*i*SSB – a Synergetic NEO Deflection Campaign and Mitigation Effects Test Mission Scenario, IAA-WPP-323 S5_0910_2162714

[167] L. Riu, J-P. Bibring, V. Hamm, et al., Calibration of MicrOmega Hayabusa-2 Flight Model – First Results, 47th LPSC 2016, #2109. – also: C. Pilorget, J.-P. Bibring, NIR reflectance hyperspectral microscopy for planetary science: Application to the MicrOmega instrument. Planetary and Space Science, 76(1):42{52, 2013. ISSN 00320633. doi: 10.1016/j.pss.2012.11.004.

[168] R. Jaumann, N. Schmitz, A. Koncz, H. Michaelis, S.E. Schroeder, S. Mottola, F. Trauthan, H. Hoffmann, T. Roatsch, D. Jobs, J. Kachlicki, B. Pforte, R. Terzer, M. Tschentscher, S. Weisse, U. Mueller, L. Perez-Prieto, B. Broll, A. Kruselburger, T.-M. Ho, J. Biele, S. Ulamec, C. Krause, M. Grott, J.-P. Bibring, S. Watanabe, S. Sugita, T. Okada, M. Yoshikawa, H. Yabuta, The Camera of the MASCOT Asteroid Lander on Board Hayabusa2; Space Science Reviews, 2016, DOI 10.1007/s11214-016-0263-2

[169] M. Grott, J. Knollenberg, B. Borgs, F. Hänschke, E. Kessler, J. Helbert, A. Maturilli, N. Müller, The MASCOT Radiometer MARA for the Hayabusa 2 Mission, Space Science Reviews, 2016, DOI 10.1007/s11214-016-0272-1

[170] David Herčík, Hans-Ulrich Auster, Jürgen Blum, Karl-Heinz Fornaçon, Masaki Fujimoto, Kathrin Gebauer, Carsten Güttler, Olaf Hillenmaier, Andreas Hördt, Evelyn Liebert, Ayako Matsuoka, Reiko Nomura, Ingo Richter, Bernd Stoll, Benjamin P. Weiss, Karl-Heinz Glassmeier, The MASCOT Magnetometer; Space Science Reviews, 2016, DOI 10.1007/s11214-016-0236-5

[171] JAXA press release, Name Selection of Asteroid 1999 JU3 Target of the Asteroid Explorer "Hayabusa2", http://global.jaxa.jp/press/2015/10/20151005_ryugu.html , also http://www.minorplanetcenter.net/iau/lists/Numbered MPs160001.html , http://scully.cfa.harvard.edu/cgi-bin/showcitation.cgi?num=162173 (09OCT2015)

[172] C. Ziach, et al., MASCOT, the Small Mobile Asteroid Landing Package on its Piggyback Journey to 1999 JU3: Pre-Launch and Post-Launch Activities, IAC-15-A3.4.6

[173] C. Lange, R. Findlay, C. Grimm, et al., "How to build a 10 kg autonomous Asteroid landing package with 3 kg of instruments in 6 years?" – Systems Engineering challenges of a high-density deep space system in the DLR MASCOT project, 2624640 (1325), SECESA 2012.

[174] R. Findlay, T.-M. Ho, C. Lange, et al., A Small Asteroid Lander Mission to Accompany HAYABUSA-II, Proceedings of the 63rd International Aeronautical Congress, Naples, Italy, 2012, IAC-12-A3.4.7.

[175] C. Ziach, T.-M. Ho, C. Grimm, R. Findlay, C. Lange, et al., The Final Stages of MASCOT, a Small Asteroid Lander to Accompany HAYABUSA-II, IAC-13-A.3.4.6.

[176] M. Lange, O. Mierheim, C. Hühne. MASCOT - Structures Design and Qualification of an "Organic" Mobile Lander Platform for Low Gravity Bodies. Proc. of '13th European Conference on Space Structures, Materials & Environmental Testing', Braunschweig, Germany, ESA SP-727 (June 2014)

[177] M. Lange, et al. MASCOT - A Lightweight Multi-Purpose Lander Platform. Proc. of 12th European Conf. on Space Structures, Materials & Environmental Testing, Noordwijk, ESA SP-691 (July 2012)

[178] E. Canalias, M. Deleuze, et al., Analysis of the Descent and Bouncing Trajectory of MASCOT on 1999JU3, IPPW2015-6105, International Planetary Probe Workshop, 2015, Cologne

[179] L. Celotti, et al., MASCOT thermal subsystem design challenges and solution for contrasting requirements, 45th Intern'l Conf. on Environmental Systems, ICES-2015-83

[180] P. Michel, A. Cheng, et al., Science case for the Asteroid Impact Mission (AIM): A component of the Asteroid Impact & Deflection Assessment (AIDA) mission, Advances in Space Research (57): 2529-2547 (2016).

[181] A.F. Cheng, J. Atchison, et al., Asteroid impact and deflection assessment mission, Acta Astronautica 115: 262-269 (2015).

[182] A.F. Cheng, P Michel, M. Jutzi, et al., Asteroid Impact & Deflection Assessment mission: Kinetic impactor. Planetary and Space Science 121 (2016), 27–35. doi:10.1016/j.pss.2015.12.004

[183] A.F. Cheng, C.L.B. Reed, Asteroid Impact & Deflection Assessment: Double Asteroid Redirection Test, IAC-16-A3.4.10

[184] A. Herique, D. Plettemeier, V. Ciarletti, B. Agnus, J. Du, W. Fa, O. Gassot, R. Granados-Alfaro, J. Grygorczuk, C. Hoarau, W. Kofman, M. Laabs, C. Le Gac, M.

Mütze, S. Rochat, Y. Rogez, P. Schaffer, M. Tokarz, A.-J. Vieau, J. Biele, C. Buck, I. Carnelli , J. Gil Fernandez, A. Galvez, B. Grieger, J.T. Grundmann, T.-M. Ho, C. Krause, M. Küppers, C. Lange, C. Philippe, R. Rodriguez Suquet, S. Ulamec, Radar Package for a Direct Observation of the Asteroid's Structure from Deep Interior to Regolith, *this conference*, IAA-PDC-17-05-P18

[185]   A. Herique, V. Ciarletti, A Direct Observation of the Asteroid's Structure from Deep Interior to Regolith: Two Radars on the AIM Mission. 47th Lunar and Planetary Science Conference (2016).

[186]   A. Herique, B. Agnus, E. Asphaug, et al., Direct Observations of Asteroid Interior and Regolith Structure: Science Measurement Requirements, Advances in Space Research, 2018 (*submitted*)

[187]   S. Ulamec, J. Biele, J.T. Grundmann, J. Hendrikse, C. Krause, Relevance of PHILAE and MASCOT in-situ Investigations for Planetary Defense, IAA-PDC15-04-08.

[188]   J.T. Grundmann, J. Biele, B. Dachwald, C.D. Grimm, C. Lange, J.-G. Meß, P. Seefeldt, P. Spietz, T. Spröwitz, S. Ulamec, Small Spacecraft in Small Solar System Body Applications, IEEE 2017, 2.1212.

[189]   A. Herique, J. Biele, P. Bousquet, V. Ciarletti, V., T.-M. Ho, J.L. Issler, W. Kofman, P. Michel, D. Plettemeier, P. Puget, J.C. Souyris, S. Ulamec, T. van Zoest, S. Zine, FANTINA: Fathom Asteroids Now: Tomography and Imagery of a NEA - Payload For Marco Polo R CV3 / ESA mission. EGU General Assembly Conference Abstracts, p. 9633

[190]   VRmDC-8 PRO (color), VRmagic, 2009.

[191]   Techspec Fixed Focal Length Lens Specifications, Edmund Optics, 2015.

[192]   For Machine Vision H1214-M, 12 mm 1:1.4, Pentax Optics, 2003.

[193]   M. Hamm, M. Grott, I. Pelivan, J. Knollenberg, J.T. Grundmann, T. Okada, S. Tanaka, H. Senshu, T. Arai, N. Sakatani, In-Situ Determination of Asteroid Thermal Inertia using the MASCOT Radiometer, *this conference*, IAA-PDC-17-03-P18

[194]   A.W. Harris, L. Drube, How to find Metal-Rich Asteroids, ApJ, 2014, 785, L4

[195]   Ostro, S.J., Margot, J.-L., Benner, L.A.M., Giorgini, J.D., Scheeres, D.J., Fahnestock, E.G., Broschart, S.B., Bellerose, J., Nolan, M.C., Magri, C., Pravec, P., Scheirich, P., Rose, R., Jurgens, R.F., De Jong, E.M., Suzuki, S., 2006. Radar Imaging of Binary Near-Earth Asteroid (66391) 1999 KW4. Science 314, 1276–1280. doi:10.1126/science.1133622

[196]   P. C. Thomas, J. A. Burns, M. S. Tiscareno, M. M. Hedman, P. Helfenstein, Saturn's Mysterious Arc-Embedded Moons: Recycled Fluff?, 44th Lunar and Planetary Science Conference, 2013, #1598

[197]   D. Takir, V. Reddy, J.A. Sanchez, M.K. Shepard, J.P. Emery, Detection of Water and/or Hydroxyl on Asteroid (16) Psyche, 2016

[198]   Naidu, S.P. L.A.M. Benner, M. Brozovic, J.D. Giorgini, M.W. Busch, J. S. Jao, C.G. Lee, L.G. Snedeker, M.A. Silva, M.A. Slade, K.J. Lawrence. Goldstone radar images of near-Earth asteroids (469896) 2007 WV4, 2014 JO25, 2017 BQ6, and 2017 CS. AGU Fall Meeting, 2017 December, New Orleans. also: http://nineplanets.org/news/2017-bq6/

[199]   R.C. Boden, O. Mori, T. Saiki, J. Kawaguchi, et al., Design of a Lander for In-Situ Investigation and Sample-Return from a Jupiter Trojan Asteroid on the Solar Power Sail Mission, 25th Workshop on JAXA Astrodynamics and Flight Mechanics, 2015, http://www.hayabusa.isas.jaxa.jp/kawalab/astro/abst/2015A_6_abst.txt

[200] S. Ulamec, R.C. Boden, C. Lange, J. Biele, J.T. Grundmann T.-M. Ho, K. Sasaki, C. Ziach, T. Okada, H. Yano, Y. Shirasawa, Lander Element for Jupiter Trojan Mission, in: Jupiter Trojan, 2016.

[201] J.T. Grundmann, W. Bauer, J. Biele, F. Cordero, B. Dachwald, A. Koncz, C. Krause, T. Mikschl, S. Montenegro, D. Quantius, M. Ruffer, K. Sasaki, N. Schmitz, P. Seefeldt, N. Toth, E. Wejmo, From Sail to Soil – Getting Sailcraft Out of the Harbour on a Visit to One of Earth's Nearest Neighbours, IAA-PDC15-04-17, 4th IAA Planetary Defense Conference 2015, Frascati, Italy.

[202] J.T. Grundmann, R. Boden, M. Ceriotti, B. Dachwald, E. Dumont, C.D. Grimm, C. Lange, R. Lichtenheldt, I. Pelivan, A. Peloni, J. Riemann, T. Spröwitz, S. Tardivel, Soil to Sail – Asteroid Landers on Near-Term Sailcraft as an Evolution of the GOSSAMER Small Spacecraft Solar Sail Concept for In-Situ Characterization, IAA-PDC-17-05-19, 5th IAA Planetary Defense Conference , May, 15th-19th, 2017, Tokyo, Japan.

[203] P.W. Chodas, S.R. Chesley, D.K. Yeomans, Impact Hazard Assessment for 2011 AG_5, IAA-PDC13-03-11.

[204] N. Sullo, A. Peloni, M. Ceriotti, From Low Thrust to Solar Sailing: A Homotopic Approach, 26th AAS/AIAA Space Flight Mechanics Meeting, AAS Paper 16-426, 2016.

[205] Sullo, N., Peloni, A. and Ceriotti, M., "Low-Thrust to Solar-Sail Trajectories: A Homotopic Approach", Journal of Guidance, Control, and Dynamics, Vol. 40, No. 11, 2017. pp. 2796-2806.. doi: 10.2514/1.G002552

[206] PPSO solver. Retrieved on 16th April 2017 at https://uk.mathworks.com/matlabcentral/fileexchange/58895-ppso.

[207] Peloni, A., Rao, A.V. and Ceriotti, M., "Automated Trajectory Optimizer for Solar Sailing (ATOSS)", Aerospace Science and Technology, Vol. 72, 2018, pp. 465-475, doi: 10.1016/j.ast.2017.11.025

[208] A. Peloni, A.V. Rao, M. Ceriotti, ATOSS: Automated Trajectory Optimiser for Solar Sailing, Fourth European Optimisation in Space Engineering (OSE) Workshop, 27-30 March 2017, Bremen, Germany.

[209] Data available online at https://cneos.jpl.nasa.gov/pd/cs/pdc17/ , retrieved 26APR2017.

[210] Gibbings A, Bowles N, Snodgrass C, Sanchez J.P, Henning H, Braukhane A., A Deep Space Inventory Tour of the Main Asteroid Belt, IAC-16.A3.1.6x32749, 67th International Astronautical Congress (IAC), Guadalajara, Mexico, 26-30 September 2016.

[211] J.P. Sánchez Cuartielles, A. Gibbings, C. Snodgrass, S. Green, N. Bowles, ASTEROID BELT MULTIPLE FLY-BY OPTIONS FOR M-CLASS MISSIONS, IAC-16.C1.5.7x33119, 67th International Astronautical Congress (IAC), Guadalajara, Mexico, 26-30 September 2016.

[212] H. F. Levison, C. Olkin, K. S. Noll, S. Marchi, and the Lucy Team, LUCY: SURVEYING THE DIVERSITY OF THE TROJAN ASTEROIDS: THE FOSSILS OF PLANET FORMATION, Lunar and Planetary Science XLVIII (2017), #2025

[213] J.Veverka, M.Belton, K.Klaasen, C.Chapman, Galileo's Encounter with 951 Gaspra: Overview, Icarus, Volume 107, Issue 1, January 1994, Pages 2-17, https://doi.org/10.1006/icar.1994.1002

[214] P.E. Beyer, R.C. O'Connor, Galileo Early Cruise, Including Venus, First Earth, and Gaspra Encounters, TDA Progress Report 42-109, 1992, https://ipnpr.jpl.nasa.gov/progress_report/42-109/109T.PDF

[215] NASA, Galileo Jupiter Arrival Press Kit, Dec. 1995, https://www.jpl.nasa.gov/news/press_kits/gllarpk.pdf

[216] R.Schulz, H.Sierks, M.Küppers, A.Accomazzo, Rosetta fly-by at asteroid (21) Lutetia: An overview, Planetary and Space Science, Volume 66, Issue 1, June 2012, Pages 2-8, https://doi.org/10.1016/j.pss.2011.11.013

[217] Duxbury, Thomas C.; Newburn, Ray L.; Acton, Charles H.; Carranza, Eric; McElrath, Timothy P.; Ryan, Robert E.; et al. (2004). "Asteroid 5535 Annefrank size, shape, and orientation: Stardust first results". Journal of Geophysical Research. doi:10.1029/2003JE002108

[218] M. Henderson, Deep Impact – A Review of the World's Pioneering Hypervelocity Impact Mission, 13th Hypervelocity Impact Symposium 2015, session 11, #22

[219] PIA02449: Masursky, https://photojournal.jpl.nasa.gov/catalog/PIA02449

[220] Olkin, Catherine B.; Reuter, D.; Lunsford, A.; Binzel, R. P.; Stern, S. A., The New Horizons Distant Flyby of Asteroid 2002 JF56, http://adsabs.harvard.edu/abs/2006DPS....38.5922O

[221] V. Maiwald, About Combining Tisserand Graph Gravity-Assist Sequencing with Low-Thrust Trajectory Optimization. International Conference on Astrodynamics Tools and Techniques, 14.-17. März 2016, Darmstadt, Deutschland.

[222] V. Maiwald, Initial Results of a New Method for Optimizing Low-Thrust Gravity-Assist Missions. International Symposium on Space Technology and Science, 3-9 Jun 2017, Matsuyama, Japan.

[223] V. Maiwald, Applicability of Tisserand Criterion for Optimization of Gravity-Assist Sequences for Low-Thrust Missions. 66th International Astronautical Congress, 12-16 October 2015, Jerusalem, Israel

[224] V. Maiwald, A New Method for Optimization of Low-Thrust Gravity-Assist Sequences. CEAS Space Journal. 2017, DOI: DOI 10.1007/s12567-017-0147-7 ISSN 1868-2502

[225] C. Lange, J.T. Grundmann, Responsive Development of Optimized Small Spacecraft through Balanced Ad-hoc and Strategic Re-Use with Model-Based System Engineering for Planetary Defence, Science and Emerging Applications, *this conference*, IAA-PDC-17-05-P22

based on the conference papers:

5th IAA Planetary Defense Conference – PDC 2017
15-19 May 2017, Tokyo, Japan

IAA-PDC-17-05-19
SOIL TO SAIL – ASTEROID LANDERS ON NEAR-TERM SAILCRAFT AS AN EVOLUTION OF THE GOSSAMER SMALL SPACECRAFT SOLAR SAIL CONCEPT FOR IN-SITU CHARACTERIZATION

Jan Thimo Grundmann, Ralf Boden, Matteo Ceriotti, Bernd Dachwald, Etienne Dumont, Christian D. Grimm, Caroline Lange, Roy Lichtenheldt, Ivanka Pelivan, Alessandro Peloni, Johannes Riemann, Tom Spröwitz, Simon Tardivel

4th IAA Planetary Defense Conference – PDC 2015
13-17 April 2015, Frascati, Roma, Italy

IAA-PDC-15-04-17
FROM SAIL TO SOIL – GETTING SAILCRAFT OUT OF THE HARBOUR
ON A VISIT TO ONE OF EARTH'S NEAREST NEIGHBOURS

Jan Thimo Grundmann, Waldemar Bauer, Jens Biele, Federico Cordero, Bernd Dachwald, Christian D. Grimm, David Herčík, Aaron D. Koch, Alexander Koncz, Christian Krause, Caroline Lange, Tobias Mikschl, Sergio Montenegro, Alessandro Peloni, Dominik Quantius, Michael Ruffer, Kaname Sasaki, Nicole Schmitz, Wolfgang Seboldt, Patric Seefeldt, Maciej Sznajder, Norbert Tóth, Elisabet Wejmo, Friederike Wolff

APPENDIX / SUPPLEMENT

Parameters of the asteroids appearing in MNR trajectories by Peloni et al. in [71], [72], and this paper, according to [110] [111] [112].

object	table
1989 UQ	A4
2000 EA14	A5b
2000 SG344	2, 7
2001 QJ142	A5a
2002 AW	A2
2002 RW25	A4
2003 WT153	A4
2004 VJ1	A3
2005 TG50	11, A3
2006 BZ147	A1
2007 UY1	A5a
2008 DB	A5b
2008 EV5	2, 7
2008 TX3	A5b
2009 UZ87	A2
2009 YF	A2
2011 AG5	7
2011 CG2	A1, A3
2011 UX275	A2
2012 BB4	A1
2012 BB14	11
2012 EC	A2
2012 KB4	2, 7
2012 WH	A5a
2013 BS45	A1
2014 EK24	A5a
2014 MP	2
2014 UN114	A5a
2014 YN	11, A1
2015 JD3	2, 7, Ax
2015 JF11	11, A3

Table A1 – Properties of the encounters of Table 1 in [72].

Object	2012 BB$_{14}$	2011 CG$_2$	2006 BZ$_{147}$	2013 BS$_{45}$	2014 YN
Orbital type	Apollo	Apollo	Apollo	Aten	Aten
Semi-major axis [AU]	1.0644	1.1775	1.0234	0.9918	0.89227
Eccentricity	0.0994	0.9908	0.0986	0.0837	0.13429
Inclination [deg]	2.645	2.757	1.410	0.7725	1.208
Absolute magnitude [mag]	25.0	21.4	25.4	25.9	25.7
Estimated size [m] geometric albedo	17-78	130-300	20-50	17-37	13-56
EMOID [AU]	0.01712	0.03002	0.00188	0.01139	0.00497
PHA	No	Yes	No	No	No
NHATS	Yes	Yes	Yes	Yes	Yes
Taxonomic type					
Albedo					
Rotation period [h]		10.813			
Light-curve amplitude [mag]		1.3			
Radar observation				Yes	
Spectral observation					
IR observation					
Ascending node Earth separation [AU]	0.06773	0.08951	0.03512	0.07756	-0.2359
Descending node Earth separation [AU]	0.04104	0.20895	-0.00844	-0.09775	0.01767

Table A2 – Properties of the encounters of Table 2 in [72].

Object	2011 UX$_{275}$	2012 EC	2009 YF	(350751) 2002 AW	2009 UZ$_{87}$
Orbital type	Apollo	Apollo	Aten	Apollo	Aten
Semi-major axis [AU]	1.0349	1.1516	0.9359	1.0708	0.9233
Eccentricity	0.0762	0.1374	0.1216	0.2563	0.1883
Inclination [deg]	4.5448	0.9134	1.5268	0.5744	3.7815
Absolute magnitude [mag]	25.8	23.4	24.7	20.8	25.9
Estimated size [m]	18-40	50-120	30-70	180-400	17-37
geometric albedo					
EMOID [AU]	0.0191	0.0022	0.0173	0.0049	0.0115
PHA	No	No	No	Yes	No
NHATS	Yes	Yes	Yes		Yes
Taxonomic type				B	
Albedo					
Rotation period [h]					
Light-curve amplitude [mag]					
Radar observation					
Spectral observation					
IR observation					
Ascending node Earth separation [AU]	-0.02623	-0.00964	0.06103	0.15214	-0.22073
Descending node Earth separation [AU]	0.08863	0.30379	-0.19112	-0.11964	0.0337

Object	2011 CG$_2$	2004 VJ$_1$	2005 TG$_{50}$	2015 JF$_{11}$	-
Orbital type	Apollo	Aten	Aten	Aten	
Semi-major axis [AU]	1.1775	0.9437	0.92348	0.99547	
Eccentricity	0.9908	0.1641	0.134504	0.16669	
Inclination [deg]	2.757	1.2939	2.401	9.317	
Absolute magnitude [mag]	21.4	24.2	24.8	20.8	
Estimated size [m]	140-315	38-90	19-85	120-538	
geometric albedo					
EMOID [AU]	0.03002	0.01364	0.01240	0.1143	
PHA	Yes	No	No	No	
NHATS	Yes	Yes	Yes	Yes	
Taxonomic type					
Albedo					
Rotation period [h]	10.813				
Light-curve amplitude [mag]	1.3				
Radar observation					
Spectral observation					
IR observation					
Ascending node Earth separation [AU]	0.08951	-0.20866	0.02879	0.13308	
Descending node Earth separation [AU]	0.20895	0.08442	-0.18638	-0.15138	

Table A3 – Properties of the encounters of Table 3 in [72].

Table A4 – Properties of the encounters of Table 5, update of Table 4 in [72].

Object	2003 WT$_{153}$	(65679) 1989 UQ	(401954) 2002 RW$_{25}$	-	-
Orbital type	Aten	Aten	Aten		
Semi-major axis [AU]	0.8935	0.9151	0.8263		
Eccentricity	0.1777	0.2647	0.2869		
Inclination [deg]	0.3684	1.299	1.327		
Absolute magnitude [mag]	28.0	19.4	18.8		
Estimated size [m]	7-15	918 ±10	420-940		
geometric albedo		0.033 ±0.007			
EMOID [AU]	0.00153	0.01406	0.01607		
PHA	No	Yes	Yes		
NHATS					
Taxonomic type		B;C			
Albedo		0.06			
Rotation period [h]	0.117	7.733			
Light-curve amplitude [mag]	0.2	0.27			
Radar observation		No			
Spectral observation					
IR observation					
Ascending node Earth separation [AU]	0.03547	-0.31793	-0.28839		
Descending node Earth separation [AU]	-0.26124	0.13912	-0.18346		

Table A5a – Properties of the other encounters of Fig.4 in [72].

Object	2001 QJ$_{142}$	2014 UN$_{114}$	2012 WH	2007 UY$_1$	(459872) 2014 EK$_{24}$
Orbital type	Apollo	Aten	Aten	Aten	Apollo
Semi-major axis [AU]	1.0621	0.8973	0.9072	0.9511	1.0075
Eccentricity	0.0862	0.1600	0.1452	0.1753	0.0701
Inclination [deg]	3.1038	3.4143	4.0938	1.0194	4.8060
Absolute magnitude [mag]	23.7	24.5	25.5	22.9	23.3
Estimated size [m]	46-110	35-75	20-50	70-160	55-130
geometric albedo					
EMOID [AU]	0.00969	0.00078	0.03348	0.00555	0.03173
PHA	No	No	No	No	No
NHATS					
Taxonomic type					
Albedo					
Rotation period [h]	~0.16				0.0978
Light-curve amplitude [mag]	large				0.83
Radar observation					
Spectral observation					
IR observation					
Ascending node Earth separation [AU]	0.01853	-0.22566	-0.2346	-0.09787	-0.03697
Descending node Earth separation [AU]	0.09282	0.0019	0.04759	-0.05841	0.04387

Table A5b – Properties of the other encounters of Fig.4 in [72].

Object	2008 TX$_3$	(350523) 2000 EA$_{14}$	2008 DB	-	-
Orbital type	Apollo	Apollo	Apollo		
Semi-major axis [AU]	1.1793	1.1170	1.0547		
Eccentricity	0.1866	0.2026	0.2332		
Inclination [deg]	2.3816	3.5556	4.2239		
Absolute magnitude [mag]	24.9	21.1	25.7		
Estimated size [m]	27-63	160-355	19-45		
geometric albedo					
EMOID [AU]	0.02053	0.04365	0.00152		
PHA	No	Yes	No		
NHATS					
Taxonomic type		Q			
Albedo					
Rotation period [h]					
Light-curve amplitude [mag]					
Radar observation					
Spectral observation					
IR observation					
Ascending node Earth separation [AU]	0.21665	0.3068	-0.0097		
Descending node Earth separation [AU]	0.06912	-0.09114	0.00493		